

UNCLASSIFIED

AD 294 354

*Reproduced
by the*

ARMED SERVICES TECHNICAL INFORMATION AGENCY
ARLINGTON HALL STATION
ARLINGTON 12, VIRGINIA



UNCLASSIFIED

NOTICE: When government or other drawings, specifications or other data are used for any purpose other than in connection with a definitely related government procurement operation, the U. S. Government thereby incurs no responsibility, nor any obligation whatsoever; and the fact that the Government may have formulated, furnished, or in any way supplied the said drawings, specifications, or other data is not to be regarded by implication or otherwise as in any manner licensing the holder or any other person or corporation, or conveying any rights or permission to manufacture, use or sell any patented invention that may in any way be related thereto.

294354

22100

(1) N-63-2-

AIR FORCE MISSILE DEVELOPMENT CENTER

DEPUTY FOR GUIDANCE TEST

GUIDANCE AND CONTROL DIVISION

AD No. _____
ASTIA FILE COPY

CENTRAL INERTIAL GUIDANCE TEST FACILITY

ARMA LIGHTWEIGHT INERTIAL GUIDANCE SYSTEM

SLED TEST PROGRAM SUMMARY REPORT

VOLUME II



SEPTEMBER 1962

ASTIA
RECEIVED
JAN 22 1963
ASTIA

294 354

UNITED STATES AIR FORCE

HOLLOMAN AIR FORCE BASE, NEW MEXICO

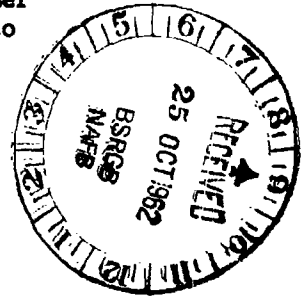
\$10.50

Copy 11 of _____
copies.

ARMA LIGHTWEIGHT INERTIAL GUIDANCE SYSTEM
SLED TEST PROGRAM SUMMARY REPORT

VOLUME II

GUIDANCE AND CONTROL DIVISION
DEPUTY OF GUIDANCE TEST
Air Force Missile Development Center
Holloman Air Force Base, New Mexico



This document is unclassified

NOTICES

SECURITY CLASSIFICATION

This document is unclassified

PROPRIETARY INFORMATION

This document does not contain proprietary information

DISTRIBUTION LIMITATION

There is no restriction on distribution of this document

TABLE OF CONTENTS

APPENDIX A

ANALYSIS PHILOSOPHY, DATA PROCESSING AND PARTIAL ERROR ANALYSIS

	Page
A-1 INTRODUCTION	A-1
A-2 HISTORICAL SPACE/TIME DATA REDUCTION	A-3
A-3 COMPARISON OF AVERAGES	A-5
Introduction	A-5
Error Analysis	A-6
A-4 FREQUENCY RESPONSE OF COMPARISON OF AVERAGES	A-11
A-5 GEODETIC COORDINATE TRANSFORMATION REQUIREMENTS	A-13
Introduction	A-13
Space/Time Geodetic Transformation - Tangent Plane	A-13
A-6 SPACE/TIME DATA HANDLING	A-18
A-7 VIBRATING STRING ACCELEROMETER CALIBRATION MODELS	A-33
A-8 VSA SUM FREQUENCY - SCALE FACTOR CORRELATION	A-38
A-9 VSA DATA HANDLING	A-42
Difference Frequency Model Calculations	A-47
Sum Frequency Model Computations	A-47
Filter Design for Acceleration Information	A-48
A-10 DATA FLOW DISCUSSION	A-62
A-11 LABORATORY SCALING PROGRAMS	A-71
VSA Alignment and Calibration Positions	A-71
Regular Scaling	A-75
Arma Scaling Program No. 178	A-82

	Page
Alternate Scaling Approach	A-89
Alternate Scaling Program No. 179	A-94
Input Data for Arms Scaling Programs	A-97
A-12 COHERENT OSCILLATION OR SERVO ERROR, PLATFORM BALANCING	A-99
A-13 DYNAMIC SIMULATION	A-103
The Simulation Program	A-103
The Simulation Results	A-124

LIST OF FIGURES

APPENDIX A

Figure No.	Title	Page No.
A-1	VSA	A-33
A-2a	Data Flow Diagram - Space/Time	A-54
A-2b	Data Flow Diagram - VSA Data Flow	A-55
A-2c	Data Flow Diagram - Vector Comparison	A-56
A-2d	Data Flow Diagram - Regression	A-57
A-2e	Data Flow Diagram - Pre and Post Run	A-58
A-2f	Data Flow Diagram - Laboratory Programs	A-59
A-3a	Automatic Edit (Flow Diagram) f_{1n} Loop	A-64
A-3b	Automatic Edit (Flow Diagram) f_{2n} Loop	A-65
A-3c	Automatic Edit (Flow Diagram) Sum Check Loop	A-66
A-4	Acceleration and Velocity Profile - Sled Run 3-5c	A-107
A-5	Block Diagram of Simulated Data Flow	A-108
A-6a-b	Effect of Time Shift between Integration	A-111
A-7	Effect of Round-Off Errors	A-112
A-8	Flow Diagram of VSA Simulation	A-116
A-9	Final Version Simulation ΔV Error	A-118
A-10	Observed Quadratic and Cubic Effects	A-119
A-11	δK_0 (Bias) Recovery	A-125
A-12	δK_1 (Scale Factor) Recovery	A-126
A-13	δK_2 (Quadratic) Recovery	A-127
A-14	δK_3 (Cubic) Recovery	A-128
A-15	δK_A (Servo Lag) Recovery	A-129
A-16	Constant (Offset) Recovery	A-130

APPENDIX A

ANALYSIS PHILOSOPHY, DATA PROCESSING AND PARTIAL ERROR ANALYSIS

A-1 INTRODUCTION

This appendix is intended to serve a dual purpose. First it is meant to document the actually accomplished Arma sled test analysis scheme including the pertinent data processing aspects involved. Second, it appears desirable to have the explanations for and partial error analysis of the various steps taken all in one place and in a form which may be understood by those not dealing immediately with the effort.

The problem of evaluating IMU performance by track testing is basically a problem of establishing a highly accurate reference quantity in the proper coordinate system which may be compared with a similar quantity as indicated by the IMU. Except for very small errors, the difference between indicated and reference quantities should represent the IMU error quantity. This error quantity may be analyzed as to magnitude and forms and an attempt made to calibrate all determinable error sources. The residual error quantity (after removal of calibratable errors) should represent the sum of the uncalibratable system errors and the reference system errors. If at all possible, the analysis of the system error quantity should break down the calibration into specific error sources, e.g., gyros or accelerometers. Such a breakdown, however, may require a dual reference quantity such as Space/Time velocity and photo-autocollimator indicated platform position. The dual reference system was not available for the Arma test sequence.

The primary reference system for the analysis of sled test data is the Space/Time system. The Space/Time system consists of: A set of very accurately surveyed markers (± 0.0005 foot rms leading edge placement as surveyed from the north end of the track); an accurate one-megacycle clock time base; a real time digitizer which digitizes and places on magnetic tape in binary form the time of the transducer passage by the fixed marker, ± 1 microsecond; and the S/T head or transducer which senses the passage by the interrupters and transmits the pulse to the digitizer indicating this event.

Thus, from a sled run ~~we obtain~~ ^{we obtain} a set of times indicating sled (transducer) passage by the surveyed markers. This is the input information from which ~~we form our~~ ^{we form our} reference quantity.

The Space/Time data reduction, as previously accomplished, was aimed at the accurate definition of sled velocity at the times of passage of the surveyed interrupters. An error analysis of the velocity measuring system from an instrumentation point of view has been accomplished by H. P. Greinel and published as a technical report AFMDC-TR-59-25 in June 1959. This error

analysis points up certain inherent limitations of the S/T instrumentation in defining the velocity at the instantaneous sled center of mass. The error analysis completely ignores the problem of transforming this velocity information to meaningful velocity as would be sensed by an ideal inertial guidance system in the face of relative motion between the guidance system and the sled center of mass. Greinel's error analysis defines a part of the "raw data" error and is not at all concerned with the data reduction errors. One "raw data" error which has been recognized which was not considered by Greinel is that of digitizer drift (loss or gain of time counts). This raw data error arises through improper instrumentation and has been effectively eliminated at AFMDC. Nonetheless, a periodic check has been included in the data reduction to insure that this error remains insignificantly small. Another raw data error which was not considered by Greinel is that of a systematic miscorrelation in time between the events from the Space/Time and the events from the guidance system under test. This error is very difficult to eliminate entirely and places a good deal of doubt upon any attempt to recover an instrument's servo lag term from track testing. The recovery of this term is better suited to transient tests specifically designed for that purpose. This point should become clear as one follows through the rest of this appendix.

The main results of Greinel's error analysis may be stated as:

1. Greinel's estimate of the rms error in downtrack position determination neglecting relative motion and timing error is $\sigma_x = 2.5 \times 10^{-3}$ ft.
2. Greinel's estimate of the rms (random) timing error is $\sigma_t = 6$ microseconds.

Using the above estimates we can say that the instantaneous downtrack position determination error (neglecting relative motion, digitizer drift, time correlation, and coordinate transformation errors) may be approximated as:

$$\sigma_{\text{Sled position}} \approx \left(\sqrt{6.25 \times 10^{-6} + 36V^2 \times 10^{-12}} \right) \text{ ft.}$$

where V = the average velocity in ft/second near the sled position being determined.

It will be shown later using Arma VSA data that this estimate is quite pessimistic and more nearly realistic but still cautious figures would be $\sigma_x = 1 \times 10^{-3}$ ft and $\sigma_t = 2$ microsecond. Using these figures we obtain

$$\sigma_{\text{Sled position}} \approx \left(\sqrt{1 \times 10^{-6} + 4V^2 \times 10^{-12}} \right) \text{ ft.}$$

The significance of this estimate will be seen later, after the comparison of averages technique is discussed.

A-2 HISTORICAL SPACE/TIME DATA REDUCTION

In the past the assumption was made that a sampled measure of the instantaneous sled velocity was the required quantity for the reference system against which the guidance system was to be compared. The raw S/T data was and still is first edited to eliminate spurious pulses and correct obviously erroneous data. Since the edited S/T data is in the form of a set of times (t_c) for measured distances, this information must be differentiated to obtain velocity measurements. In the past it was assumed that the times involved were adequately represented by a 3rd degree polynomial in distance and that all errors were timing errors; i.e., there were no position errors. Then the edited observed times (t_c) were fit with a 3rd degree polynomial in distance over seven points in a least squares sense. The mid-interval time was re-evaluated as the mid-point on this curve and this value taken as the adjusted or smoothed time (t_s). The estimated velocity at the mid-point was evaluated by differentiating with respect to distance the 3rd degree polynomial and inverting the results. This value was taken as S/T indicated velocity as a function of smoothed interrupter times, t_s . The difference ($t_c - t_s$) was evaluated for use as an error estimator for the velocity information. The $\sigma(t_c - t_s)$ for each point was evaluated over a twenty-five point spread symmetrically placed about the point in question.

A complete error analysis of the process outlined above is impossible because of the lack of information on the statistics of the velocity signal being considered. A partial error analysis has been done by Roger Moore of STL and documented in STL Inter-office Correspondence, GM 43.11-9, 14 November 1958. The result of this analysis is an estimate of velocity error. The following assumptions are made in R. Moore's approach:

1. A cubic polynomial in distance is the true characteristic of the raw data, t_c .
2. The errors are all timing errors.
3. Timing error can be represented as a random process of zero mean.
4. The data sampling rate is always high enough to prevent aliasing of high frequency information into a lower frequency variation in t_c .
5. The velocity of the S/T head is the quantity desired.

Under these assumptions R. Moore comes up with a standard error in velocity (ft/sec) of:

$$\sigma_V = .0483 V^2 \sigma(t_c - t_s) \quad \text{where } V \text{ is in ft/sec and} \\ \sigma(t_c - t_s) \text{ is in seconds.}$$

For a sled run of maximum velocity < 1600 ft/sec and $\sigma_t \approx 1$ μ sec this estimate gives us a maximum σ_v of .124 ft/sec. This is a slightly optimistic estimate for the 7 point cubic method since over a major portion of the run the position uncertainty effects actually exceed the timing uncertainty effects. Also, the 7 point cubic polynomial is inadequate to represent the dynamics which occur around first motion, boost cut off, water braking, etc. In addition, at very low velocities, the sampling rate is so bad that the above method of velocity determination breaks down entirely. As a result of these problems, a choice had to be made for the Arma sled runs between the alternatives of:

1. Finding a better way of getting instantaneous velocity.
2. Eliminating the requirement for the determination of instantaneous velocity altogether.

The comparison of averages technique effectively eliminated the instantaneous velocity requirement while accomplishing the desired test goals.

A-3 COMPARISON OF AVERAGES

Introduction

The need for an instantaneous velocity measurement has been definitely over-stressed in the past. The basic need is for an accurate reference quantity against which the major error trends of the IMU may be calibrated. Thus, we might perform the calibration on the distance level instead of the velocity level in order to make the comparison with the greatest possible accuracy using the raw (edited and coordinate transformed) Space/Time data. In the attempted IMU calibration certain confusion factors soon appear. For example: We can define the distance reference best, but a least squares adjustment on the distance domain tends to break down due to correlation between the form of the error trends from different error sources. This correlation is not as bad on the velocity level and so we might want to make a velocity comparison instead of a distance comparison. Actually, the solution is to take the best advantage of both the velocity and distance aspects of the problem and perform an average velocity comparison which has been named the comparison of averages. The averaging time used provides the trade-off between accuracy requirements on the trend of the comparison quantity and the frequency response of the comparison made.

The comparison of averages comes about simply by the application of a linear operation; namely, time averaging, to the ΔV quantity.

$$\Delta V(t_1) = V_{\text{system}}(t_1) - V_{\text{reference}}(t_1)$$

Let us find the average ΔV over the time interval from t_1 to t_2 . This would be the mean or trend value as long as $t_2 - t_1$ is kept reasonably short. (S indicates distance.)

$$\frac{1}{t_2 - t_1} \int_{t_1}^{t_2} \Delta V(t_1) dt = \overline{\Delta V} = \frac{[S_{\text{system}}(t_2) - S_{\text{ref}}(t_2)] - [S_{\text{system}}(t_1) - S_{\text{ref}}(t_1)]}{t_2 - t_1}$$

It should be immediately apparent that we can find $\overline{\Delta V}$ simply from a knowledge of t_1 , t_2 and distance quantities at those times. We do not need to smooth (fit) the S/T data and differentiate it to estimate a velocity value at all!

Thus, $\overline{\Delta V}$ may be defined to the limiting accuracies of the raw measurements. No more accurate measure of a function of velocity can be made using the same time interval for evaluation. The partial error analysis which follows is meant to point up the inherent limits of this method. The analysis is for the downtrack comparison only. Similar analyses can be done for the crosstrack and vertical direction, but better methods of handling

the survey results in these directions must be found before these comparisons can be accomplished with an accuracy approaching that of the downtrack comparison.

Error Analysis

All quantities in this section are in ft, second units.

Let $S_T(t)$ be the true instantaneous distance that would be sensed by an ideal inertial system as it proceeds down the track.

Let $S_M(t)$ be the measured distance function which is intended to estimate $S_T(t)$.

The average true velocity over an interval $(t_2 - t_1)$ is given by:

$$\bar{V}_T(t_2-t_1) = \frac{1}{t_2-t_1} \int_{t_1}^{t_2} V_T(t) dt = \frac{S_T(t_2) - S_T(t_1)}{t_2 - t_1}$$

The error in the definition of \bar{V}_T is given as:

$$\epsilon \bar{V}_T = \bar{V}_T - \bar{V}_M = \left\{ \frac{S_T(t_2) - S_T(t_1)}{t_{T_2} - t_{T_1}} - \frac{S_M(t_2) - S_M(t_1)}{t_{M_2} - t_{M_1}} \right\}$$

where $t_T = t_M + \delta t$.

The knowledge of true instantaneous downtrack position is hampered due to data uncertainties which we will presume to come from independent error sources of the following nature:

$SS(t)$ = the systematic error in the knowledge of interrupter positioning in the tangent plane coordinates.

σ_x = the rms error in the knowledge of the downtrack true instantaneous position caused by the addition of vibrational relative motion effects and the random error in the knowledge of interrupter positioning. It is estimated that σ_x (for the Arma sled test series) is approximately equal to 1×10^{-3} ft over most of the sled run although it is not really a stationary process which gives rise to this error.

$D_x(t)$ = the instantaneous error associated with σ_x .

$\delta S(t)$ = the equivalent position error due to timing inaccuracy; i.e., $\delta S(t) \approx V(t)_t \cdot \delta t$ where δt is the timing error and \approx means approximately equal. The approximation is an excellent one as long as δt is small. A large systematic time miscorrelation is not considered in this δt quantity since such an error can be analyzed out of the comparison at a later point in the analysis and does not give rise to a large error. Thus, $\delta t \leq 6 \mu\text{sec}$ for most of the sled run. We will assume $\sigma_{\delta t} \approx 2 \mu\text{sec}$.

The true instantaneous downtrack position can then be expressed as:

$$S_T(t) = S_M(t) + SS(t) + D_X(t) + V(t) \cdot \delta t$$

Placing this expression into our estimate of the error in the definition of \bar{V}_T we get

$$\epsilon \bar{V}_T = \frac{\{SS(t_2) + D_X(t_2) + V(t_2) \cdot \delta t_2 - SS(t_1) - D_X(t_1) - V(t_1) \cdot \delta t_1\}}{t_2 - t_1 + \delta t_2 - \delta t_1} - \frac{\{S_M(t_2) - S_M(t_1)\}}{(t_2 - t_1)(t_2 - t_1 + \delta t_2 - \delta t_1)}$$

For practical situations, $t_2 - t_1 \geq .01$ second and $|\delta t_2| + |\delta t_1| \leq 20 \mu\text{seconds}$. Thus, with less than .2% error in our estimation of $\epsilon \bar{V}_T$, we may neglect the δt_2 and δt_1 terms in the denominator of the above expression. This leaves us with

$$\epsilon \bar{V}_T = \left\{ \frac{SS(t_2) + D_X(t_2) - SS(t_1) - D_X(t_1)}{(t_2 - t_1)} \right\} + \left\{ \frac{[V_T(t_2) - \bar{V}_M] \delta t_2 + [\bar{V}_M - V_T(t_1)] \delta t_1}{t_2 - t_1} \right\}$$

In order to further simplify our expression for $\epsilon \bar{V}_T$ we will now assume that

$$\bar{V}_M = \frac{V_T(t_2) + V_T(t_1)}{2}$$

This approximation is good to 1% over most of the run as long as $t_2 - t_1 \leq 1$ second. However, this approximation tends to break down for areas of rapid change in acceleration level and must be examined critically in those areas. With these words of caution our approximate expression for $\epsilon \bar{V}_T$ becomes:

$$\epsilon \bar{V}_T = \frac{SS(t_2) - SS(t_1)}{t_2 - t_1} + \frac{Dx(t_2) - Dx(t_1)}{t_2 - t_1} + \bar{A}_T (\delta t_2 + \delta t_1)$$

where \bar{A}_T = the true average acceleration in the interval t_1 to t_2 .

Let us consider the effective contribution to $\epsilon \bar{V}_T$ of each of these three terms in order.

The first term represents the systematic interrupter positioning error. Since we are dealing with differences in this error, we need only consider the maximum change in this error over the interval t_1 to t_2 .

$$\text{Let } \frac{d(SS(t))}{dS} = 5.72 \times 10^{-6} \text{ ft/ft of track.}$$

This is equivalent to a .2 ft error accumulated over the 35,000 ft of the track. The geodetic transformation has been accomplished in such a manner as to keep this error source less than .1 ft over the length of the track. However, primary survey uncertainties may exist which amount to something closer to .2 ft over the entire track length.

The number of feet passed in the interval $t_2 - t_1$ is simply $\bar{V}_T (t_2 - t_1)$. Thus,

$$\frac{SS(t_2) - SS(t_1)}{t_2 - t_1} \leq 5.72 \times 10^{-6} \bar{V}_T$$

This error source thus looks like an accelerometer scale factor error and has a maximum value at maximum velocity. Taking our maximum velocity to be 1500 ft/sec, this error source would amount to approximately .0086 ft/sec or 1 part in 175,000 of sensed velocity. The track may actually be a little better than this, but something close to this figure probably represents the present limitation on testing of inertial guidance systems and components. If modern survey techniques can be applied (interferometer, etc.) to reduce this over-all track length uncertainty, the ultimate sled test accuracy figure may be closer to a part in one million.

The mean squared error contribution due to this source may be estimated as:

$$E \left\{ \left[\frac{SS(t_2) - SS(t_1)}{t_2 - t_1} \right]^2 \right\} = E \left[5.72 \times 10^{-6} \bar{V}_T^2 \right] = 32.7 \bar{V}_T^2 \times 10^{-12}$$

The second term in our estimate of the error of the measured average velocity is due to the uncertainty of interrupter positioning and to vibrational relative motion. We will assume that the vibrational relative motion belongs to a zero mean random process. The more systematic relative motion effects are handled as if they were a legitimate part of the $\bar{\Delta V}$ measured and later removed from the data.

The mean squared error contribution of this second term may be estimated as:

$$E \left\{ \left[\frac{D_X(t_2) - D_X(t_1)}{t_2 - t_1} \right]^2 \right\} = \frac{2 \sigma_X^2}{(t_2 - t_1)^2} \approx \frac{2 \times 10^{-6}}{(t_2 - t_1)^2}$$

The third term in our estimate of the error of the measured average velocity is due to the combination of timing uncertainty and acceleration. The mean squared error contribution from this effect may be estimated as:

$$E \left\{ \left[\bar{A}_T (\delta t_2 + \delta t_1) \right]^2 \right\} = \bar{A}_T^2 \cdot 2 \sigma_{\delta t}^2 \approx 8 \times 10^{-12} \bar{A}_T^2$$

Thus, from our simplified estimation formula we obtain an estimate of the mean squared error of measured average velocity (taking appropriate note of zero mean processes) which becomes:

$$\sigma_{e\bar{V}_T}^2 = 32.7 \times 10^{-12} \bar{V}_T^2 + \frac{2 \times 10^{-6}}{(t_2 - t_1)^2} + 8 \times 10^{-12} \bar{A}_T^2$$

Note that for reasonable values of acceleration, the effects of position uncertainty completely overshadow the effects of timing uncertainty. Note also that the error due to relative motion rises sharply as we allow our averaging time ($t_2 - t_1$) to approach zero.

If we choose an averaging time equal to .2 seconds and assume worst conditions of maximum velocity ($\bar{V}_T = 1500$ ft/sec) and maximum acceleration ($\bar{A}_T = 300$ ft/sec²) the estimate of the standard error in average velocity measurement becomes

$$\sigma_{\Delta V_T} \leq \sqrt{73.6 \times 10^{-8} + 50 \times 10^{-8} + .72 \times 10^{-8}}$$

$$\sigma_{\Delta V_T} \leq .011 \text{ ft/sec}$$

This estimate is somewhat pessimistic from the point of view that it presumes worst conditions, but in reality it is probably a bit optimistic due to other uncertainties (such as data processing) which have not entered into the above rationale. Actual hot run ΔV 's have shown a typical random standard error of $\approx .015$ ft/sec using $t_2 - t_1 = .25$ sec.

A-4 FREQUENCY RESPONSE OF COMPARISON OF AVERAGES

Let us examine a side light at this point for the benefit of those who want to see what the frequency response of any data handling procedure will be. It is possible to interpret the formula for average velocity as an attempt to differentiate distance data to get instantaneous velocity information.

In the continuous sense the computations we are performing would estimate a velocity (\dot{V}) according to

$$\dot{V}(t - \frac{h}{2}) = \frac{S(t) - S(t - h)}{h} \quad \text{where } h = t_2 - t_1 = \text{the averaging interval.}$$

The transfer function of this differentiating filter is given by (take Laplace Transform and set $p = i\omega$)

$$Y(\omega) = \frac{\sin(\frac{h\omega}{2})}{h/2} \cdot e^{i(\frac{\pi}{2} - \frac{h\omega}{2})}$$

$$\text{and } V(\omega) = S(\omega) Y(\omega)$$

Now, if we interpret the output as velocity at a delayed time (midpoint of interval), then the ideal differentiator has a transform

$$e^{-\frac{h}{2}p} \cdot p = e^{-\frac{h}{2}i\omega} \cdot i\omega = e^{i(\frac{\pi}{2} - \frac{h\omega}{2})}$$

We can define an error; actual-ideal = error. On this basis, the error in instantaneous velocity at the midpoint is given by

$$\text{LT}^{-1} V_e(\omega) = \text{LT}^{-1} \{S(\omega) Y_e(\omega)\}$$

$$\text{where } Y_e(\omega) = \left\{ \frac{\sin(\frac{h\omega}{2})}{h/2} - \omega \right\} \cdot e^{i(\frac{\pi}{2} - \frac{h\omega}{2})}$$

The $e^{i(\frac{\pi}{2} - \frac{h\omega}{2})}$ term merely serves the purpose of differentiation and the required delay of $\frac{h}{2}$ to get mid-interval velocity. Thus, we look at the first term which causes the error.

$$\text{Now } \frac{V_e(\omega)}{V(\omega)} = \text{relative error in } V(\omega).$$

$$\frac{V_e(\omega)}{V(\omega)} = \omega e^{-i\left(\frac{\pi}{2} - \frac{h\omega}{2}\right)} \cdot \left\{ \frac{\sin \frac{h\omega}{2}}{h/2 - \omega} \right\}$$

The above shows that as an instantaneous velocity, almost all of the high frequency components are underestimated (missed) for reasonable values of $h \geq .05$ sec. Thus, this is a pretty poor estimate of instantaneous velocity. Note, however, that the estimate is best for mid-interval time, so our using mid-interval times to tag it makes sense.

A-5 GEODETIC COORDINATE TRANSFORMATION REQUIREMENTS

Introduction

In order to compare S/T information with the IMU generated information we must deal with vector quantities in the same coordinate system. This requires a coordinate transformation from IMU to S/T or vice-versa. An arbitrary choice was made some time ago which stated that we would transform the S/T data into the coordinate set consistent with the IMU. On the basis of this choice, it appears practical to divide the transformation into several distinct steps:

1. Transform S/T information which is gathered as a one-dimensional quantity into a three-dimensional vector set in a tangent plane coordinate system.
2. Transform tangent plane information into the nominal coordinate set consistent with the IMU transducers.
3. Transform from nominal coordinates to coordinates which drift with time, etc., including the transformation to inertial space for those systems which maintain an inertial reference.

The process may be varied if desired; however, regardless of what else is done, it makes good sense to transform S/T information into tangent plane coordinates. In this way, the same geodetic transformations may be used for different systems under test. Of course, the parameters vary slightly if a run is made from one end of the track or the other, but once a tangent plane is set up, any sled run which starts reasonably close to the origin of this tangent plane may use it as a reference coordinate set for calculations.

Space/Time Geodetic Transformation - Tangent Plane

For any inertial guidance system being tested, a tangent plane coordinate set is defined at the center of mass of the inertial measuring unit in the following way:

X, Y, Z make up a right-handed orthogonal coordinate set in Cartesian coordinates with:

1. Z pointing directly up along the local vertical,
2. X pointing directly downtrack in the intended direction of motion for the guidance system (X lies in the tangent plane),

3. Y completing the orthogonal set, lying in the tangent plane and oriented by the right hand rule of $+X$ into $+Y$ yields a + rotation about $+Z$.

The one-dimensional Space/Time measurements are converted to three-dimensional measurements by a geodetic survey which essentially expresses the tangent plane position coordinate of each interrupter. This survey information is contained in what is known as the "Master File."

The track facility consists of a pair of specially constructed steel rails supported on concrete beams. The total length is approximately 35,000 ft. The general direction is north-south.

The west rail is called the reference or "master rail." All "master file" positions are determined as points at top center of the master rail.

On the west side of the track a very accurate base line was established by the "United States Coast and Geodetic Survey." This base line is commonly referred to as the fiducial line. It is identified by bench marks approximately 100 ft. apart.

On the east side of the track and parallel to the rail is a row of small rectangular steel plates called interrupters. These are placed upright parallel to the track at intervals of approximately 13 feet. A vertical plane at 90° to the fiducial line and containing the north edge of an interrupter defines that interrupter station on top of the master rail. All measurements along the track were determined with respect to the fiducial line.

A "master file" containing interrupter position downtrack, height, horizontal offset, and local gravity as determined from the best available geodetic information from both a north track reference point and a south track reference point has been compiled and studied. This master file was reported upon in an AFMDC technical memo released early in 1961.

The results of this study show that the required track coordinate transformation to get to tangent plane coordinates is a simple one as long as the accuracy requirements are within bounds. The X (downtrack) distance is simply the distance function indicated by the Space/Time system. The error in this assumption will not accumulate to as much as .1 ft. displacement over the length of the track. The Y (crosstrack) and Z (vertically up) distances are simply the values listed in the "master file" as revised by a continual survey effort. In order to properly handle the Y and Z comparisons these listed values should be used directly and no assumption made as

to the smoothness, etc., of the Y and Z track coordinates. Unfortunately, such use of master file data in a routine program would put a prohibitive time burden on the 1103A computers presently available at the AFMDC Computation Division. As a consequence, we are forced to compromise some of our accuracy capabilities in the Y and Z directions (none is compromised in X) to achieve program structure efficiency.

The sacrifice is not great, but it is sufficient to cast a great deal of doubt upon any accelerometer or gyre calibration coefficients recovered from Y or Z velocity comparisons. Since the major effort for the Arma sled test sequence was to recover VSA (vibrating string accelerometer) calibration coefficients, it was felt sufficient to recover coefficients for the down-track accelerometer and use the Y and Z accelerometers to compensate for platform misorientations during the sled run. Note that this is not a fundamental sled test limitation, but merely one imposed for reasons of efficiency. Thus, the following assumptions were made:

1. Y (cross track) distance = 0
2. Z (vertically up) distance = the distance indicated by a sectionalized (10 segments) fit over long track segments of the form

$$Z = A_0 + A_1 X + A_2 X^2$$

where Z comes from master file information A_0 , A_1 , A_2 are found in a least squares sense. The residual distance from the fitted segments turns out to have a standard deviation of approximately .01 ft. Unfortunately, the individual deviations are not random, and the localized effects of short length trends can be seen in the Z velocity comparison which amount to around .1 ft/sec. These effects are repeatable (from run to run) and do not interfere with the use of the Z comparison for attitude reference purposes, but they would interfere with coefficient recovery attempts.

3. Local gravity at each interrupter may be expressed as:

$$\epsilon_{x_i} = \frac{-g_0 X_i}{R_0} \quad \text{where } g_0 \text{ is the origin gravity value and } R_0 \text{ is approximately } 21 \times 10^6 \text{ ft.}$$

$$\epsilon_{y_i} = 0$$

$$\epsilon_{z_i} = g_0 \text{ or } \epsilon_{\text{nominal}}$$

In addition to the above geodetic information, the following quantities are required to properly accomplish any inertial guidance system sled test:

1. Astronomic azimuth of track at origin (launch point).
2. Astronomic latitude of origin (launch point).
3. Deflection of the vertical at the origin (launch point).

With the above quantities supplied, the necessary conversion of earth rate into tangent plane coordinates proceeds as follows:

1. Take the angular velocity vector of the earth with respect to inertial space as

$$|\vec{W}_E| = 7.29211 \times 10^{-5} \text{ inertial rad/mean solar sec.}$$

2. Project $|\vec{W}_E|$ into two components

$$W_N = |\vec{W}_E| \cos (\text{astronomic latitude of launch point})$$

$$W_{\perp} = |\vec{W}_E| \sin (\text{astronomic latitude})$$

3. Project W_{\perp} into two components

$$W_z = W_{\perp} \cdot \cos (\text{east or west deflection of the vertical})$$

$$W_{\perp}^{\circ} = W_{\perp} \cdot \sin (\text{east deflection of vertical, minus if west})$$

4. Let $\alpha = 360^{\circ}$ or 180° - astronomic azimuth of track
(a small angle)

Then

$$W_{Nx} = W_N \cos \alpha + W_{\perp}^{\circ} \sin \alpha$$

$$W_{Ny} = -W_N \sin \alpha + W_{\perp}^{\circ} \cos \alpha$$

where W_{Nx} is the X component of $|\vec{W}_E|$ for a shot from the south to the north end, etc.

or

$$W_{S_x} = -W_N \cos \alpha - W_{\perp} \sin \alpha$$

$$W_{S_y} = +W_N \sin \alpha - W_{\perp} \cos \alpha$$

where W_{S_x} is the X component of $|\vec{W}_E|$ for a shot from north to south end, etc.

Accomplishing these calculations for the Arma launch point yields
(running from north to south)

$$W_x = -12.5857 \text{ arc sec/sec}$$

$$W_y = .8857 \text{ arc sec/sec}$$

$$W_z = 8.1870 \text{ arc sec/sec}$$

A-6 SPACE/TIME DATA HANDLING

The raw S/T data is edited as necessary and a set of t_c values determined. These are the times of passage of the successive interrupters. This series is then inverted to form a series of distance values as a function of sampled times. This is the S/T distance function $S_{ST}(t_1)$. In this inversion process it is presently assumed that the distance between successive interrupters is exactly 13.00000000 ft. Using this number we get an accumulated error of 0.2 ft. over the length of the track due to the fact that the base line length divided by the number of interrupters comes out 12.99992584. Thus, in our $S_{T,jp}$ calculation (which follows shortly) we can multiply our α_1 factor by $\frac{12.99992584}{13.0} = .999994295$ and compensate for this factor with no appreciable error.

The S/T distance function $S_{ST}(t_1)$ may be broken into three components consistent with the geodetic transformation assumptions made above. These become:

$S_{ST_y} = 0$ = the Space/Time indicated distance in the Y direction

$S_{ST_x} = S_{ST}$ = the Space/Time indicated distance in the X or downtrack direction. This distance is the distance travelled from first motion time, t_0^1 .

$S_{ST_z} = A_0 + A_1 S_{ST} + A_2 S_{ST}^2$ where the A_0 , A_1 , and A_2 are constants which take on several different sets of values as a function of S_{ST} . The A_0 , A_1 , and A_2 values are found by a least squares fit of the Z data in the master file on the X distance over sections of the track, starting from the origin concerned.

From this information plus geodetic transformation information, we can compute the distance which ideal accelerometers should indicate in tangent plane coordinates. In order to accomplish this, we first examine the true accelerations which would be indicated in tangent plane coordinates, and then integrate the significant results. Let the subscripts T = true and ST = Space/Time. Let A = acceleration and V = velocity and W = earth rate. Then,

$$A_{T_x} = A_{ST_x} + 2W_y V_{ST_z} - 2W_z V_{ST_y} - \epsilon_x$$

$$A_{T_y} = A_{ST_y} + 2W_z V_{ST_x} - 2W_x V_{ST_z} - \epsilon_y$$

$$A_{T_z} = A_{ST_z} + 2W_x V_{ST_y} - 2W_y V_{ST_x} - \epsilon_z$$

Since we make the programming approximations that

$$V_{ST_y} = 0 \text{ (or } A_{ST_y} = 0)$$

$$\epsilon_y = 0$$

$$\epsilon_z = -|\epsilon_{\text{nominal}}| = -|\epsilon_N|$$

we are led to the following:

$$A_{T_x} = A_{ST_x} + 2W_y V_{ST_z} - \epsilon_x$$

$$A_{T_y} = 2W_z V_{ST_x} - 2W_x V_{ST_z}$$

$$A_{T_z} = A_{ST_z} - 2W_y V_{ST_x} + |\epsilon_N|$$

In addition, the term $2W_x V_{ST_z}$ may be neglected since it contributes less than 0.004 ft/sec to V_{T_y} . Also, $2W_y V_{ST_z}$ may be neglected since its influence is even smaller than that of $2W_x V_{ST_z}$. For tests of future systems, both these terms may have to be included if error (calibration) coefficients are attempted using cross track comparisons. For the present, we are left with tangent plane accelerations:

$$A_{T_x} = A_{ST_x} - \epsilon_x = A_{ST_x} + \frac{|\epsilon_0|}{R_0} S_{ST_x}$$

$$A_{T_y} = 2W_z V_{ST_x}$$

$$A_{T_z} = A_{ST_z} - 2W_y V_{ST_x} + |\epsilon_N|$$

The above equations represent the reference acceleration or true acceleration seen by an ideal accelerometer in tangent plane coordinates.

These will be utilized to form reference velocities and distances. Under the approximations which led to these equations, we can expect errors in our reference (neglecting dynamic or sampling errors) downtrack velocity of considerably less than .01 ft/sec. Thus, the coordinate transformations contribute negligible errors to the overall comparison. Of course, obvious dynamic and sampling errors creep into the definition of our reference quantities, but these must be considered separately.

We now define the computational quantity $P_{ST}(t_1)$ as:

$$P_{ST}(t_1) = \int_{t_0}^t S_{ST}(t) dt = \text{the integral from 1st motion time } (t_0^1) \text{ to time } t \text{ of the S/T distance function. Numerically, this integration is accomplished using the trapezoidal rule.}$$

Then, in tangent plane coordinates the velocities become:

$$V_{Tx} = V_{ST} + \frac{|S_0|}{R_0} P_{ST}$$

$$V_{Ty} = 2W_z S_{ST}$$

$$V_{Tz} = A_1 \cdot V_{ST} + 2A_2 \cdot S_{ST} V_{ST} - 2W_y S_{ST} + |S_N| \cdot (t-t_0)$$

where t_0 represents computation zero time, which is either prior to or at first motion time, t_0^1 . The computation of V_{Tz} is made every 0.1 second starting at t_0 up till 1st motion time, t_0^1 , at which time the calculation switches to interrupter times.

Also, in tangent plane coordinates the distances become:

$$S_{Tx} = S_{ST} + \frac{|S_0|}{R_0} \int_{t_0^1}^t P_{ST}(t) dt$$

$$S_{Ty} = 2W_x P_{ST}$$

$$S_{Tz} = A_1 S_{ST} + 2A_2 \int_{t_0^1}^t S_{ST}(t) V_{ST}(t) dt - 2W_y P_{ST} + \frac{|S_N|}{2} (t-t_0)^2$$

where t_0 represents computation zero time. The computation of S_{Tz} is made every 0.1 second starting at t_0 and continuing up till 1st motion² time, t_0^1 , at which time the calculation switches to interrupter times.

For data handling purposes we now define t_j = the time of sled passage by the j th interrupter from launch point origin.

We compute the Space/Time indicated velocity at t_j times by a seven point cubic polynomial arc smoothing technique whereby we differentiate the least squares cubic polynomial and take one over the mid-point slope as $V_{ST}(t_j)$.

We compute the Space/Time indicated distance at t_j times by a direct addition of 13 foot increments for each interrupter passed except the first. This is denoted $S_{ST}(t_j)$.

From geodetic survey information on the Z coordinate we establish a set of triplets of constants $(A_0, A_1, A_2)_n$ defined over intervals of distance which are identified by critical values of distance S_{ST_k} . From first motion time (t_0) until a first critical distance (S_{ST_1}) is reached, the first triplet of constants $(A_0, A_1, A_2)_1$ will be used. In the interval from the first critical distance (S_{ST_1}) to the second critical distance, (S_{ST_2}), the second triplet of constants $(A_0, A_1, A_2)_2$ will be used, etc. No more than ten sets of these constants are used for a sled run.

The digital program then calculates the two Space/Time distance components as:

$$S_{ST_x} = S_{ST}$$

$$S_{ST_z} = \left[A_0 + A_1 S_{ST} + A_2 S_{ST}^2 \right]_k \quad \text{where } k \text{ denotes the use of the proper constants over the proper intervals.}$$

The digital program then calculates the two Space/Time velocity components as:

$$V_{ST_x} = V_{ST}$$

$$V_{ST_z} = V_{ST} \cdot \left[A_1 + 2A_2 S_{ST} \right]_k \quad \text{where } k \text{ denotes the use of the proper constants over the proper intervals.}$$

These quantities are then transformed into reference indications in tangent plane coordinates. In order to accomplish this, we define a set

of constants A_3 , A_4 , A_5 , and A_6 plus computation zero time (t_0). The computation zero time (t_0) will in general be before the first motion time (t_0'). The constants are:

$$A_3 = \frac{|S_0|}{R_0}$$

$$A_4 = 2W_z$$

$$A_5 = -2W_y$$

$$A_6 = |S_N|$$

The program then computes (starting with first motion time (t_0')) the integral of Space/Time distance by the trapezoidal rule defining a new quantity $P_{ST}(t_j)$ as:

$$P_{ST}(t_j) = \int_{t_0'}^{t_j} S_{STx}(t_j) dt$$

This quantity is kept distinct for future operations. In addition, it is integrated from first motion time (t_0') to t_j by the rectangular rule thus defining another new quantity as:

$$U_{ST}(t_j) = \int_{t_0'}^{t_j} P_{ST}(t_j) dt$$

This quantity is also kept distinct for future operations.

The program then adjusts the $\{t_j\}$ time series for the fact that we want our calculations to start at t_0 (computation zero time) and not necessarily t_0' (first motion time). The new series of times is labelled $\{t_1\}$. This new series of times starts at t_0 and goes at 0.1 second intervals until a time t_1 is reached such that $(t_0' - t_0) - t_1 \leq 0.1$ second. Then, the 0.1 second interval is dropped, and the next time taken as $(t_0' - t_0)$. Each interrupter time thereafter has $(t_0' - t_0)$ added to it to become consistent with the new time series $\{t_1\}$. The following calculations are done on the basis of this new time series thus defining outputs on the times $\{t_1\}$. However, it is to be noted that up to and including the t_1 value signifying first motion (namely $t_0' - t_0$) the following quantities must be inserted as zeros and the proper values used thereafter:

V_{ST_x} , V_{ST_z} , S_{ST_x} , S_{ST_z} , P_{ST} , and U_{ST}

The program then computes on the basis of these adjusted times $\{t_1\}$ the quantities:

$$V_{T_x} = V_{ST_x}(t_1) + A_3 P_{ST}(t_1)$$

$$V_{T_y} = A_4 S_{ST}(t_1)$$

$$V_{T_z} = V_{ST_z}(t_1) + A_5 S_{ST_x}(t_1) + A_6 (t_1 - t_0)$$

$$S_{T_x} = S_{ST_x}(t_1) + A_3 U_{ST}(t_1)$$

$$S_{T_y} = A_4 P_{ST}(t_1)$$

$$S_{T_z} = S_{ST_z}(t_1) + A_5 P_{ST}(t_1) + A_6 \frac{(t_1 - t_0)^2}{2}$$

These are the reference velocities and distances in tangent plane coordinates. They are placed in vector form (3 components in serial order x, y, z) and eventually printed out along with the $\{t_1\}$ series upon which they are defined. In the printout these are denoted as X, Y, Z distance functions and VX, VY, VZ velocity functions. In order to make a proper comparison with the accelerometer indicated quantities, these tangent plane results must be modified by drift compensations and other coordinate transformations.

Examination of typical sled run conditions allows us to state that the platform misorientation from initial conditions hardly ever exceeds 7 arc min, and this is reached only by the system which goes inertial at the time t_0 , or computation zero time. Thus, we may make small angle approximations to the drift experienced during a sled run and calculate the reference quantities along the slightly misoriented platform axes which were originally aligned with tangent plane coordinates. Maximum velocity errors associated with this approximation are on the order of 2 parts per million of sensed velocity. If greater accuracies are required, this transformation will have to be re-accomplished differently.

Define: $\phi_1(t)$ = the platform drift angle as a function of time about the tangent plane 1th axis.

X_p, Y_p, Z_p = platform axes which are originally aligned to the tangent plane coordinates, x, y, z .

Then, by our small angle approximations we get:

$$\begin{Bmatrix} A_{T_x p} \\ A_{T_y p} \\ A_{T_z p} \end{Bmatrix} = \begin{bmatrix} 1.0 & \phi_z & -\phi_y \\ -\phi_z & 1.0 & \phi_x \\ \phi_y & -\phi_x & 1.0 \end{bmatrix} \begin{Bmatrix} A_{T_x} \\ A_{T_y} \\ A_{T_z} \end{Bmatrix}$$

$$= \begin{Bmatrix} A_{T_x} \\ A_{T_y} \\ A_{T_z} \end{Bmatrix} + \begin{Bmatrix} \delta A_{T_x} \\ \delta A_{T_y} \\ \delta A_{T_z} \end{Bmatrix}$$

where

$$\begin{Bmatrix} \delta A_{T_x} \\ \delta A_{T_y} \\ \delta A_{T_z} \end{Bmatrix} = \begin{bmatrix} 0 & \phi_z & -\phi_y \\ -\phi_z & 0 & \phi_x \\ \phi_y & -\phi_x & 0 \end{bmatrix} \begin{Bmatrix} A_{T_x} \\ A_{T_y} \\ A_{T_z} \end{Bmatrix}$$

$$\begin{Bmatrix} v_{T_x p} \\ v_{T_y p} \\ v_{T_z p} \end{Bmatrix} = \begin{Bmatrix} v_{T_x} \\ v_{T_y} \\ v_{T_z} \end{Bmatrix} + \int_{t_0}^t \begin{bmatrix} 0 & \phi_z & -\phi_y \\ -\phi_z & 0 & \phi_x \\ \phi_y & -\phi_x & 0 \end{bmatrix} \begin{Bmatrix} A_{T_x} \\ A_{T_y} \\ A_{T_z} \end{Bmatrix} dt$$

or

$$\begin{Bmatrix} V_{Txp} \\ V_{Typ} \\ V_{Tzp} \end{Bmatrix} = \begin{Bmatrix} V_{Tx} \\ V_{Ty} \\ V_{Tz} \end{Bmatrix} + \begin{Bmatrix} \delta V_{Tx} \\ \delta V_{Ty} \\ \delta V_{Tz} \end{Bmatrix}$$

where

$$\begin{Bmatrix} \delta V_{Tx} \\ \delta V_{Ty} \\ \delta V_{Tz} \end{Bmatrix} = \int_{t_0}^t \begin{bmatrix} 0 & \phi_z & -\phi_y \\ -\phi_z & 0 & \phi_x \\ \phi_y & -\phi_x & 0 \end{bmatrix} \begin{Bmatrix} A_{Tx} \\ A_{Ty} \\ A_{Tz} \end{Bmatrix} dt$$

Assuming that each term $\phi_i(t)$ is a linear drift in time (constant drift rate) over short intervals of time (note that all time values are measured from computation zero time, t_0) we obtain:

From t_0 to t_1 ,

$$\phi_{x1}(t) = C_{x1} \cdot t$$

$$\phi_{y1}(t) = C_{y1} \cdot t$$

$$\phi_{z1}(t) = C_{z1} \cdot t$$

From t_1 to t_2 ,

$$\phi_{x2}(t) = C_{x1} \cdot t_1 + C_{x2} \cdot (t-t_1)$$

$$\phi_{y2}(t) = C_{y1} \cdot t_1 + C_{y2} \cdot (t-t_1)$$

$$\phi_{z2}(t) = C_{z1} \cdot t_1 + C_{z2} \cdot (t-t_1)$$

From t_2 to t_3 ,

$$\phi_{x3}(t) = C_{x3} \cdot (t-t_2) + C_{x1} \cdot t_1 + C_{x2} \cdot (t_2-t_1)$$

$$\phi_{y3}(t) = C_{y3} \cdot (t-t_2) + C_{y1} \cdot t_1 + C_{y2} \cdot (t_2-t_1)$$

$$\phi_{z3}(t) = C_{z3} \cdot (t-t_2) + C_{z1} \cdot t_1 + C_{z2} \cdot (t_2-t_1)$$

Or in general in the interval from t_{j-1} to t_j

$$\phi_{xj}(t) = C_{xj} \cdot (t-t_{j-1}) + C_{xj-1} \cdot t_{j-1} + \sum_{i=1}^{j-2} (C_{xi} - C_{xi+1}) \cdot t_i$$

$$\phi_{yj}(t) = C_{yj} \cdot (t-t_{j-1}) + C_{yj-1} \cdot t_{j-1} + \sum_{i=1}^{j-2} (C_{yi} - C_{yi+1}) \cdot t_i$$

$$\phi_{zj}(t) = C_{zj} \cdot (t-t_{j-1}) + C_{zj-1} \cdot t_{j-1} + \sum_{i=1}^{j-2} (C_{zi} - C_{zi+1}) \cdot t_i$$

Note that the following recursion formula holds between the j th interval (from t_{j-1} to t_j) and the $(j-1)$ th interval (from t_{j-2} to t_{j-1}). The calculation of $\phi_{xi}(t)$, etc., may be programmed by this recursion formula:

$$\phi_{xj}(t) = \phi_x(t_{j-1}) + C_{xj} \cdot (t-t_{j-1})$$

$$\phi_{yj}(t) = \phi_y(t_{j-1}) + C_{yj} \cdot (t-t_{j-1})$$

$$\phi_{zj}(t) = \phi_z(t_{j-1}) + C_{zj} \cdot (t-t_{j-1})$$

Note also that the derivatives over any interval from t_{j-1} to t_j (j th interval) are given by:

$$\frac{d}{dt} [\phi_{xj}(t)] = C_{xj}$$

$$\frac{d}{dt} [\phi_{yj}(t)] = C_{yj}$$

$$\frac{d}{dt} [\phi_{zj}(t)] = C_{zj}$$

Under the conditions imposed on the drift function by the above assumptions, let us examine an integration by parts over the time interval t_{j-1} to t_n (where $t_n \leq t_j$) of the term:

$$\begin{Bmatrix} \delta V_{T_x} \\ \delta V_{T_y} \\ \delta V_{T_z} \end{Bmatrix}_{t_{j-1}}^{t_n} = \int_{t_{j-1}}^{t_n} \begin{bmatrix} 0 & \phi_z & -\phi_y \\ -\phi_z & 0 & \phi_x \\ \phi_y & -\phi_x & 0 \end{bmatrix} \begin{Bmatrix} A_{T_x} \\ A_{T_y} \\ A_{T_z} \end{Bmatrix} dt$$

From the general relation

$$\int_{t_{j-1}}^{t_n} u \, d v = u \cdot v \Big|_{t_{j-1}}^{t_n} - \int_{t_{j-1}}^{t_n} (du) \cdot v$$

plus the associations

$$u_j = \begin{bmatrix} 0 & \phi_{zj} & -\phi_{yj} \\ -\phi_{zj} & 0 & \phi_{xj} \\ \phi_{yj} & -\phi_{xj} & 0 \end{bmatrix}, \quad d u_j = \begin{bmatrix} 0 & C_{zj} & -C_{yj} \\ -C_{zj} & 0 & C_{xj} \\ C_{yj} & -C_{xj} & 0 \end{bmatrix} dt$$

$$d v = \begin{Bmatrix} A_{T_x} \\ A_{T_y} \\ A_{T_z} \end{Bmatrix} dt, \quad v = \begin{Bmatrix} V_{T_x} \\ V_{T_y} \\ V_{T_z} \end{Bmatrix}$$

we have the relationship:

$$\int_{t_{j-1}}^{t_n} \begin{bmatrix} 0 & \phi_z & -\phi_y \\ -\phi_z & 0 & \phi_x \\ \phi_y & -\phi_x & 0 \end{bmatrix} \begin{Bmatrix} A_{T_x} \\ A_{T_y} \\ A_{T_z} \end{Bmatrix} dt =$$

$$\begin{aligned}
& \begin{bmatrix} 0 & \phi_{zj} & -\phi_{yj} \\ -\phi_{zj} & 0 & \phi_{xj} \\ \phi_{yj} & -\phi_{xj} & 0 \end{bmatrix} \begin{Bmatrix} V_{Tx} \\ V_{Ty} \\ V_{Tz} \end{Bmatrix} \Big|_{t_{j-1}}^{t_n} - \begin{Bmatrix} 0 & C_{zj} & -C_{yj} \\ -C_{zj} & 0 & C_{xj} \\ C_{yj} & -C_{xj} & 0 \end{Bmatrix} \begin{Bmatrix} V_{Tx} \\ V_{Ty} \\ V_{Tz} \end{Bmatrix} \Big|_{t_{j-1}}^{t_n} \quad dt \\
& = \begin{bmatrix} 0 & \phi_{zj} & -\phi_{yj} \\ -\phi_{zj} & 0 & \phi_{xj} \\ \phi_{yj} & -\phi_{xj} & 0 \end{bmatrix} \begin{Bmatrix} V_{Tx} \\ V_{Ty} \\ V_{Tz} \end{Bmatrix} \Big|_{t_{j-1}}^{t_n} - \begin{bmatrix} 0 & C_{zj} & -C_{yj} \\ -C_{zj} & 0 & C_{xj} \\ C_{yj} & -C_{xj} & 0 \end{bmatrix} \begin{Bmatrix} S_{Tx} \\ S_{Ty} \\ S_{Tz} \end{Bmatrix} \Big|_{t_{j-1}}^{t_n} \\
& = \begin{bmatrix} 0 & \phi_z(t_n) & -\phi_y(t_n) \\ -\phi_z(t_n) & 0 & \phi_x(t_n) \\ \phi_y(t_n) & -\phi_x(t_n) & 0 \end{bmatrix} \begin{Bmatrix} V_{Tx}(t_n) \\ V_{Ty}(t_n) \\ V_{Tz}(t_n) \end{Bmatrix} \\
& - \begin{bmatrix} 0 & \phi_z(t_{j-1}) & -\phi_y(t_{j-1}) \\ -\phi_z(t_{j-1}) & 0 & \phi_x(t_{j-1}) \\ \phi_y(t_{j-1}) & -\phi_x(t_{j-1}) & 0 \end{bmatrix} \begin{Bmatrix} V_{Tx}(t_{j-1}) \\ V_{Ty}(t_{j-1}) \\ V_{Tz}(t_{j-1}) \end{Bmatrix} \\
& - \begin{bmatrix} 0 & C_{zj} & -C_{yj} \\ -C_{zj} & 0 & C_{xj} \\ C_{yj} & -C_{xj} & 0 \end{bmatrix} \begin{Bmatrix} S_{Tx}(t_n) - S_{Tx}(t_{j-1}) \\ S_{Ty}(t_n) - S_{Ty}(t_{j-1}) \\ S_{Tz}(t_n) - S_{Tz}(t_{j-1}) \end{Bmatrix}
\end{aligned}$$

Since $\begin{Bmatrix} \delta V_{T_x} \\ \delta V_{T_y} \\ \delta V_{T_z} \end{Bmatrix}$ for any time t_n , where $t_{j-1} \leq t_n \leq t_j$, must be found by

integrating over successive intervals from t_0 to t_n , we have

$$\begin{Bmatrix} \delta V_{T_x}(t_n) \\ \delta V_{T_y}(t_n) \\ \delta V_{T_z}(t_n) \end{Bmatrix} = \begin{bmatrix} 0 & \phi_z(t_n) & -\phi_y(t_n) \\ -\phi_z(t_n) & 0 & \phi_x(t_n) \\ \phi_y(t_n) & -\phi_x(t_n) & 0 \end{bmatrix} \begin{Bmatrix} V_{T_x}(t_n) \\ V_{T_y}(t_n) \\ V_{T_z}(t_n) \end{Bmatrix} \\ + \sum_{i=1}^{j-1} \begin{bmatrix} 0 & (C_{z_{i+1}} - C_{z_i}) & -(C_{y_{i+1}} - C_{y_i}) \\ -(C_{z_{i+1}} - C_{z_i}) & 0 & (C_{x_{i+1}} - C_{x_i}) \\ (C_{y_{i+1}} - C_{y_i}) & -(C_{x_{i+1}} - C_{x_i}) & 0 \end{bmatrix} \begin{Bmatrix} S_{T_x}(t_i) \\ S_{T_y}(t_i) \\ S_{T_z}(t_i) \end{Bmatrix} \\ - \begin{bmatrix} 0 & C_{z_j} & -C_{y_j} \\ -C_{z_j} & 0 & C_{x_j} \\ C_{y_j} & -C_{x_j} & 0 \end{bmatrix} \begin{Bmatrix} S_{T_x}(t_n) \\ S_{T_y}(t_n) \\ S_{T_z}(t_n) \end{Bmatrix}$$

For any t_n in the j^{th} interval, i.e., such that $t_{j-1} \leq t_n \leq t_j$.

These represent the velocity correction terms by which tangent plane velocities are corrected to be velocities which belong to the platform coordinate set which drifts with time in the specified (linear segment) manner. These components are printed out by the program as DVX, DVY, and DVZ. The digital program accepts up to ten time segments over which the linear drifts apply.

Once the velocity has been corrected for drift we may find the velocity that would be seen along any other coordinate set, merely by a coordinate transformation.

The reference velocity in drifting platform coordinates is computed by adding the V_T vector and DV vector together and printed out as V_{XP} , V_{YP} , and V_{ZP} components.

$$\begin{Bmatrix} V_{T_{XP}}(t_1) \\ V_{T_{YP}}(t_1) \\ V_{T_{ZP}}(t_1) \end{Bmatrix} = \begin{Bmatrix} V_{T_X}(t_1) \\ V_{T_Y}(t_1) \\ V_{T_Z}(t_1) \end{Bmatrix} + \begin{Bmatrix} \delta V_{T_X}(t_1) \\ \delta V_{T_Y}(t_1) \\ \delta V_{T_Z}(t_1) \end{Bmatrix}$$

The correction to the reference distance required is computed by integration of the DV vector with respect to time using the trapezoidal rule. These results are printed out as DX, DY, and DZ.

Then the reference distance is computed according to:

$$\begin{Bmatrix} S_{T_{XP}} \\ S_{T_{YP}} \\ S_{T_{ZP}} \end{Bmatrix} = \int_{t_0}^t \begin{Bmatrix} V_{T_X} \\ V_{T_Y} \\ V_{T_Z} \end{Bmatrix} dt + \int_{t_0}^t \begin{Bmatrix} \delta V_{T_X} \\ \delta V_{T_Y} \\ \delta V_{T_Z} \end{Bmatrix} dt = \begin{Bmatrix} S_{T_X} \\ S_{T_Y} \\ S_{T_Z} \end{Bmatrix} + \int_{t_0}^t \begin{Bmatrix} \delta V_{T_X} \\ \delta V_{T_Y} \\ \delta V_{T_Z} \end{Bmatrix} dt$$

with the results printed out as X_p , Y_p , and Z_p components.

A vector quantity is independent of the coordinate system in which it might be expressed. Consequently, once a vector has been specified in one coordinate set it is simply a matter of a coordinate transformation (linear operator) to express that vector in another coordinate set, orthogonal or non-orthogonal, which is fixed with respect to the first. We have found the vectors for acceleration, velocity, and distance in the x_p , y_p , z_p axes, which were fixed in the platform and aligned to the tangent plane at time t_0 , computation zero time. These quantities may be transformed to any other coordinate set fixed in the platform. This will now be accomplished:

Let us define: $[\theta]$ = the general matrix which transforms vectors expressed in the x_p , y_p , z_p axes to vectors expressed in the u , v , w , axes, where u , v and w may or may not be orthogonal.

Then, if \vec{B} is any vector at all, we have

$$\begin{Bmatrix} B_u \\ B_v \\ B_w \end{Bmatrix} = [\theta] \begin{Bmatrix} B_{xp} \\ B_{yp} \\ B_{zp} \end{Bmatrix}$$

The digital program takes the vectors

$$\begin{Bmatrix} V_{T_{xp}}(t_1) \\ V_{T_{yp}}(t_1) \\ V_{T_{zp}}(t_1) \end{Bmatrix} \quad \text{and} \quad \begin{Bmatrix} S_{T_{xp}}(t_1) \\ S_{T_{yp}}(t_1) \\ S_{T_{zp}}(t_1) \end{Bmatrix}$$

and converts them to the vectors

$$\begin{Bmatrix} V_u \\ V_v \\ V_w \end{Bmatrix} \quad \text{and} \quad \begin{Bmatrix} S_u \\ S_v \\ S_w \end{Bmatrix} \quad \text{respectively.}$$

These are the final reference quantities in the desired coordinate system. They are printed out as VHATU, VHATV, VHATW, U, V, and W components respectively. The detailed break-down of the transformation matrix is given by

$$[\theta] = \left[[\theta]_1 + [\theta]_2 \right] \cdot [\theta]_3$$

where

$$[\theta]_1 = \begin{bmatrix} \alpha_1 & \alpha_2 & \alpha_3 \\ \alpha_4 & \alpha_5 & \alpha_6 \\ \alpha_7 & \alpha_8 & \alpha_9 \end{bmatrix}$$

$$[\theta]_2 = \begin{bmatrix} \alpha_{10} & \alpha_{11} & \alpha_{12} \\ \alpha_{13} & \alpha_{14} & \alpha_{15} \\ \alpha_{16} & \alpha_{17} & \alpha_{18} \end{bmatrix}$$

$$[\theta]_s = \begin{bmatrix} \alpha_{18} & \alpha_{20} & \alpha_{21} \\ \alpha_{22} & \alpha_{23} & \alpha_{24} \\ \alpha_{25} & \alpha_{26} & \alpha_{27} \end{bmatrix}$$

where α_1 through α_{27} are insertable program constants.

This, in essence, completes the Space/Time data handling which can be considered by itself.

A-7 VIBRATING STRING ACCELEROMETER CALIBRATION MODELS

The difference frequency of an Arma vibrating string accelerometer represents a very close approximation to the acceleration applied along its input axis (modified by a scale factor). The integral of this difference frequency (the phase) then represents very accurately the velocity information we seek. The integral of this, of course, represents distance information. The basic problem to be solved, then, was the recovery of this information from the accelerometer in such a fashion that it could be compared accurately with our Space/Time reference system. In addition, before comparison certain known small non-linearities of the VSA were taken into account and the data modified accordingly. The difference between the VSA indicated quantity and the Space/Time indicated quantity was then analyzed for the source of further errors or non-linearities.

A very simplified view of the VSA shows that it is basically a device wherein two strings (or tapes) are each anchored at one end to a firm support and at the other end to a mass which is otherwise free to move short distances along the input axis of the VSA:

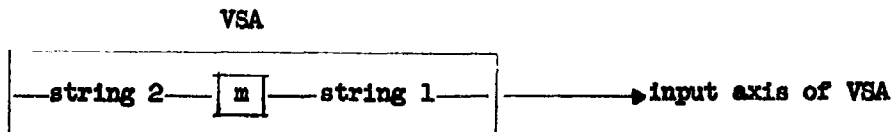


FIGURE A-1

The strings are forced to vibrate transversely at (or near) their natural frequencies under the influence of no input acceleration. When an acceleration along the input axis occurs (we ignore the cross axis temporarily) the inertial reaction of the mass in opposing this acceleration increases the tension in one string and decreases the tension in the other.

If we examine the approximate equation of motion for a freely vibrating string lying along the X axis and restrained at both ends, under a tension T with a mass density ρ , we have (See Hildebrand, Advanced Calculus for Engineers, Ch. 5):

$$\frac{d}{dx} \left(T \frac{dy}{dx} \right) + \rho w^2 y = 0 \quad \text{where } w \text{ is the angular frequency of vibration.}$$

If T is a constant then

$$T \frac{d^2 y}{dx^2} + \rho w^2 y = 0 \quad \text{or} \quad \frac{d^2 y}{dx^2} + \lambda y = 0.$$

For the various values of λ which satisfy the above relationship we obtain the various natural modes of oscillation.

$$\lambda = \frac{\rho w^2}{T} \quad \therefore \quad w = \sqrt{\frac{\lambda T}{\rho}}$$

Thus we see that the natural frequency of the string is related to the tension through a square root relationship.

Returning to the case of the individual strings of the VSA we note that we can approximately relate the frequency of the i^{th} string to its tension by

$$f_i = \alpha \sqrt{T_i} \quad \text{where } \alpha \text{ is a constant of proportionality.}$$

Let us denote as f_{0i} the natural frequency of the i^{th} string under equilibrium conditions with no acceleration input. Then let τ_i be a positive constant denoting the rate of increase (or decrease) in tension per unit initial tension per unit of input acceleration. Let "a" be the input acceleration along the instrument's input axis.

Then:

$$f_1 = f_{01} \sqrt{1 + \tau_1 a} \quad \text{and} \quad f_2 = f_{02} \sqrt{1 - \tau_2 a}$$

This, of course: Neglects any possible cross axis coupling effects; assumes no friction on the vibration tapes; ignores the non-linear tendency due to stretching of the tapes; ignores non-linear reactions of a coupling spring employed in the actual instrument; ignores temperature transient effects; and in general greatly simplifies a very complex physical situation. However, the examination of the simplified equations as presented above leads us directly to the rationale behind the two widely employed models for the operation of the VSA, the sum model, and the difference model (as we shall call them).

We define the sum frequency of the strings to be $f_1 + f_2 = \Sigma f$ and the difference frequency to be $f_1 - f_2 = \Delta f$.

We note that

$$\begin{aligned}(\Delta f) (\Sigma f) &= (f_1 - f_2)(f_1 + f_2) = (f_1^2 - f_2^2) \\ &= (f_{01}^2 - f_{02}^2) + (f_{01}^2 \tau_1 + f_{02}^2 \tau_2)a\end{aligned}$$

or when inverted, this expression becomes

$$a = \beta(\Delta f)(\Sigma f) - \gamma$$

$$\text{where } \beta = \frac{1}{f_{01}^2 \tau_1 + f_{02}^2 \tau_2}$$

$$\text{and } \gamma = \frac{f_{01}^2 - f_{02}^2}{f_{01}^2 \tau_1 + f_{02}^2 \tau_2} = (f_{01}^2 - f_{02}^2) \beta$$

This expression for acceleration in terms of the product of the string difference frequency and the string sum frequency is known as the "sum model" at HAFB.

It cannot be expected that this model should apply too closely to the physical operation of the VSA because of the factors which were ignored (some of which were noted previously) in its development. Nonetheless, the model does come close enough to the actual facts to make it a useful tool with the VSA. It was part of the purpose of the planned analysis of the VSA to determine the relative validity of this model and thus possible areas of application.

We have seen that according to our simplified assumptions

$$f_1 = f_{01} \sqrt{1 + \tau_1 a} \quad \text{and} \quad f_2 = f_{02} \sqrt{1 - \tau_2 a}$$

Using the binomial expansion of $(x + y)^n$ we obtain:

$$f_1 = f_{01} \left(1 + \frac{\tau_1 a}{2} - \frac{\tau_1^2 a^2}{8} + \frac{\tau_1^3 a^3}{16} - \frac{5}{128} \tau_1^4 a^4 + \dots \right)$$

$$f_2 = f_{02} \left(1 - \frac{\tau_2 a}{2} - \frac{\tau_2^2 a^2}{8} - \frac{\tau_2^3 a^3}{16} - \frac{5}{128} \tau_2^4 a^4 + \dots \right)$$

The values of τ_1 and τ_2 are very nearly the same, but they differ by the fact that the initial tensions on the two strings are slightly different and also by the fact that the effective masses acting on each string are slightly different. Note that the convergence of the binomial expansion

requires that $\tau_1^2 a^2$ be ≤ 1 . Thus, we would expect that as higher and higher accelerations were encountered the higher order non-linearities would become increasingly significant, which can be seen intuitively anyway.

Calculating the difference frequency, we get

$$\Delta f = f_1 - f_2 = (f_{01} - f_{02}) + \left(\frac{f_{01}\tau_1}{2} + \frac{f_{02}\tau_2}{2} \right) a - \left(\frac{f_{01}\tau_1^2}{8} - \frac{f_{02}\tau_2^2}{8} \right) a^2 + \left(\frac{f_{01}\tau_1^3}{16} + \frac{f_{02}\tau_2^3}{16} \right) a^3 - \left(\frac{5 f_{01}\tau_1^4}{128} - \frac{5 f_{02}\tau_2^4}{128} \right) a^4 + \dots$$

(Denote the zero offset frequency ($f_{01} - f_{02}$) as (Δf_0).

Note that in the above representation of difference frequency, the coefficients are terms which alternately add and subtract two nearly equal quantities. Thus, the sensitivity of the difference frequency to an input acceleration is expected to be nearly twice the single string sensitivity. The squared non-linearity of each string is relatively high, but the difference between two such non-linearities is low making the coefficient of the squared non-linearity low. The cubic non-linearity of a single string is very low but the coefficient for the cubic term in acceleration is the sum of two such non-linearities. Finally, the fourth order non-linearity of a single string is low and the difference between two strings is lower yet. Consequently, we may safely ignore all terms above the cubic for input accelerations under twenty g's. This is seen more clearly if we recognize that τ is on the order of 2×10^{-4} and f_{01} is on the order of 10^4 . Consequently, the single string fourth order non-linearity at 20 g's contributes approximately .1 cps to the single string frequency. The series for difference frequency is seen to converge rapidly for moderate input accelerations.

Thus

$$\Delta f = K_0 + K_1 a + K_2 a^2 + K_3 a^3$$

This is known as the "difference model" at HAFB, where we expect the various K's to be somewhere nearly consistent with the following expressions:

$$K_0 \approx \Delta f_0 \qquad K_1 \approx \left(\frac{f_{01}\tau_1 + f_{02}\tau_2}{2} \right)$$

$$K_2 \approx \left(\frac{f_{02}\tau_2^2 - f_{01}\tau_1^2}{8} \right) \qquad K_3 \approx \left(\frac{f_{01}\tau_1^3 + f_{02}\tau_2^3}{16} \right)$$

The difference model was derived from the same assumptions as the sum model, but it has the following advantage: The K's we solve for do not have to follow the functional square root relationships of the sum model and the

difference model may be thought of as an arbitrary fit of accelerometer output to a power series of acceleration (the input). This means that although many of the physical complications were ignored in deriving the difference model, this model may still be capable of fitting these effects in the physical situation.

Other relationships which are of use may be derived from the same linear approximations which led to the formulation of the calibration models above. Some specific examples (used in Section III of the main text of the report) are:

$$\Sigma f \text{ under zero g's} = (f_{01} + f_{02})$$

$$\frac{\Sigma f_{+1g} + \Sigma f_{-1g}}{2} = (f_{01} + f_{02}) - \frac{g^2}{8} (f_{01}\tau_1^2 + f_{02}\tau_2^2)$$

$$\Sigma f_{+1g} - \Sigma f_{-1g} = g (f_{01}\tau_1 - f_{02}\tau_2)$$

The next section of this appendix uses the same linear rationale to predict scale factor and sum frequency correlations.

A-8 VSA SUM FREQUENCY - SCALE FACTOR CORRELATION

(Reference Technical Note of B. W. Parkinson, 6 July 1962, Internal Document, HAFB, MDSGA)

A very heuristic approach to the problem of predicting the VSA scale factor for various temperatures leads us directly to the result that we may be able to use the VSA itself as our thermometer, i.e., the scale factor and sum frequency variation appear to be intimately related.

In the previous section, we used the approximate formulae:

$$f_1 = f_{01} \sqrt{1 + \tau_{1a}}$$

$$f_2 = f_{02} \sqrt{1 - \tau_{2a}}$$

Let us assume that the tension of both strings is affected exactly the same by a change in the VSA thermal equilibrium temperature (no gradient changes of note considered). Let us further assume that this change is a linear variation of tension with temperature. Thus we may assume

$$f_1 = f_{01} \sqrt{1 + \tau_{1a} + kT}$$

$$f_2 = f_{02} \sqrt{1 - \tau_{2a} + kT}$$

where T = the change from normal (zero or initial condition) operating temperature

and k = a proportionality constant

Since the effect of temperature will be very small relative to the initial conditions, we may expand and truncate these expressions to give:

$$f_1 = f_{01}(1 + \tau_{1a})^{\frac{1}{2}} + \frac{1}{2} \frac{kTf_{01}}{(1 + \tau_{1a})^{\frac{1}{2}}} - \frac{1}{8} \frac{(kT)^2 f_{01}}{(1 + \tau_{1a})^{\frac{3}{2}}} + \frac{1}{16} \frac{(kT)^3 f_{01}}{(1 + \tau_{1a})^{\frac{5}{2}}} + \dots$$

or

$$f_1 \approx f_{01}(1 + \tau_{1a})^{\frac{1}{2}} + \frac{1}{2} kTf_{01}(1 - \frac{\tau_{1a}}{2}) - \frac{1}{8} (kT)^2 f_{01}(1 - \frac{3\tau_{1a}}{2}) + \frac{(kT)^3 f_{01}}{16} (1 - \frac{5}{2} \tau_{1a}) + \dots$$

Similarly

$$f_2 \approx f_{02} (1 - \tau_{2a})^{\frac{1}{2}} + \frac{1}{2} kT f_{02} (1 + \frac{\tau_{2a}}{2}) \\ - \frac{1}{8} (kT)^2 f_{02} (1 + \frac{3\tau_{2a}}{2}) + \frac{(kT)^3 f_{02}}{16} (1 + \frac{5}{2} \tau_{2a}) + \dots$$

Calculating the sum frequency and rearranging the results yields:

$$\Sigma f = [f_{01} + f_{02}] \left[1 + \frac{1}{2} kT - \frac{1}{8} (kT)^2 + \frac{1}{16} (kT)^3 \right] \\ - \frac{a^2}{8} [\tau_1^2 f_{01} + \tau_2^2 f_{02}] \\ + \frac{a}{2} [f_{01} \tau_1 - f_{02} \tau_2] \left[1 - \frac{1}{2} kT + \frac{3}{8} (kT)^2 - \frac{5}{16} (kT)^3 \right] \\ + \frac{a^3}{16} [\tau_1^3 f_{01} - \tau_1^3 f_{02}] + \dots$$

Similarly for the difference frequency

$$\Delta f = [f_{01} - f_{02}] \left[1 + \frac{1}{2} kT - \frac{1}{8} (kT)^2 + \frac{1}{16} (kT)^3 \right] \\ - \frac{a^2}{8} [\tau_1^2 f_{01} - \tau_2^2 f_{02}] \\ + \frac{a}{2} [f_{01} \tau_1 + f_{02} \tau_2] \left[1 - \frac{1}{2} kT + \frac{3}{8} (kT)^2 - \frac{5}{16} (kT)^3 \right] \\ + \frac{a^3}{16} [\tau_1^3 f_{01} - \tau_2^3 f_{02}] + \dots$$

Examination of the difference frequency under the influence of temperature shows that the scale factor may be approximately given by:

$$SF = \frac{[f_{01}\tau_1 + f_{02}\tau_2]}{2} \left[1 - \frac{1}{2} kT + \frac{3}{8} (kT)^2 - \frac{5}{16} (kT)^3 \right]$$

Taking the partial derivative of scale factor relative to temperature variation, we find

$$\frac{\partial SF}{\partial T} = \left[\frac{f_{01}\tau_1 + f_{02}\tau_2}{2} \right] \left[-\frac{k}{2} + \frac{3}{4} k^2 T - \frac{15}{16} k^3 T^2 \right]$$

Similarly (ignoring dynamically coupled acceleration effects by setting $a = 0$)

$$\frac{\partial \Sigma f}{\partial T} \approx [f_{01} + f_{02}] \left[\frac{k}{2} - \frac{1}{4} k^2 T + \frac{3}{16} k^3 T^2 \right]$$

Thus if we set our initial (no temperature variation) scale factor and sum frequencies up as

$$SF_0 = \frac{f_{01}\tau_1 + f_{02}\tau_2}{2}$$

$$\Sigma f_0 = f_{01} + f_{02}$$

and then find the ratio of scale factor variation to sum frequency variation we find:

$$\frac{\partial SF}{\partial \Sigma f} = \frac{SF_0}{\Sigma f_0} \cdot \frac{\left[-\frac{k}{2} + \frac{3}{4} k^2 T - \frac{15}{16} k^3 T^2 \right]}{\left[\frac{k}{2} - \frac{1}{4} k^2 T + \frac{3}{16} k^3 T^2 \right]}$$

By long division we obtain the truncated series

$$\begin{aligned} \frac{\partial SF}{\partial \Sigma f} &= -\frac{SF_0}{\Sigma f_0} \left[1 - kT + k^2 T^2 - \frac{7}{8} k^3 T^3 \right] \\ &\approx -\frac{SF_0}{\Sigma f_0} \end{aligned}$$

or

$$SF = SF_0 - \frac{SF_0}{\Sigma f_0} [\Sigma f - \Sigma f_0]$$

This equation is somewhat experimentally verified and it appears applicable to improve the estimation of scale factor at missile launch. For example, sum frequency could be evaluated for the 100 seconds before launch. This would yield a current evaluation of scale factor. With this, and knowledge of accelerometer position relative to the local vertical, an evaluation of bias can be performed. The missile shot would be made with current values of both bias and scale factor calculated according to this scheme. For the actual results of this approach, see the scale factor results in the main text of the report (Section III).

A-9 VSA DATA HANDLING

The first in a chain of IMU data handling operations is the proper digitization of the VSA outputs. The goal is to recover properly the accumulated phase of the string difference frequency and to interpret this phase in terms of its velocity indication.

We could have observed the difference frequency directly as an analog signal, digitized this, and then integrated to get phase information. This procedure is fraught with problems of accuracy, however, because the frequency cannot be determined with sufficient accuracy to allow the integrated quantity to be assumed to be correct.

We could have operated as the Arma Airborne Computer was designed to operate and accepted pulses at the times one full (or one-half) cycle of phase (and thus a given constant velocity increment) was accumulated. This would have put the VSA data in a format very similar to that found for the Minuteman and/or Titan systems sled tests, i.e., the constant velocity increments would have been received at a series of unequal time samples.

Because of the difficulty of applying constant frequency response filters to uneven time-sampled data, the above approach was abandoned in favor of a scheme which yields velocity samples on the basis of equal time increments of t_w second. The basic approach was to calculate frequency in such a manner that when all the frequency computations were added up, they gave the correct phase information rather than allowing errors to accumulate.

The very first step in the VSA data reduction was to take the individual string frequencies (or heterodyned string frequencies) which were transmitted and recorded (versus a 100 KC clock) during the sled run and digitize them. The digitization consisted of timing (relative to 100 KC clock multiplied up to 1 megacycle) the occurrence of each positive going zero crossing of the string frequency and putting this time value on tape in digital form. A 1/2 second timing grid was included in the raw data and its effects had to be edited out by the digital program upon digitization. The purpose of the timing grid was to check on and insure very low digitizer drifts (less than 20 μ seconds for the whole sled run).

The next step in the data reduction was to compute the average string frequency from the digitized string information over a short interval of time which defined a sampling rate f_s .

$f_s = \frac{1}{t_w}$, where t_w is a constant time interval called "window time." The value of t_w may be varied by changing a parameter in the counting program, but it was normally set at .004 seconds so that $f_s = 250$ cps.

This sampling rate was sufficient to define most of the important dynamics which occurred on the Arma platform due to the soft shock-mounting system employed.

In the basic string frequency computing program, the computer applies the window time (t_w) to the string signal, finds the integral number of positive going zero crossings within the n^{th} interval (Z_n), and finds LT_n (lag time, n^{th} interval) and OT_n (over time, n^{th} interval). OT_n is equal to the time from the last positive going zero crossing within the interval to the end of the interval, and LT_n is equal to the time from the beginning of the interval to the first positive going zero crossing.

From this information, we can calculate a frequency such that when it is accumulated into counts (zero crossings) it will only be in error due to initial and end conditions plus the round-off errors introduced by calculation, which should be insignificant. A glance at later data processing requirements shows that eventually we will need acceleration (frequency) information for the determination of such things as coordinate functions for a least squares analysis, etc. Thus, we proceed to calculate this frequency and integrate the results to get phase information. Actually, it was determined (after the program was in operation) that there was a better way to proceed and thus avoid a systematic round-off error which amounted to .003 ft/sec in velocity or 1 part in 500,000 of maximum sled velocity. Although this error is insignificant, the alternative method will be described later in this section.

The string frequency which was actually computed was a heterodyned string frequency, so we will use a prime (') symbol on it. It was also an average frequency over the window time, so we will place a bar over it.

For the first interval:

$$\bar{f}'_1 = \frac{(Z_1 - 1) + \frac{(OT_1)}{(OT_1 + LT_2)} + \frac{(LT_1)(Z_1 - 1)}{(t_w - OT_1 - LT_1)}}{t_w}$$

For the second interval:

$$\bar{f}'_2 = \frac{Z_2 + \frac{(OT_2)}{(OT_2 + LT_3)} - \frac{(OT_1)}{(OT_1 + LT_2)}}{t_w}$$

For the third interval:

$$\bar{f}'_3 = \frac{Z_3 + \frac{(OT_3)}{(OT_3 + LT_4)} - \frac{(OT_2)}{(OT_2 + LT_3)}}{t_w}$$

.....

For the n^{th} interval:

$$\bar{F}_n = \frac{Z_n + \frac{(OT_n)}{(OT_n + LT_{n+1})} - \frac{(OT_{n-1})}{(OT_{n-1} + LT_n)}}{t_w}$$

As can be seen, the total number of counts (zero crossings) can be found as t_w times the sum of the above average frequencies. Note that successive intervals cancel out errors in OT or LT determination and thus make the sum accurate up to initial and end point conditions. It is not difficult to show that round-off errors introduced by the above calculations are not excessive. In addition, the actual program has a built-in round-off check capability which really amounts to the alternative method of computation previously mentioned.

The error which is desirable to keep negligible is the accumulated pulse error since this accumulation represents velocity information. For this reason, it is very desirable to accomplish all frequency calculations on the basis of a rounding operation rather than a dropping operation. This should insure that any error thus introduced will belong to a zero mean random process and not have distinct biasing effects. However, even for such a process it should be noticed that the accumulation error of a zero mean random process may certainly have character which we would call biasing were we to plot as a function of time the accumulated error function. For a discussion of this situation see Feller, An Introduction to Probability Theory and Its Applications, Vol. I, Ch. III.3. The saving grace in such a situation is that although the accumulated error may look like a bias term it never gets to large magnitudes in a limited number of steps for a zero mean random process where each incremental error is itself very small. Of course, the situation we face is not identical to the random walk discussed by Feller because the calculations of frequency are made in such a way that the individual round-offs are not entirely independent.

Faced with this situation, one could spend an enormous amount of time and effort deriving the specific statistics of the accumulated velocity error due to round-off operations in the various steps of calculation. This effort would hardly be worthwhile when a simple empirical check can insure us that in any given set of data this error does not become significant. This check takes the form of a comparison of the computed accumulated count derived from frequency calculations with the actual accumulated count available as part of the information processed from the Arma Airborne Computer. We will state here the velocity according to the difference model partially in terms of the accumulated counts so that it will be available for later comparison with the accumulated difference frequency. This velocity expression is easily derived, but it will only be stated here.

$$(D) V_j(tk) = (D)V_j(tr) + \sum_{n=r+1}^{n=k} (t_w) \cdot (D) \bar{A}_{jn}$$

where \bar{A}_{jn} is the average acceleration seen by the j^{th} VSA over the n^{th} interval according to the "difference" frequency model (D).

or

$$(D) V_j(tk) = (D)V_j(tr) + \frac{1}{K_1} \left\{ \sum_{n=r+1}^{n=k} N_{1jn} - \sum_{n=r+1}^{n=k} N_{2jn} - t_w K_0 (k-r) \right\} \\ - \sum_{n=r+1}^{n=k} \left\{ \frac{K_2}{K_1} \left(\frac{\Delta \bar{F}_{jn} - K_0}{K_1} \right)^2 + \frac{K_3}{K_1} \left(\frac{\Delta \bar{F}_{jn} - K_0}{K_1} \right)^3 \right\} t_w$$

This equation states that the Velocity (V) indicated by the j^{th} VSA at time t_k according to the difference frequency model (D) is equal to a prior indicated velocity at time t_r plus the scale factor modified

$\left(\frac{1}{K_1}\right)$ sum of the difference count less the bias offset from t_r to t_k , plus non-linearity terms. By setting $K_2 = K_3 = 0$ in this expression we arrive at the desired checking equation for round-off errors.

$$(D) V_j(tk) = (D) V_j(tr) + \frac{1}{K_1} \left\{ \sum_{n=r+1}^{n=k} N_{1jn} - \sum_{n=r+1}^{n=k} N_{2jn} - t_w K_0 (k-r) \right\}$$

The above equations represent the way we could have and should have calculated our velocity function in order to avoid the .003 ft/sec error due to accumulated round-off operations. This was not accomplished, however, and should be programmed for any future VSA computations. One reason this was not accomplished is that a simplified approximation to the round-off errors involved assured us that the errors would be less than .006 ft/sec. At the time this computation was performed, errors of this size were considered negligible relative to the velocity reference uncertainties involved.

In order to properly compare the outputs of the VSA with the Space/Time system, we must first correct the VSA outputs for known non-linearities. In order to do this, acceleration is calculated from the digitized frequencies of the preceding section. This acceleration represents an average acceleration over a window time so that its time weighted sum should represent a correct measure of velocity. In addition, this information is utilized to form various environmental coordinate functions for subsequent least squares analysis.

The acceleration calculations may be expected to contain a slight amount of jitter. In order to suppress as much of this jitter as possible, an optional digital filtering is included in the program which calculates acceleration. This programming will now be presented.

Let us define:

N'_{ijn} = the number of counts (positive going zero crossings plus fractions) of the i th (1 or 2) heterodyned (prime) string frequency on the j th (x, y, or z) VSA over the n th time interval (each time interval is of width t_w) from the start of the program, t_0 .

\bar{F}'_{ijn} = the average heterodyned frequency of the i th string on the j th VSA over the n th time interval as calculated from the equations given previously.

We must calculate the average difference frequency of the j th VSA over the n th time interval as:

$$\bar{\Delta f}'_{jn} = \bar{F}'_{1jn} - \bar{F}'_{2jn}$$

We also find the average heterodyned sum count over the $q+1$ intervals (q an even integer) in the form:

$$\bar{N}'_{ijn} = \frac{1}{q+1} \sum_{k=n-\frac{q}{2}}^{k=n+\frac{q}{2}} N'_{ijk} \quad \text{for } n > \frac{q}{2}$$

and

$$\bar{N}'_{ijn} = \frac{1}{q+1} \sum_{k=1}^{k=q+1} N'_{ijk} \quad \text{for } n \leq \frac{q}{2}$$

where k is the index of summation; n is an index representing the n th interval of width t_w from program initiation, t_0 ; and q is a program parameter = 0, 2, 4 ... any positive even integer.

Now, an individual count determination for one interval may be presumed to have a uniformly distributed and rounded random error component. Since the counting process is accomplished in such a way that (except for round-off) the errors committed at the end of one interval are balanced by those committed at the beginning of the next interval, we may logically

assume that the sum count over $(q+1)$ intervals will have a triangularly distributed error component. Our interest here was to choose a value of q large enough to make the influence of jitter in sum frequency determination less than .1 cycles per second if possible and yet maintain a level of dynamic response (small enough q) in the calculations to allow transient information on rapid changes in sum frequency to get through. A choice of $q = 16$ was taken to allow a fairly good transient response (bandwidth to 3 db pt. of ~ 2.6 cps) and at the same time to allow the error in the average count information to be fairly reasonable. For reasons of flexibility the value of q was left as a parameter which may be easily changed in the program.

Difference Frequency Model Calculations

Let:

(D) \bar{A}_{jn} = the average acceleration indicated by the j^{th} VSA over the n^{th} time interval of width t_w from the start of the program, t_0 , according to the difference frequency model, (D).

Then the difference frequency model states:

$$\bar{\Delta f}_{jn} = K_0 + K_1 \bar{A}_{jn} + K_2 \bar{A}_{jn}^2 + K_3 \bar{A}_{jn}^3$$

which we can invert to find:

$$(D) \bar{A}_{jn} = \left[\frac{\bar{\Delta f}_{jn} - K_0}{K_1} \right] - \frac{K_2}{K_1} \left[\frac{\bar{\Delta f}_{jn} - K_0}{K_1} \right]^2 - \frac{K_3}{K_1} \left[\frac{\bar{\Delta f}_{jn} - K_0}{K_1} \right]^3$$

where K_0 , K_1 , K_2 , and K_3 are arbitrary signed constants determined prior to the run and inserted as program parameters except for limitation $K_1 \neq 0$.

Since the quadratic and cubic terms are very small, we may assume that almost all of the error in (D) \bar{A}_{jn} comes from the first term in the above expression. We have no way of knowing how large the systematic error in (D) \bar{A}_{jn} may get. In fact, the determination of this factor is one of the major goals of track testing. The random error in (D) \bar{A}_{jn} may be expected to have a standard deviation around .6 ft/sec². This random component (as noted previously) should not be cumulative in its effects.

Sum Frequency Model Computations

Let:

(S) \bar{A}_{jn} = the average acceleration indicated by the j^{th} VSA over the n^{th} time interval of width t_w from the start of the program, t_0 , according to the sum frequency model, (S).

Then the sum frequency model states:

$$(S) \bar{A}_{jn} = \beta \left[\frac{\bar{\Delta f}_{jn} (\bar{N}'_{1jn} + \bar{N}'_{2jn})}{t_w} + \bar{\Delta f}_{jn} (\bar{f}_{l0(1jn)} + \bar{f}_{l0(2jn)}) \right] - \gamma$$

where β and γ are arbitrary signed constants determined from system calibration data and inserted as program parameters and where $(\bar{f}_{l0(1jn)} + \bar{f}_{l0(2jn)})$ is the average sum of the local oscillator frequencies which are heterodyned with strings one and two of the j^{th} VSA. The value of $(\bar{f}_{l0(1jn)} + \bar{f}_{l0(2jn)})$ was determined by counting the output of the hot run local oscillator and comparing this with prerun determined values. The two were found to be nearly identical and constant, so the prerun determined values were utilized in lieu of counting the hot run local oscillator data.

The acceleration derived from the sum model may be expected to contain slightly more jitter than that derived from the difference model. However, this difference should be slight and non-cumulative in its effects.

Filter Design for Acceleration Information

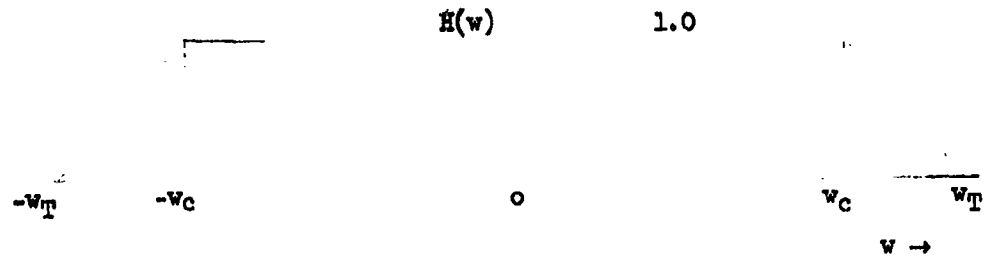
Introduction

It appeared desirable to look into the possibility of designing a digital filter to operate upon the acceleration information derived above to eliminate as much as possible of the undesirable jitter and noise while retrieving most of the signal information. The design was not optimized in any sense according to minimum mean squared errors or integral errors, etc. Instead, a logical choice of cut-off frequency was made and the results analyzed to see if the filter resulted in a significantly improved situation. The filter design described below is essentially that of a type described by J. Ormsby in an STL publication, "Design of Numerical Filters with Applications to Missile Data Processing," STL/TR60-0000-09123, March 1960.

Filter Theory - Linear

Let us assume that the data to be filtered contains noise and signal spectrum which are, to a large extent, non-overlapping. We want to design a digital filter to serve as a mid-point estimation device which

separates the signal from the noise. We will presume the signal to be of a low frequency nature so that we desire a low pass filter which has a frequency function as shown below:



The pass band is from 0 to w_c and the phase response within the pass band is perfect, i.e., no phase shift between input and output. The rejection band is from w_T to ∞ .

We denote:

w_c = cut-off frequency

w_T = filter roll-off termination frequency

The spectrum noted above may be described mathematically as:

$$H(w) = \left\{ \begin{array}{ll} 0 & |w| > w_T \\ 1.0 & |w| \leq w_c \\ \left(\frac{w+w_T}{w_T-w_c} \right) & -w_T \leq w < -w_c \\ - \left(\frac{w-w_T}{w_T-w_c} \right) & w_c < w \leq w_T \end{array} \right\}$$

The equivalent time weighting set may be found from:

$$h(t) = \frac{1}{2} \pi \int_{-\infty}^{\infty} H(w) e^{j\omega t} d\omega$$

$$\begin{aligned}
h(t) &= \frac{1}{2\pi} \int_{-w_{\pi}}^{-w_c} e^{j\omega t} \left(\frac{w - w_{\pi}}{w_{\pi} - w_c} \right) d\omega \\
&+ \frac{1}{2\pi} \int_{w_c}^{w_{\pi}} e^{j\omega t} (-1) \left(\frac{w - w_{\pi}}{w_{\pi} - w_c} \right) d\omega \\
&+ \frac{1}{2\pi} \int_{-w_c}^{w_c} e^{j\omega t} (1.0) d\omega
\end{aligned}$$

This when evaluated becomes:

$$h(t) = \frac{\cos w_c t - \cos w_{\pi} t}{\pi (w_{\pi} - w_c) t^2}$$

For a particular sampling rate f_s (cycles/sec) we have a time interval between data points $\frac{1}{f_s} = \Delta t$. For the case at hand $\Delta t = t_w$.

In digital filtering of equally spaced data we must approximate a convolution integral of the form:

$$y(t) = \int_{-\infty}^{\infty} h(t-\tau) x(\tau) d\tau,$$

where $h(t)$ is the system's unit impulse response, $x(t)$ is the system's input and $y(t)$ is the system's output, by an approximation of the form:

$$y(t) \approx \sum_{n=-\infty}^{n=+\infty} h(t-n\Delta t) x(n\Delta t) \Delta t.$$

We must, of course, limit ourselves to a finite number of data points and in the practical case our approximation using $(2N+1)$ points becomes:

$$y(t) \approx \sum_{n=-N}^{n=+N} h(t-n\Delta t) x(n\Delta t) \Delta t$$

We will not enter into an error analysis of the approximation so expressed since this is adequately covered in Ormsby's publication noted above. What needs to be done, however, is to choose a proper set of cut-off and termination frequencies and a proper number of data points, and to adjust the convolution integral approximation above for the fact that the acceleration data for time t_n actually applies as an estimate of the acceleration at $(t_n - \frac{t_w}{2})$. In addition, the resulting set of weighting coefficients must be normalized (their sum set equal to one) so that the truncation of the above series will not yield a bias in the determination of acceleration.

Characteristics of Signal and Noise to be Filtered

The acceleration signal which we were trying to retrieve was the acceleration seen by the inertial platform. Recognizing the fact that our sampling rate was only 250 cps, we note that we could not hope to recover meaningful information (due to aliasing or foldover effects) in a frequency range exceeding 125 cps (the nyquist frequency). The inertial system is mounted in a very soft shock-mount system with resonant frequencies from eight to fourteen cycles per second. Thus, whatever the acceleration is (which acts as an input to the platform) it will be attenuated by as much as one logarithmic unit (10 db power ratio or 20 db amplitude ratio) by the time the frequency reaches twenty-five cycles per second. Consequently, we do not expect very much signal content beyond 25 cps.

The jitter or noise, on the other hand, may be expected to have relatively wide band characteristics. Consider the acceleration noise due to jitter. The fact that we are not sampling randomly but at a discrete rate of 250 samples per second will cause a dependency of the error in one interval in the overtime count with that of another interval. This dependency is the only immediately apparent factor which keeps us from declaring the error in acceleration to be a zero mean stationary and ergodic random process with a pseudo white noise (broad band) character. Due to this dependency there will be undesirable harmonic components of the noise in the low frequency region of interest. In effect, this dependency is the same as the aliasing phenomenon or foldover effect due to any set sampling rate. Thus, there is no way that we can eliminate all of the jitter in the low frequency band. What we can do is to limit ourselves strictly to the signal spectrum of interest and reject all higher frequencies. If we assume the signal spectrum of interest to be from 0 to 20 cps, which is twice the natural frequency of the x axis shock-mounting, the design of the filter follows as shown below.

Design of Fourteen Point Acceleration Filter - Choosing

$$f_c = 20 \text{ cps}, f_T = 30 \text{ cps}, f_s = 100 \text{ cps}$$

$$\lambda_C = .2, \lambda_R = .1, \lambda_T = .3, N = 14$$

Entering Ormsby's paper, p. 10, we estimate that for $N=14$ points the error will be less than 1.5% in the region 0 to 19 cps and above 31 cps. Specifying that the lower frequencies must be passed to within .05% (1 part in 2,000) gives us the estimate that from 0 to 3 cps are so handled. This is considered to be sufficient accuracy to meet the present needs since the filter accuracy is the best at lower frequencies where accuracy is needed.

We now calculate the weights $h_n = h(t_n)$ as:

$$w_C = (2\pi) (20) \cdot \cdot \cdot .01 w_C \text{ equivalent to } 72 \text{ degrees}$$

$$\text{and } .005 w_C \text{ equivalent to } 36 \text{ degrees}$$

$$w_T = (2\pi) (30) \cdot \cdot \cdot .01 w_T \text{ equivalent to } 108 \text{ degrees}$$

$$.005 w_T \text{ equivalent to } 54 \text{ degrees}$$

n	$w_C \Delta t_n$	$w_T \Delta t_n$	$\cos w_C \Delta t_n$	$\cos w_T \Delta t_n$	$\cos w_C \Delta t_n - \cos w_T \Delta t_n$
0,+1	36°	54°	+ .809 016 99	+ .587 785 25	+ .221 231 74
-1,+2	108°	162°	- .309 016 99	- .951 056 52	+ .642 039 53
-2,+3	180°	270°	-1.000 000 00	.000 000 00	-1.000 000 00
-3,+4	252°	18°	- .309 016 99	+ .951 056 52	-1.260 073 51
-4,+5	324°	126°	+ .809 016 99	- .587 785 25	+1.396 802 24
-5,+6	36°	234°	+ .809 016 99	- .587 785 25	+1.396 802 24
-6,+7	108°	342°	- .309 016 99	+ .951 056 52	-1.260 073 51

$$\begin{aligned} \pi(w_T - w_C) &= \pi(2\pi 30 - 2\pi 20) = 2\pi^2 \\ &= 197.392088 \end{aligned}$$

$$\therefore \frac{1}{\pi(w_T - w_C)} = .005 066 05918$$

n	h_n (raw)	h_n (bias corrected)
0,+1	+ 44.830 923 493	+ .445 697 61
-1,+2	+ 14.456 045 577	+ .143 718 32
-2,+3	- 8.105 694 688	- .080 584 75
-3,+4	- 5.211 107 692	- .051 807 50
-4,+5	+ 3.494 460 647	+ .034 741 03
-5,+6	+ 2.339 267 045	+ .023 256 39
-6,+7	- 1.510 912 893	- .015 021 11
$\Sigma h_n =$	+ 100.585 962 98	$\Sigma h_n =$ 1.000 000 00
$\frac{1}{\Sigma h_n} =$.009 941 745 05	. . . No D.C. Bias

We instrument the equation:

$$A_j(p) = \sum_{n=-6}^{n=+7} h_n \cdot \bar{A}_j(p+n)$$

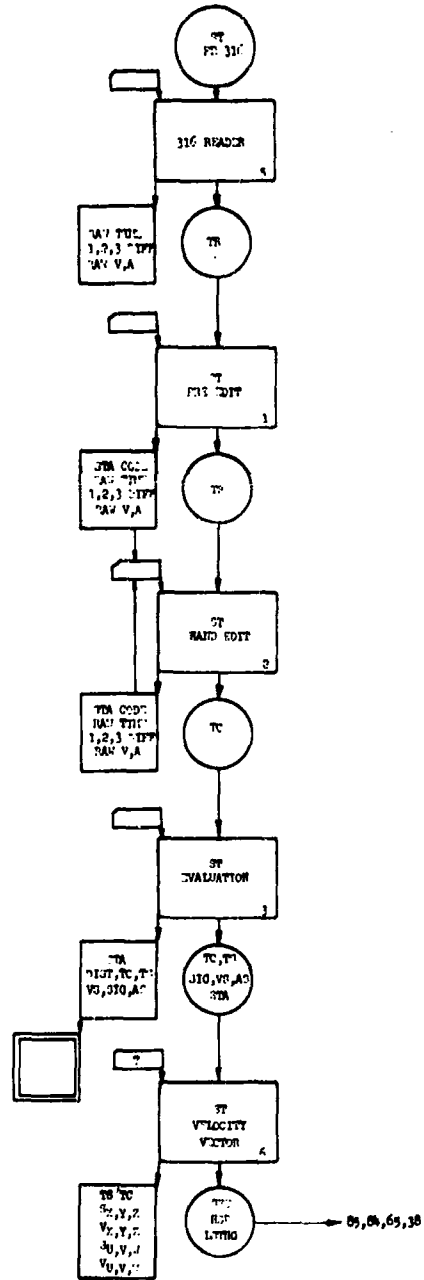
where $A_j(p)$ represents the best estimate of the acceleration at the end of the p th interval; $\bar{A}_j(p+n)$ represents the average acceleration calculated over the $(p+n)$ th interval; and h_n make up the set of linear weights calculated above.

Various definitions of bandwidth of interest will lead to various different filters. As a result, the filter weights were left as input parameters to the program which calculated acceleration. In actual practice, the results with and without fairly heavy acceleration filtering were found to be indistinguishable in the results on the rest of the programs and/or coefficient evaluations. At one time, a straight averaging over 14 pts was used.

At this point, it seems advisable to present a flow diagram of the digital computer programs used for the Phase III Arma analysis. Figures A2a through A2f will clarify the data handling already discussed and set the stage for future discussion.

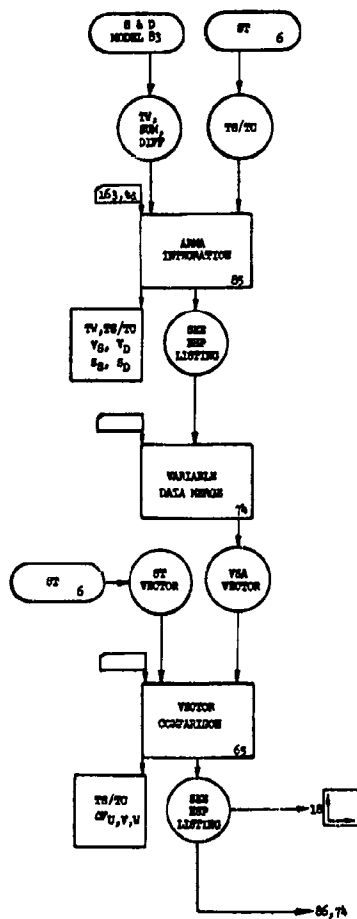
SPACE TIME

FIGURE A-2a



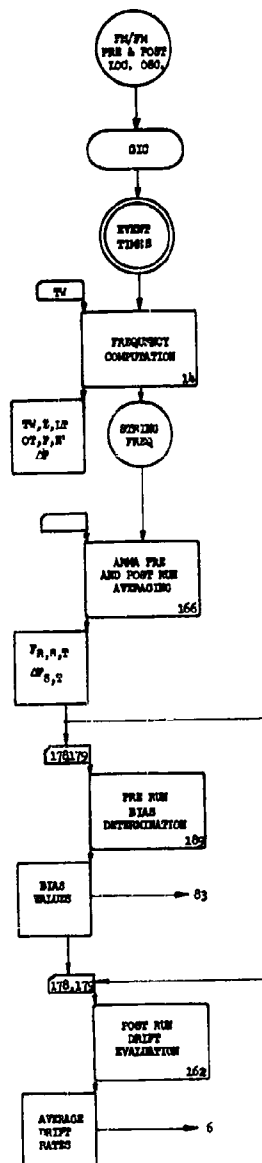
VECTOR COMPARISON

FIGURE A-2c

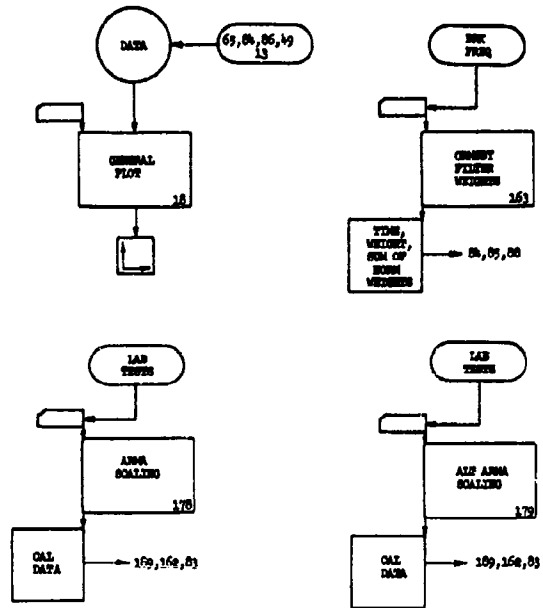


PRE AND POST RUN

FIGURE A-2e

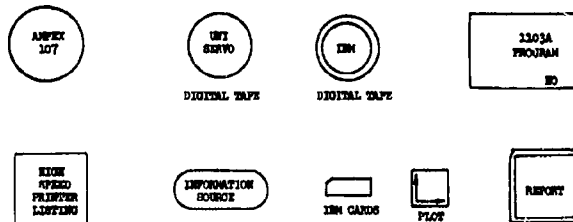


LABORATORY PROGRAMS FIGURE A-2f



LEGEND

See attached list of abbreviations and symbols



ABBREVIATIONS AND SYMBOLS
FOR FIGURE A-2

ALT	Alternate
AS	Acceleration, smoothed
BRK	Break
CAL	Calibration
\bar{A}	Average acceleration over window width acc. to diff. model
DIFF	Difference
ΔF	Difference function
$\overline{\Delta F}$	Average heterodyned diff. frequency of string one and string two over window width
$\overline{\Delta V}$	Delta V bar
\bar{F}	Average heterodyned frequency over window width
FCTN	Function
FILTRD	Filtered
$F_{U,V,W}$	Vector function of time in U,V,W coordinates
GIC	General input converter
HSP	High speed
IMU	Inertial measuring unit
LOC OSC	Local oscillator
LISTNG	Listing
LT	Lag time
N°	Total number of counts of the heterodyned string
NORM	Normalized

OT	Overtime
S	Distance
\overline{SA}	Average acceleration over window width acc. to sum model
S&D	Sum and difference
S_D	Distance, difference model
S_S	Distance, sum model
ST	Space/Time
STA	Station (track)
STRNG	String
\overline{SF}	Average heterodyned sum frequency of string one and two over window width
\overline{EF}	Filtered average heterodyned sum frequency of string one and two
σ , SIG	Sigma, standard deviation
TC	Corrected time
td	Interpolation time
TR	Raw time
TS	Smoothed time
TW	Window time
U,V,W	IMU coordinates
V	Velocity
VECTOR	Vector
V_D	Velocity, difference model
V_S	Velocity, sum model
VS	Velocity, smoothed (Space/Time)
VSA	Vibrating string accelerometer
X, Y, Z	Tangent plane coordinates
Z	Integral number of positive going zero crossings

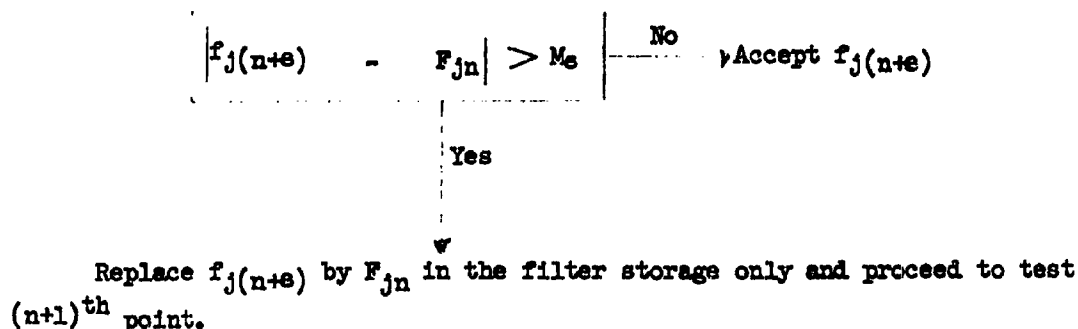
A-10 DATA FLOW DISCUSSION

Figure A-2a shows the digital program structure of the Space/Time data handling previously discussed. The Space/Time Velocity Vector program (#6) computes the best estimate of the vector distance which would be indicated by an ideal IMU and puts this information out as a time series defined on Space/Time times. As already described, program #6 takes into account any known platform drift, etc. It also puts out a velocity vector based upon a seven point cubic fit which may be used if desired. This velocity measure was not seriously used in the Arma analysis effort.

Figure A-2b shows the program structure for the string frequency computation, the string editing, and the sum and difference model computations. Except for the editing, these operations have already been discussed. The digital filter on acceleration which has been described is used on option in program #84 (Coordinate Function Generator, Figure A-2d) and not #83. At the output of program #83, we have a measure of VSA indicated acceleration which may be used in various ways. Before describing this use, we will outline the editing accomplished in program #88 (Figure A-2b).

The VSA strings are counted separately in the GIC and merged on the input to the automatic editing program #88. The auto-edit program takes in six input parameters M_1 through M_6 and performs checks against the individual string frequencies, over times, lag times, and various combinations of the two string information trains. Parameter M_6 is used to pre-test future data which is approaching the editing and keeps very bad data points out of the frequency prediction function.

Consider the n^{th} point to be under observation for editing. The program computes a best estimate F_{jn} (predicted frequency of string 1 in the n^{th} frame) from filtering of 15 points symmetrically around the n^{th} point. Very bad data is prevented from entering the prediction filtering by a check on M_6 prior to bringing in new data. This check may be shown schematically as:



Using the best estimate of frequency, the program computes a maximum possible period as:

$$P_{in \max} = \frac{1}{F_{in} - K \tau w} \quad \text{where } K \text{ is a program stored parameter.}$$

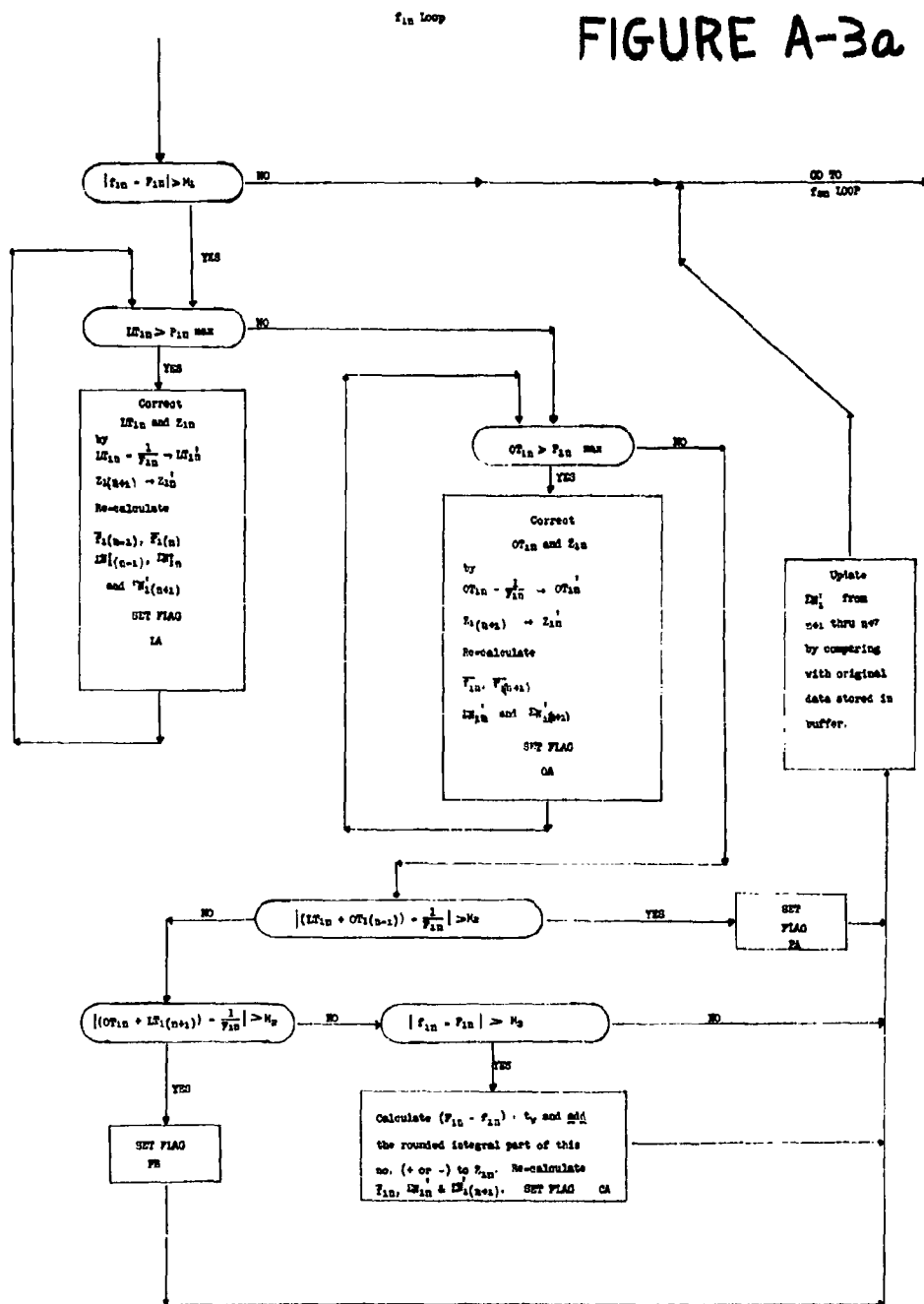
The actual checks accomplished in the auto-edit can then best be described by a flow diagram. This is done in Figures A-3a through A-3c.

At this point in the data processing, we have a reference distance vector defined at Space/Time times and an indicated acceleration vector (from the IMU) defined at VSA times. It is the job of the Arma integration program (#85) (Figure A-2c) to integrate the VSA output to the distance level and then interpolate the resulting time series to S/T times. The first integration (from acceleration to velocity) takes the form of a pure summation taking advantage of the built-in error cancelling effects already described. The next integration step is accomplished using a Simpson's rule integration. It is fairly easy to show that the truncation error associated with this step of integration is negligible. The interpolation to Space/Time times takes the form of a linear (straight line) interpolation between two VSA data points. This (or any other) interpolation scheme brings up the question of whether or not there could be significant vibration components over one-half of the sampling rate which lead to significant aliasing (foldover) errors. The answer in this case is no. The sampling rate on the VSA information is normally 250 samples/second, and the resultant velocity aliasing (over a bandwidth of D.C. to 3 cps) is less than .004 ft/sec. The corresponding distance aliasing is reduced even further by the integration from velocity to distance. To obtain this estimate one observes the VSA acceleration power spectral density and transforms this to the spectrum on the velocity and distance domains. The area under the curve ± 3 cycles about the sampling frequency gives the estimate involved.

The output of the Arma integration program (#85) (Figure A-2c) is the VSA indicated distance defined at S/T times for a single VSA. The outputs for the three VSA's are merged (using program #74) to form a system indicated distance vector. This vector is then compared with the S/T reference distance vector using the vector comparison program (#65).

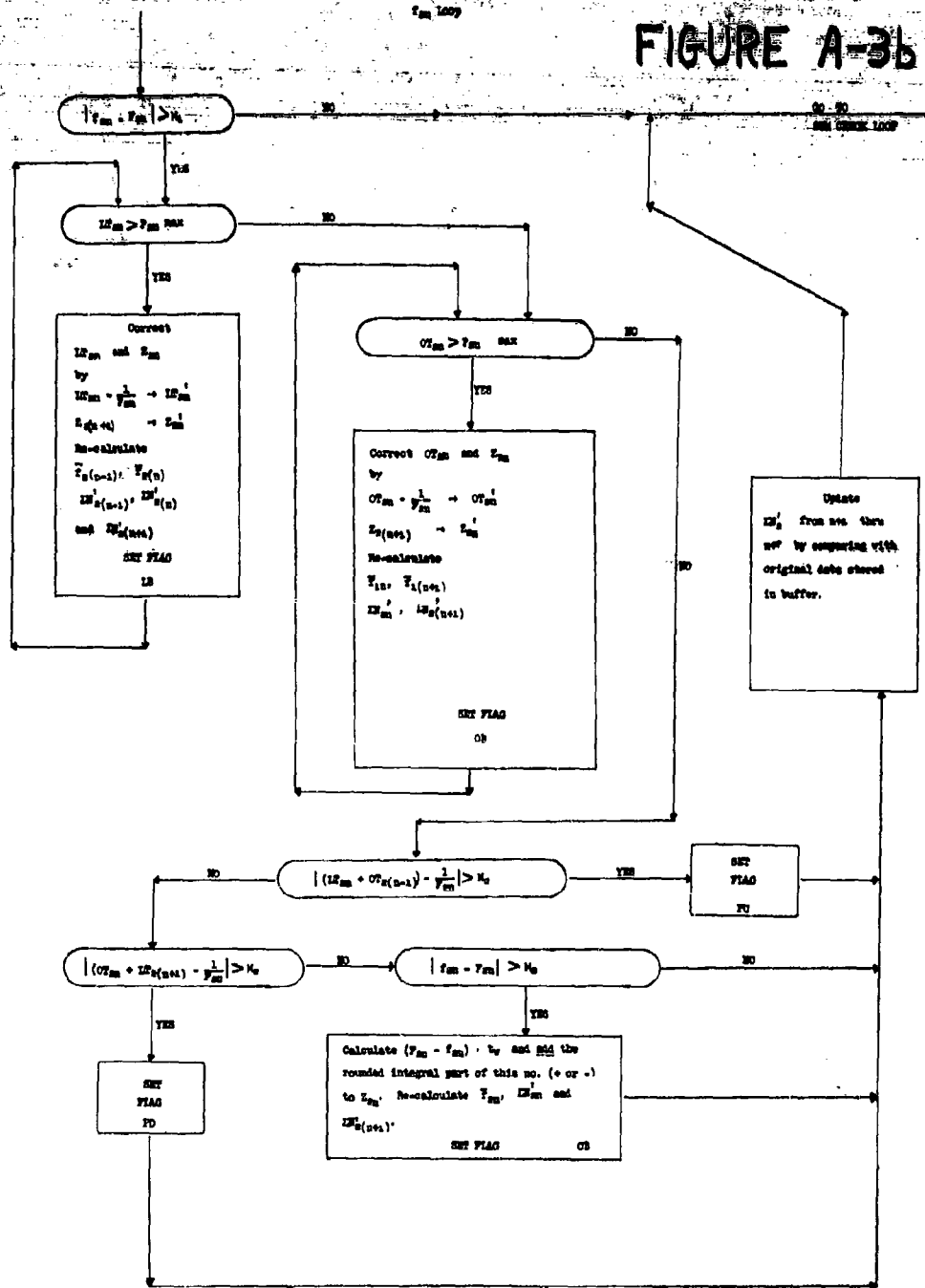
AUTOMATIC EDIT (FLOW DIAGRAM)

FIGURE A-3a



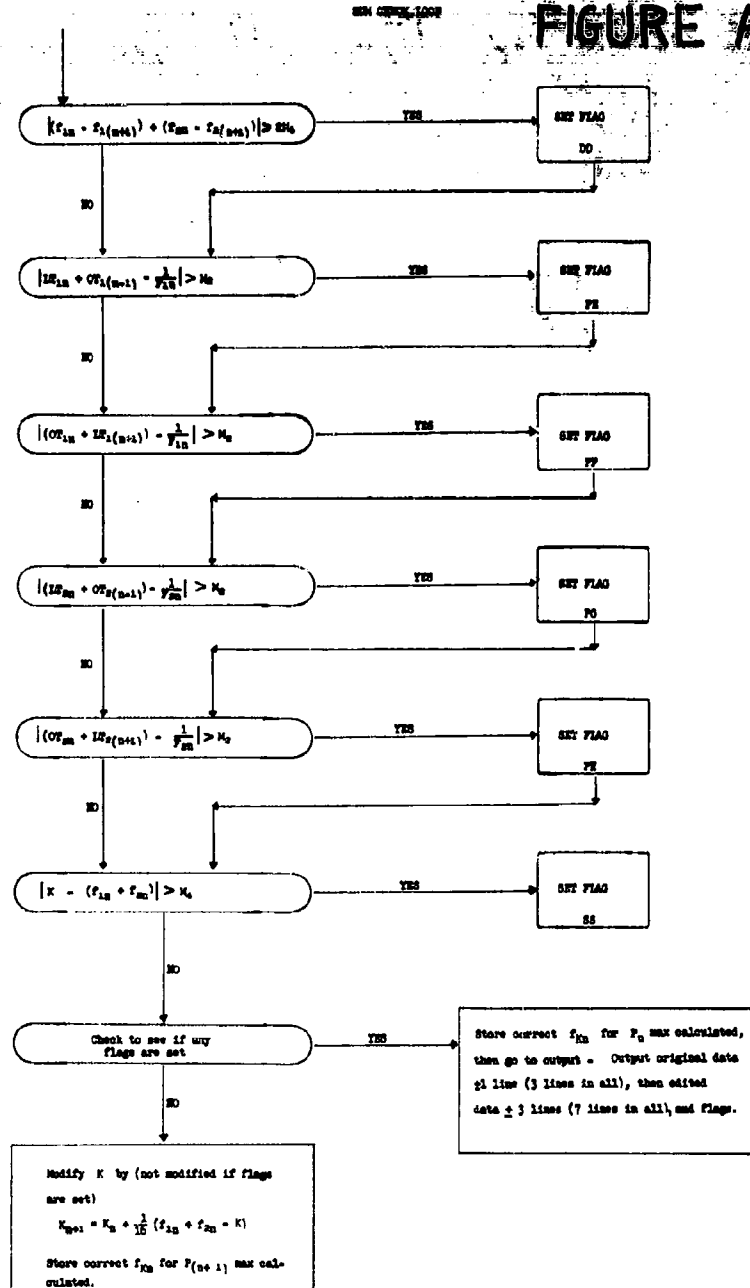
AUTOMATIC EDIT (FLOW DIAGRAM)

FIGURE A-3b



AUTOMATIC EDIT (FLOW DIAGRAM)

FIGURE A-3c



$$\vec{\Delta S} = \begin{Bmatrix} \Delta S_x \\ \Delta S_y \\ \Delta S_z \end{Bmatrix} = \vec{S}_{IMU} - \vec{S}_{S/T}$$

Although the present programming on this vector comparison and the computations leading to it are adequate for most purposes, they should be modified to reach the ultimate capabilities of the track as a reference system. Presently, 8 decimal place floating point arithmetic is being employed in the operations leading to the $\vec{\Delta S}$ comparison. When \vec{S}_{IMU} or $\vec{S}_{S/T}$ exceeds 10,000, there are only three significant places left behind the decimal point. This implies that we can only know the reference or indicated distance to the nearest .001 ft. Various schemes may be employed to remove this shortcoming, but it definitely should be removed.

The distance comparison ($\vec{\Delta S}$) then goes to the average derivative program (#86) which transforms it into a comparison of average velocities. The operation of program #86 is essentially to find the average derivative of the quantity it takes as an input with the averaging time (τ) inserted as a program parameter. In essence it operates on the $\vec{\Delta S}$ such that:

$$\frac{\Delta S(t_2) - \Delta S(t_1)}{t_2 - t_1} = \overline{\Delta V} \left(\frac{t_1 + t_2}{2} \right)$$

$$t_2 - t_1 \geq \tau$$

The program starts at one interrupter time t_1 , waits a time τ and picks up the next interrupter time as t_2 . That is, $t_2 - t_1 \geq \tau$. An option included in the program makes possible a series comparison wherein each old t_2 becomes the new t_1 for the next comparison interval; or a sliding comparison wherein the very next interrupter time after the old t_1 becomes the new t_1 for the next comparison. The choice of this optional feature may be exercised by the user.

The comparison of average velocities is then ready to be submitted to a regression analysis against our error model (sum or difference model for the VSA + other effects not due to the VSA). Before this regression analysis can be accomplished, however, the proper environmental coordinate functions must be generated and gathered together as inputs to the extended precision least squares compile and solve program (#177) (Figure A-2d). The operation of program #177 is such that it solves (in a least squares sense for the δK_j coefficients) an equation of the form:

$$\overline{\Delta V}_1 = \sum_{j=1}^n \delta K_j \phi_{j1}$$

where $\overline{\Delta V}_1$ = the average velocity error for the 1th observation interval

δK_j = the error coefficient related to the jth environmental coordinate function

ϕ_{j1} = the jth environmental coordinate function observed for the 1th interval

For the purposes of the Arma VEA analysis, the following environmental coordinate functions are required:

\bar{t} = average time, $\frac{t_1 + t_2}{2}$

$\bar{V} \Big|_{t_1}^{t_2}$ = average velocity in the interval t_1 to t_2

$\overline{\int A^2 dt} \Big|_{t_1}^{t_2}$ = average integral of squared acceleration in the interval t_1 to t_2

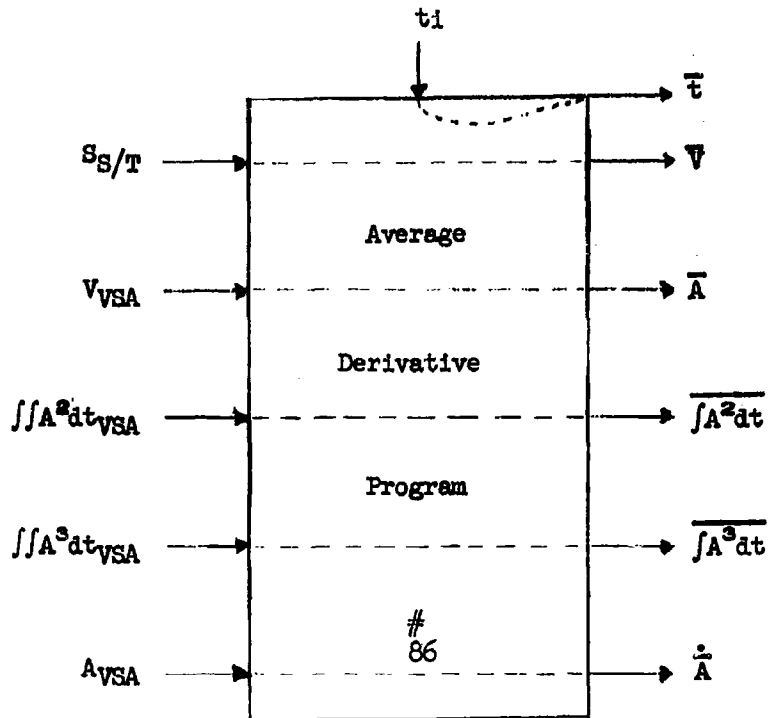
$\overline{\int A^3 dt} \Big|_{t_1}^{t_2}$ = average integral of cubed acceleration in the interval t_1 to t_2

$\bar{A} \Big|_{t_1}^{t_2}$ = average acceleration in the interval t_1 to t_2

$\dot{\bar{A}}$ = average derivative of acceleration (jerk) in the interval t_1 to t_2

The purpose of the coordinate function generator (program #84) is to provide the quantities $\int \int A^2 dt$, $\int \int A^3 dt$, and filtered or unfiltered A . The distance function comes from the S/T velocity vector program (#61),

and the velocity function comes from the Arma integration program (#85). These are merged and put through the average derivative program to obtain the coordinate functions required as shown below:



These coordinate functions are then merged with the $\overline{\Delta V}$ and taken to the compile and solve program (#177) for the least squares regression analysis (Figure A-2d).

Program #49 functions to generate the best estimate of the residuals from the least squares fit and a best estimate of the fit itself. These quantities may be plotted if desired.

The above discussion presumes that the $\overline{\Delta V}$ as generated is a true indication of VSA effects plus other effects which are describable in terms of a coordinate function of our error model. This is not always the case and the $\overline{\Delta V}$ must sometimes be adjusted by some arbitrary amount to take out a known error in its measurement. This is the function of programs #12 and #13. An analog tape containing the time history of the correction to

be applied is fed to program #12. There it is digitized and placed on tape in digital format. Program #13 applies the correction quantity to the ΔV with the proper sign and magnitude and with time correlation. For the Arma analysis, this correction loop was used extensively to correct for a geometrically induced rectification error known at HAFB as coherent oscillation. (See Appendix A-12 for a more complete description of this error source and treatment.)

Figure A-2e shows the digital program structure for the pre- and post-run evaluations. These evaluations are made within a few seconds of the actual sled run, and establish a majority of the initial and end conditions related to the sled run. The information used for these evaluations comes directly from the VSA's under test. The individual string frequencies are digitized (GIC) and a frequency computed (#14) for a period of approximately 100 seconds prior to first motion and 100 seconds after last motion. The pre- and post-run averaging program (#166) edits and averages this frequency information to give the average string frequencies (and their rates of change) during the pre- and post-run periods. Then program #189 (pre-run bias determination) takes the average string frequencies during pre-run and calculates the best estimate of VSA bias (K_0), just prior to first motion. Program #189 requires the known initial platform orientation information as an input. Program #162 (post-run drift evaluation) takes the average string frequencies and their rates of change during the post-run period and computes the best estimate of platform orientation and drift rate during the post-run. This information may be used to generate an average drift rate of the platform during the sled run. Only roll and pitch drift rates can be determined in this manner. Azimuth drift rate must be determined from other information such as the Y velocity (cross track) comparison.

Figure A-2f shows the digital program structure for the laboratory scalings of the IMU plus miscellaneous programs associated with the overall evaluation. The laboratory scaling programs are described in detail in the next section.

A-11 LABORATORY SCALING PROGRAMS

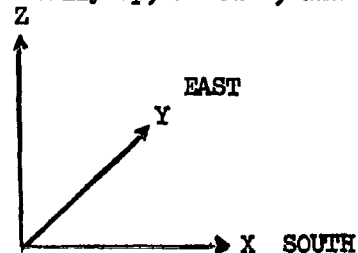
VSA Alignment and Calibration Positions

In order to measure the VSA scale factors and bias (zero offset) values as well as to determine the actual orientations of the input axes of the instruments as mounted on the IMU, a laboratory alignment and calibration routine was established as outlined below. In addition, the information gathered during this laboratory test provided a way of measuring approximate values of the VSA non-linearities which agreed remarkably well with the values provided by the centrifuge testing accomplished at the Arma plant.

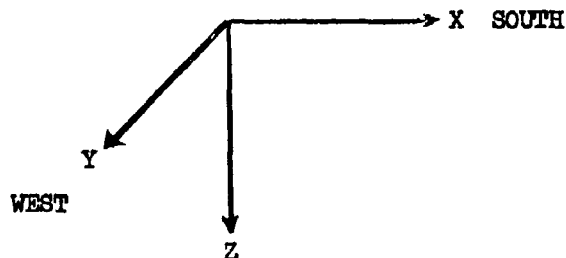
The reference coordinate system for the IMU is established by a cube fastened to the platform with the X axis, Y axis, and Z axis being perpendicular to visible faces of this cube. The coordinate system is right-handed and taken to be orthogonal. Actual deviation of the cube faces from orthogonality is less than two arc seconds (as specified by the platform department optical group of the Arma plant). As a result, the non-orthogonality of the cube faces may be ignored. During the laboratory test sequence, the platform is aligned in six different positions such that the positive and negative axes for X, Y, and Z are essentially straight up. The accuracy of positioning is determined by optically monitoring the cube faces using two pre-leveled (level reference = Davidson pendulous mirror ± 2 arc sec) Wild T3 autocollimators whose optical axes are 90° apart in the level plane.

The orientations used for the alignment check and calibration are numbered from one through six. They may be listed as:

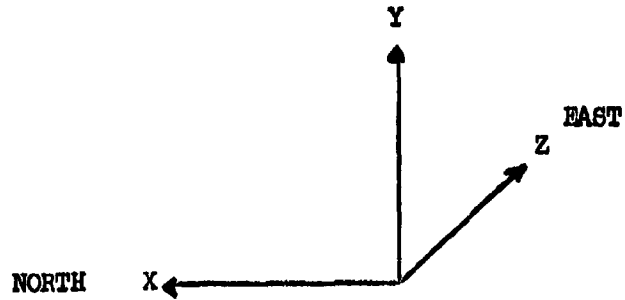
1. Position one: Z vertically up, X south, and Y east.



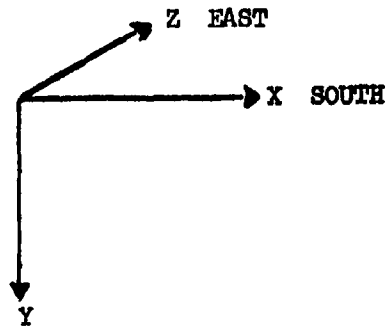
2. Position two: Z vertically down, X south, and Y west.



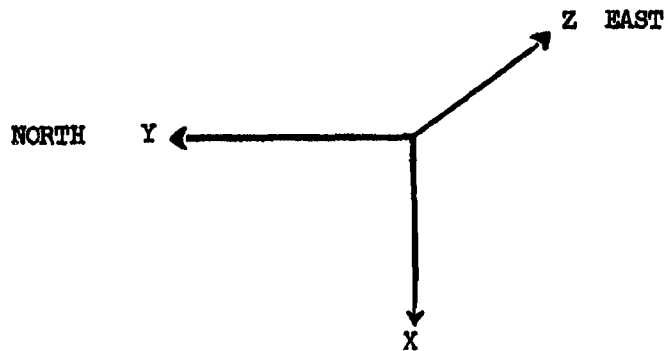
3. Position three: Y vertically up, X north, and Z east.



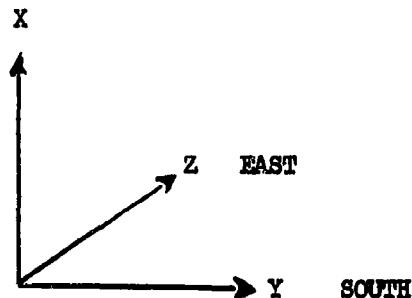
4. Position four: Y vertically down, X south, and Z east.



5. Position five: X vertically down, Y north, and Z east.



6. Position six: X vertically up, Y south, and Z east.



It should be pointed out that the north-south reference line is not exactly north and south in its direction, but this fact does not play any significant role until gyro drift measurements are considered. Therefore, this factor is ignored here.

By definition (at HAFB) we have stated that for the vibrating string accelerometer f_1 = the frequency of the string which undergoes increased tension when a positive acceleration is applied along the instrument's input axis. Thus, f_{1X} is the string of the X accelerometer which would be furthest downtrack during the sled run. As a consequence of this definition, f_2 = the frequency of the string which undergoes decreased tension when a positive acceleration is applied along the instrument's input axis. One of the first tasks to be accomplished in IMU laboratory testing is the tagging of the f_1 and f_2 strings for the X, Y, and Z accelerometers. This is easily accomplished by noting that if a given axis is pointed nearly straight up, the string with the higher frequency will be string #1. As a further consequence of this definition, we find that for track testing the signs of the zero offset (bias or K_0) term ($f_1 - f_2$) may differ from the signs provided by the manufacturer who based his definitions upon another set of criteria. The analytical models of accelerometer performance presented in section A-7 show that the changes in sign of the quadratic (K_2) nonlinearity will usually follow a change in sign associated with the bias (K_0) value and as such may also differ from the sign supplied by the manufacturer.

As previously stated, the platform is placed in positions one through six (though not necessarily in that order) through optical monitoring of the faces of the cube which is attached to the platform. The cube faces are used to define the nearly orthogonal platform reference axes X_p , Y_p , and Z_p . We consider each of the vibrating string accelerometers to have its input axis slightly misaligned with respect to the reference platform axes. The misalignments may be as large as one degree without materially affecting the results of the programs which follow.

Let λ_{ij} be defined as the misalignment angle of the i^{th} VSA (X, Y, or Z) about the j^{th} platform axis (X_p , Y_p , or Z_p). Thus, λ_{xy} is the misalignment

of the input axis of the X-VSA through having been rotated about the Y_p axis. If this number comes out negative, then the actual rotation (in the right-hand sense) was about the $-Y_p$ axis. In order to coordinate with definitions previously given by Arma and provide a little descriptive detail, the following equivalents are listed (without regard to proper sign polarity):

1. $|\lambda_{xy}| = |X_z| = \text{X-VSA misalignment in azimuth}$
2. $|\lambda_{xz}| = |X_y| = \text{X-VSA misalignment in pitch}$
3. $\lambda_{yx} = |Y_z| = \text{Y-VSA misalignment in azimuth}$
4. $\lambda_{yz} = |Y_x| = \text{Y-VSA misalignment in roll}$
5. $|\lambda_{zx}| = |Z_y| = \text{Z-VSA misalignment in pitch}$
6. $|\lambda_{zy}| = |Z_x| = \text{Z-VSA misalignment in roll}$

The size of the misalignment angles (up to 1°) has a lot to do with how complex the data reduction need be. The sine of one degree differs from the radian measure of one degree by less than an equivalent two tenths of a second of arc. Thus, we may safely presume $\sin \lambda = \lambda$. The cosine of one degree differs from one by one part in five thousand. This factor affects the scaling of the VSA. Consequently, we cannot assume $\cos \lambda = 1.0$. Under these conditions we note that any vector V in the platform coordinates is related (to the desired accuracy) to its projections into VSA coordinates by:

$$\begin{Bmatrix} V_{xVSA} \\ V_{yVSA} \\ V_{zVSA} \end{Bmatrix} = \begin{bmatrix} (\cos \lambda_{xy} \cos \lambda_{xz}) & (\lambda_{xz}) & (-\lambda_{xy}) \\ (-\lambda_{yz}) & (\cos \lambda_{yx} \cos \lambda_{yz}) & (\lambda_{yx}) \\ (\lambda_{zy}) & (-\lambda_{zx}) & (\cos \lambda_{zx} \cos \lambda_{zy}) \end{bmatrix} \begin{Bmatrix} V_{xp} \\ V_{yp} \\ V_{zp} \end{Bmatrix}$$

If we consider the various laboratory positions and the equivalent accelerations seen by the platform, we have the following input accelerations:

Position one

$$\begin{Bmatrix} 0 \\ 0 \\ +|g| \end{Bmatrix}$$

Position two

$$\begin{Bmatrix} 0 \\ 0 \\ -|g| \end{Bmatrix}$$

Position three

$$\begin{Bmatrix} 0 \\ +|g| \\ 0 \end{Bmatrix}$$

Position four

$$\begin{Bmatrix} 0 \\ -|g| \\ 0 \end{Bmatrix}$$

Position five

$$\begin{Bmatrix} -|g| \\ 0 \\ 0 \end{Bmatrix}$$

Position six

$$\begin{Bmatrix} +|g| \\ 0 \\ 0 \end{Bmatrix}$$

If we then designate the acceleration seen by the i^{th} VSA in the j^{th} position by A_{ij} we note:

$$A_{x1} = -\lambda_{xy} |g|$$

$$A_{y1} = +\lambda_{yx} |g|$$

$$A_{z1} = \cos \lambda_{zx} \cos \lambda_{zy} |g|$$

$$A_{x3} = +\lambda_{xz} |g|$$

$$A_{y3} = \cos \lambda_{yx} \cos \lambda_{yz} |g|$$

$$A_{z3} = -\lambda_{zx} |g|$$

$$A_{x5} = -\cos \lambda_{xy} \cos \lambda_{xz} |g|$$

$$A_{y5} = +\lambda_{yz} |g|$$

$$A_{z5} = -\lambda_{zy} |g|$$

$$A_{x2} = +\lambda_{xy} |g|$$

$$A_{y2} = -\lambda_{yx} |g|$$

$$A_{z2} = -\cos \lambda_{zx} \cos \lambda_{zy} |g|$$

$$A_{x4} = -\lambda_{xz} |g|$$

$$A_{y4} = -\cos \lambda_{yx} \cos \lambda_{yz} |g|$$

$$A_{z4} = +\lambda_{zx} |g|$$

$$A_{x6} = \cos \lambda_{xy} \cos \lambda_{xz} |g|$$

$$A_{y6} = -\lambda_{yz} |g|$$

$$A_{z6} = +\lambda_{zy} |g|$$

The value of $|g|$ for the laboratory installation is given as 32.12437 ft/sec².

Regular Scaling

The scaling and alignment check of the accelerometers may be accomplished on the basis of a "difference model" which states:

$$\Delta f = f_1 - f_2 = K_0 + K_1 A + K_2 A^2 + K_3 A^3$$

It may also be accomplished according to a "sum model" which states:

$$A = \beta \cdot \Delta f \cdot \Sigma f - \gamma$$

$$= \beta(f_1^2 - f_2^2) - \gamma$$

where A = input acceleration (gravity component)

β , γ , K_0 and K_1 are constants to be determined by the scaling technique.

K_2 and K_3 are constants which should be considered if their effects become important.

Designating Δf_{ij} as the difference frequency ($f_1 - f_2$) for the i^{th} VSA (x , y , or z) in the j^{th} position (1 through 6) we may write:

$$\Delta f_{xj} = K_{0x} + K_{1x} A_{xj} + K_{2x}(A_{xj})^2 + K_{3x}(A_{xj})^3$$

$$\Delta f_{yj} = K_{0y} + K_{1y} A_{yj} + K_{2y}(A_{yj})^2 + K_{3y}(A_{yj})^3$$

$$\Delta f_{zj} = K_{0z} + K_{1z} A_{zj} + K_{2z}(A_{zj})^2 + K_{3z}(A_{zj})^3$$

We examine these equations in detail and use the + and - 1 g positions to determine scale factor (K_1) and zero offset (K_0), while utilizing the zero g positions for misalignment determinations. The following equations can be written (assuming the parameters $K_0 \rightarrow K_3$ remain constant):

X-VSA

$$\frac{|\Delta f_{xs}| + |\Delta f_{xe}|}{2} = + K_{1x} (\cos \lambda_{xy} \cos \lambda_{xz} |g|) + K_{3x} (\cos \lambda_{xy} \cos \lambda_{xz} |g|)^3$$

$$\frac{|\Delta f_{xe}| - |\Delta f_{xs}|}{2} = + K_{0x} + K_{2x} (\cos \lambda_{xy} \cos \lambda_{xz} |g|)^2$$

$$\frac{(\Delta f_{xs} - \Delta f_{xe})}{2} = K_{1x} (\lambda_{xz} |g|) + K_{3x} (\lambda_{xz} |g|)^3$$

$$\frac{(\Delta f_{xe} - \Delta f_{xs})}{2} = K_{1x} (\lambda_{xy} |g|) + K_{3x} (\lambda_{xy} |g|)^3$$

Note that the last two equations need to take cognizance of the signs of Δf_x which will be plus for a given position if $f_{1x} > f_{2x}$ and negative otherwise.

Y-VSA

$$\frac{|\Delta f_{ys}| + |\Delta f_{ye}|}{2} = K_{1y} (\cos \lambda_{yx} \cos \lambda_{yz} |g|) + K_{3y} (\cos \lambda_{yx} \cos \lambda_{yz} |g|)^3$$

$$\frac{|\Delta f_{y3}| - |\Delta f_{y4}|}{2} = K_{0y} + K_{zy} (\cos \lambda_{yx} \cos \lambda_{yz} |g|)^2$$

$$\frac{(\Delta f_{y1} - \Delta f_{y2})}{2} = K_{1y} (\lambda_{yx} |g|) + K_{3y} (\lambda_{yx} |g|)^3$$

$$\frac{(\Delta f_{y5} - \Delta f_{y6})}{2} = K_{1y} (\lambda_{yz} |g|) + K_{3y} (\lambda_{yz} |g|)^3$$

Note that the last two equations need to take cognizance of the signs of Δf_y which will be plus for a given position if $f_{1y} > f_{2y}$ and negative otherwise.

Z-VSA

$$\frac{|\Delta f_{z1}| + |\Delta f_{z2}|}{2} = K_{1z} (\cos \lambda_{zx} \cos \lambda_{zy} |g|) + K_{3z} (\cos \lambda_{zx} \cos \lambda_{zy} |g|)^3$$

$$\frac{|\Delta f_{z1}| - |\Delta f_{z2}|}{2} = K_{0z} + K_{2z} (\cos \lambda_{zx} \cos \lambda_{zy} |g|)^2$$

$$\frac{(\Delta f_{z4} - \Delta f_{z3})}{2} = K_{1z} (\lambda_{zx} |g|) + K_{3z} (\lambda_{zx} |g|)^3$$

$$\frac{(\Delta f_{z6} - \Delta f_{z5})}{2} = K_{1z} (\lambda_{zy} |g|) + K_{3z} (\lambda_{zy} |g|)^3$$

Note that the last two equations need to take cognizance of the signs of Δf_z which will be plus for a given position if $f_{1z} > f_{2z}$ and negative otherwise.

In addition to the above, we may write the following redundant information equations:

X-VSA

$$\frac{(\Delta f_{x3} + \Delta f_{x4})}{2} = K_{0x} + K_{2x} (\lambda_{xz} |g|)^2$$

$$\frac{(\Delta f_{x1} + \Delta f_{x2})}{2} = K_{0x} + K_{2x} (\lambda_{xy} |g|)^2$$

Y-VSA

$$\frac{(\Delta f_{y1} + \Delta f_{y2})}{2} = K_{0y} + K_{2y} (\lambda_{yx} |g|)^2$$

$$\frac{(\Delta f_{y3} + \Delta f_{y4})}{2} = K_{0y} + K_{2y} (\lambda_{yz} |g|)^2$$

Z-VSA

$$\frac{(\Delta f_{z3} + \Delta f_{z4})}{2} = K_{0z} + K_{2z} (\lambda_{zx} |g|)^2$$

$$\frac{(\Delta f_{z5} + \Delta f_{z6})}{2} = K_{0z} + K_{2z} (\lambda_{zy} |g|)^2$$

Note that all of the redundant equations require the use of a signed difference frequency which is plus if $f_1 > f_2$ in a given position. Polarity is very important in these equations. Note also that each of the above redundant equations should yield results identical to the + and - 1 g scalings if the laboratory procedure is properly carried out and the parameters K_0 through K_3 are truly constant.

Similarly, we can write equations for the scaling of the VSA's according to the sum model. The required β and γ values can be obtained simply by placing the platform in a minimum of two different known positions in the one g field and measuring Δf and Σf for these positions. In order to make use of as much of the available data as possible, however, we used the measurements taken in all six positions for each accelerometer and found β and γ in a least squares sense. We can list for the three accelerometers the following equations:

X-VSA

$$A_{x1} = -\lambda_{xy} |g| \quad = \beta_x \Delta f_{x1} \Sigma f_{x1} - \gamma_x$$

$$A_{x2} = +\lambda_{xy} |g| \quad = \beta_x \Delta f_{x2} \Sigma f_{x2} - \gamma_x$$

$$A_{x3} = +\lambda_{xz} |g| \quad = \beta_x \Delta f_{x3} \Sigma f_{x3} - \gamma_x$$

$$A_{x4} = -\lambda_{xz} |g| \quad = \beta_x \Delta f_{x4} \Sigma f_{x4} - \gamma_x$$

$$A_{x5} = -\cos \lambda_{xy} \cos \lambda_{xz} |g| = \beta_x \Delta f_{x5} \Sigma f_{x5} - \gamma_x$$

$$A_{x6} = \cos \lambda_{xy} \cos \lambda_{xz} |g| = \beta_x \Delta f_{x6} \Sigma f_{x6} - \gamma_x$$

Y-VSA

$$A_{y1} = \lambda_{yx} |g| = \beta_y \Delta f_{y1} \Sigma f_{y1} - \gamma_y$$

$$A_{y2} = -\lambda_{yx} |g| = \beta_y \Delta f_{y2} \Sigma f_{y2} - \gamma_y$$

$$A_{y3} = \cos \lambda_{yx} \cos \lambda_{yz} |g| = \beta_y \Delta f_{y3} \Sigma f_{y3} - \gamma_y$$

$$A_{y4} = -\cos \lambda_{yx} \cos \lambda_{yz} |g| = \beta_y \Delta f_{y4} \Sigma f_{y4} - \gamma_y$$

$$A_{y5} = \lambda_{yz} |g| = \beta_y \Delta f_{y5} \Sigma f_{y5} - \gamma_y$$

$$A_{y6} = -\lambda_{yz} |g| = \beta_y \Delta f_{y6} \Sigma f_{y6} - \gamma_y$$

Z-VSA

$$A_{z1} = \cos \lambda_{zx} \cos \lambda_{zy} |g| = \beta_z \Delta f_{z1} \Sigma f_{z1} - \gamma_z$$

$$A_{z2} = -\cos \lambda_{zx} \cos \lambda_{zy} |g| = \beta_z \Delta f_{z2} \Sigma f_{z2} - \gamma_z$$

$$A_{z3} = -\lambda_{zx} |g| = \beta_z \Delta f_{z3} \Sigma f_{z3} - \gamma_z$$

$$A_{z4} = +\lambda_{zx} |g| = \beta_z \Delta f_{z4} \Sigma f_{z4} - \gamma_z$$

$$A_{z5} = -\lambda_{zy} |g| = \beta_z \Delta f_{z5} \Sigma f_{z5} - \gamma_z$$

$$A_{z6} = +\lambda_{zy} |g| = \beta_z \Delta f_{z6} \Sigma f_{z6} - \gamma_z$$

In a least squares fit over N points of an observation (V) to an independent variable (T) such that $V_1 = C_0 + C_1 T_1$, we find that our normal equations become:

$$\begin{bmatrix} N & \sum_{i=1}^N T_i \\ \sum_{i=1}^N T_i & \sum_{i=1}^N T_i^2 \end{bmatrix} \begin{Bmatrix} C_0 \\ C_1 \end{Bmatrix} = \begin{Bmatrix} \sum_{i=1}^N V_i \\ \sum_{i=1}^N V_i T_i \end{Bmatrix}$$

The solution to these normal equations yields:

$$C_1 = \frac{N \sum_{i=1}^N T_i V_i - \sum_{i=1}^N T_i \sum_{i=1}^N V_i}{N \sum_{i=1}^N T_i^2 - \left(\sum_{i=1}^N T_i \right)^2}$$

and

$$C_0 = \frac{\sum_{i=1}^N V_i - C_1 \sum_{i=1}^N T_i}{N}$$

We note that for the case at hand, $\sum_{i=1}^N V_i \equiv 0$.

This reduces the above solutions to:

$$C_1 = \frac{N \sum_{i=1}^N T_i V_i}{N \sum_{i=1}^N T_i^2 - \left(\sum_{i=1}^N T_i \right)^2}$$

$$C_0 = \frac{-C_1 \sum_{i=1}^N T_i}{N}$$

Thus we may write for the j th VSA ($j = x, y, \text{ or } z$)

$$\beta_j = \frac{6 \sum_{i=1}^6 (\Delta f_{ji} \Sigma f_{ji}) A_{ji}}{6 \sum_{i=1}^6 (\Delta f_{ji} \Sigma f_{ji})^2 - \left(\sum_{i=1}^6 \Delta f_{ji} \Sigma f_{ji} \right)^2}$$

$$\gamma_j = \frac{+ \beta_j \left(\sum_{i=1}^6 \Delta f_{ji} \Sigma f_{ji} \right)}{6}$$

In order to solve these equations for the required β_j and γ_j values, we need to know the following quantities:

$\lambda_{xy}, \lambda_{xz}, \lambda_{yx}, \lambda_{yz}, \lambda_{zx},$ and λ_{zy}

$$|g| = 32.12437 \text{ ft/sec}^2$$

$\Delta f_{x1}, \Delta f_{x2}, \Delta f_{x3}, \Delta f_{x4}, \Delta f_{x5},$ and Δf_{x6}

$\Delta f_{y1}, \Delta f_{y2}, \Delta f_{y3}, \Delta f_{y4}, \Delta f_{y5},$ and Δf_{y6}

$\Delta f_{z1}, \Delta f_{z2}, \Delta f_{z3}, \Delta f_{z4}, \Delta f_{z5},$ and Δf_{z6}

$\Sigma f_{x1}, \Sigma f_{x2}, \Sigma f_{x3}, \Sigma f_{x4}, \Sigma f_{x5},$ and Σf_{x6}

$\Sigma f_{y1}, \Sigma f_{y2}, \Sigma f_{y3}, \Sigma f_{y4}, \Sigma f_{y5},$ and Σf_{y6}

$\Sigma f_{z1}, \Sigma f_{z2}, \Sigma f_{z3}, \Sigma f_{z4}, \Sigma f_{z5},$ and Σf_{z6}

All of the above quantities are available from the calculations made for the difference frequency model. The solutions for β_j and γ_j were programmed utilizing the 43 quantities listed above. The λ 's are in radians and the Δf 's and Σf 's are in cycles per second. The following relationships also hold:

$$\beta = \frac{\text{ft/sec}^2}{(\text{cps})^2} \quad \gamma = \text{ft/sec}^2 \quad |g| = 32.12437 \text{ ft/sec}^2$$

This is part of the program run for every laboratory scaling performed, and the results are utilized in the sum model for the actual sled run's evaluation. The rest of the regular scaling program is associated with the difference model and is used in a similar manner. This part of the program is described below.

Based upon the expected magnitudes of K_2 and K_3 for the various VSA's, we may make simplifying assumptions for the difference model which lead to the program described next.

Arma Sealing Program #178

Program Description for Operators

Input, 8 parameter cards, standard 6 fields

1. Parameter Card No. 1
Field 1: Input tag No. (decimal stated point)
Fields 2 - 6: Blank
2. Parameter Card No. 2 (decimal floating point)
Field 1: $\Delta f_{x1} = f_{1x} - f_{2x}$ for position 1
Field 2: $\Delta f_{x2} = \text{etc.}$
Field 3: Δf_{x3}
Field 4: Δf_{x4}
Field 5: Δf_{x5}
Field 6: Δf_{x6}
3. Parameter Card No. 3 (decimal floating point)
Field 1: Δf_{y1}
Field 2: Δf_{y2}
Field 3: Δf_{y3}
Field 4: Δf_{y4}
Field 5: Δf_{y5}
Field 6: Δf_{y6}
4. Parameter Card No. 4 (decimal floating point)
Field 1: Δf_{z1}
Field 2: Δf_{z2}

Field 3: Δf_{z3}

Field 4: Δf_{z4}

Field 5: Δf_{z5}

Field 6: Δf_{z6}

5. Parameter Card No. 5 (decimal floating point)

Field 1: Ef_{x1}

Field 2: Ef_{x2}

Field 3: Ef_{x3}

Field 4: Ef_{x4}

Field 5: Ef_{x5}

Field 6: Ef_{x6}

6. Parameter Card No. 6 (decimal floating point)

Field 1: Ef_{y1}

Field 2: Ef_{y2}

Field 3: Ef_{y3}

Field 4: Ef_{y4}

Field 5: Ef_{y5}

Field 6: Ef_{y6}

7. Parameter Card No. 7 (decimal floating point)

Field 1: Ef_{z1}

Field 2: Ef_{z2}

Field 3: Ef_{z3}

Field 4: Σf_{24}

Field 5: Σf_{25}

Field 6: Σf_{26}

8. Parameter Card No. 8 (decimal floating point)

Field 1: $\frac{K3X}{4}$

Field 2: $\frac{K3Y}{4}$

Field 3: $\frac{K3Z}{4}$

Fields 4 - 6: Blank

Note: As many runs as required may be submitted at the same time; the sets of cards are stacked together. It is not necessary for the sets to be separated by blank cards.

Program Stop: A zero card, placed behind the last set of cards, is required to stop the program.

1. Zero Card

Field 1: Zero (decimal stated point)

Fields 2 - 6: Blank

Output: Two high speed printer listings

1. Listing of input data and tag number. Under the headline F is the listing of the data from parameter cards 2 through 4. Under the headline SUMF is the listing of the data from parameter cards 5 through 7.
2. Results of computation. The 42 quantities computed are printed out with an identifying headline for each.
3. Four sets of answers per run are printed out.

Running time: 15 seconds/set

Restrictions: None

Additional Programming and Operating Information:

Subroutines used: HOXS11, MIDAL1, RWSCF4, HOFSL1.

Space required: 1433₆ cells plus subroutines

Status: Machine checked

Operating instructions: Program tape → U3, PL(3,033),
floating point used.

Calculations

$$1. K_{OXA} = \frac{\Delta f_{x3} + \Delta f_{x4}}{2} \text{ (cps)}$$

$$K_{OXB} = \frac{\Delta f_{x1} + \Delta f_{x2}}{2} \text{ (cps)}$$

$$K_{OXC} = \frac{|\Delta f_{x3}| - |\Delta f_{x4}|}{2} \text{ (cps)}$$

If the above three bias figures are within ± .002 cps of one another, find and store.

$$K_{OxAV} = \frac{K_{OXA} + K_{OXB} + K_{OXC}}{3} \text{ (cps)}$$

If they are not within ± .002 cps of one another, store

$$K_{OxAV} = K_{OXA} \text{ (cps)}$$

$$2. K_{OYA} = \frac{\Delta f_{y1} + \Delta f_{y2}}{2} \text{ (cps)}$$

$$K_{OYB} = \frac{\Delta f_{y3} + \Delta f_{y4}}{2} \text{ (cps)}$$

$$K_{OYC} = \frac{|\Delta f_{y3}| - |\Delta f_{y4}|}{2} \text{ (cps)}$$

If the above three bias figures are within ± .002 cps of one another, find and store

$$K_{OYAV} = \frac{K_{OYA} + K_{OYB} + K_{OYC}}{3} \quad (\text{cps})$$

If they are not within $\pm .002$ cps of one another, store

$$K_{OYAV} = \frac{K_{OYA} + K_{OYB}}{2} \quad (\text{cps})$$

$$3. \quad K_{OZA} = \frac{|\Delta f_{z1}| - |\Delta f_{z2}|}{2} \quad (\text{cps})$$

$$K_{OZB} = \frac{(\Delta f_{z5} + \Delta f_{z6})}{2} \quad (\text{cps})$$

$$K_{OZC} = \frac{(\Delta f_{z3} + \Delta f_{z4})}{2} \quad (\text{cps})$$

If the above three bias figures are within $\pm .002$ cps of one another, find and store

$$K_{OZAV} = \frac{K_{OZA} + K_{OZB} + K_{OZC}}{3} \quad (\text{cps})$$

If they are not within $\pm .002$ cps of one another, store

$$K_{OZAV} = K_{OZA} \quad (\text{cps})$$

$$4. \quad K_{1X(a)} = \frac{|\Delta f_{x5}| + |\Delta f_{x6}|}{64.24874}$$

$$\lambda_{xz(a)} = \frac{\Delta f_{x3} - \Delta f_{x4}}{(64.24874) K_{1X(a)}} \quad (\text{rad})$$

$$\lambda_{xy(a)} = \frac{\Delta f_{x2} - \Delta f_{x1}}{(64.24874) K_{1X(a)}} \quad (\text{rad})$$

$$\cos \lambda_{xz(a)} \cos \lambda_{xy(a)} = \tau_{ax}$$

$$K_{1X(b)} = \frac{|\Delta f_{x5}| + |\Delta f_{x6}|}{64.24874 \tau_{ax}} - \left(\frac{K_{ax}}{4}\right) (64.24874 \tau_{ax})^2$$

$$\lambda_{xz} = \frac{K_{1x}(a) \cdot \lambda_{xz}(a)}{K_{1x}(b)} \quad (\text{rad})$$

$$\lambda_{xy} = \frac{K_{1x}(a) \cdot \lambda_{xy}(a)}{K_{1x}(b)} \quad (\text{rad})$$

$$\cos \lambda_{xy} \cos \lambda_{xz} = \tau_{bx} = \text{TAUBX}$$

$$K_{1x} = \frac{|\Delta f_{xs}| + |\Delta f_{xs}|}{64.24874 \tau_{bx}} - \left(\frac{K_{3x}}{4}\right) (64.24874 \tau_{bx})^2 \quad \text{cps/ft/sec}^2$$

$$\lambda_{xz} \text{ in arc sec} = \lambda_{xz} \cdot (2.0626481 \times 10^{+5})$$

$$\lambda_{xy} \text{ in arc sec} = \lambda_{xy} \cdot (2.0626481 \times 10^{+5})$$

$$5. \quad K_{1y}(a) = \frac{|\Delta f_{ys}| + |\Delta f_{y4}|}{64.24874}$$

$$\lambda_{yx}(a) = \frac{\Delta f_{y1} + \Delta f_{y2}}{64.24874 K_{1y}(a)} \quad (\text{radians})$$

$$\lambda_{yz}(a) = \frac{(\Delta f_{y5} - \Delta f_{y6})}{64.24874 K_{1y}(a)} \quad (\text{radians})$$

$$\cos \lambda_{yx}(a) \cos \lambda_{yz}(a) = \tau_{ay}$$

$$K_{1y}(b) = \frac{|\Delta f_{ys}| + |\Delta f_{y4}|}{64.24874 \tau_{ay}} - \left(\frac{K_{3y}}{4}\right) (64.24874 \tau_{ay})^2$$

$$\lambda_{yx} = \frac{\Delta f_{y1} - \Delta f_{y2}}{64.24874 K_{1y}(b)} \quad (\text{radians})$$

$$\lambda_{yz} = \frac{\Delta f_{y5} - \Delta f_{y6}}{64.24874 K_{1y}(b)} \quad (\text{radians})$$

$$\cos \lambda_{yx} \cos \lambda_{yz} = \tau_{by} = \text{TAUBY}$$

$$K_{1y} = \frac{|\Delta f_{ys}| + |\Delta f_{ya}|}{64.24874 \tau_{by}} - \left(\frac{K_{gy}}{4}\right) (64.24874 \tau_{by})^2 \text{ cps/ft/sec}^2$$

$$\lambda_{yx} \text{ in arc sec} = \lambda_{yx} \cdot (2.0626481 \times 10^{+5})$$

$$\lambda_{yz} \text{ in arc sec} = \lambda_{yz} \cdot (2.0626481 \times 10^{+5})$$

$$6. \quad K_{1z}(a) = \frac{|\Delta f_{z1}| + |\Delta f_{z2}|}{64.24874}$$

$$\lambda_{zx}(a) = \frac{\Delta f_{z4} - \Delta f_{z3}}{64.24874 K_{1z}(a)} \quad (\text{radians})$$

$$\lambda_{zy}(a) = \frac{\Delta f_{z6} - \Delta f_{z5}}{64.24874 K_{1z}(a)} \quad (\text{radians})$$

$$\cos \lambda_{zx}(a) \cos \lambda_{zy}(a) = \tau_{az}$$

$$K_{1z}(b) = \frac{|\Delta f_{z1}| + |\Delta f_{z2}|}{64.24874 \tau_{az}} - \left(\frac{K_{gz}}{4}\right) (64.24874 \tau_{az})^2$$

$$\lambda_{zx} = \frac{\Delta f_{z4} - \Delta f_{z3}}{64.24874 K_{1z}(b)} \quad (\text{radians})$$

$$\lambda_{zy} = \frac{\Delta f_{z6} - \Delta f_{z5}}{64.24874 K_{1z}(b)} \quad (\text{radians})$$

$$\cos \lambda_{zx} \cos \lambda_{zy} = \tau_{bz} = \tau_{aubz}$$

$$K_{1z} = \frac{|\Delta f_{z1}| + |\Delta f_{z2}|}{64.24874 \tau_{bz}} - \left(\frac{K_{gz}}{4}\right) (64.24874 \tau_{bz})^2$$

$$\lambda_{zx} \text{ in arc sec} = \lambda_{zx} (2.0626481 \times 10^{+5})$$

$$\lambda_{zy} \text{ in arc sec} = \lambda_{zy} (2.0626481 \times 10^{+5})$$

Having accomplished these calculations for the difference model, we now utilize some of them as inputs to the sum model calculations and calculate in a least squares sense

β_j and γ_j for $j = x, y,$ and z

as given in previous equations.

Program Printout - Regular Scaling

The program prints out the input parameters and tags on one page and the output on a second page. The second page consists of:

KOXA	KOXB	KOXC	KOXAV	cos λ_{xy}	cos λ_{xz}
KOYA	KOYB	KOYC	KOYAV	cos λ_{yx}	cos λ_{yz}
KOZA	KOZB	KOZC	KOZAV	cos λ_{zx}	cos λ_{zy}
$\lambda_{xy}(\text{rad})$	$\lambda_{xy}(\widehat{\text{sec}})$	$\lambda_{xz}(\text{rad})$	$\lambda_{xz}(\widehat{\text{sec}})$	KIX	TAUBX
$\lambda_{yx}(\text{rad})$	$\lambda_{yx}(\widehat{\text{sec}})$	$\lambda_{yz}(\text{rad})$	$\lambda_{yz}(\widehat{\text{sec}})$	KIY	TAUBY
$\lambda_{zx}(\text{rad})$	$\lambda_{zx}(\widehat{\text{sec}})$	$\lambda_{zy}(\text{rad})$	$\lambda_{zy}(\widehat{\text{sec}})$	KIZ	TAUBZ
BETA X	GAMMA X	BETA Y	GAMMA Y	BETA Z	GAMMA Z

Alternate Scaling Approach

Define f_{1j1} = the frequency of string one on the j^{th} VSA ($x, y,$ or z) in the 1^{th} calibration position.

Then f_{2j1} = the frequency of string two on the j^{th} VSA in the 1^{th} calibration position.

We can write the following equations:

$$f_{1x2} = f_{01x} \sqrt{1 - \tau_{1x} |g| \cos \lambda_{xy} \cos \lambda_{xz}}$$

$$f_{1x2} = f_{01x} \sqrt{1 + \tau_{1x} |g| \cos \lambda_{xy} \cos \lambda_{xz}}$$

$$f_{2x5} = f_{02x} \sqrt{1 + \tau_{2x} |g| \cos \lambda_{xy} \cos \lambda_{xz}}$$

$$f_{2x6} = f_{02x} \sqrt{1 - \tau_{2x} |g| \cos \lambda_{xy} \cos \lambda_{xz}}$$

$$f_{1y3} = f_{01y} \sqrt{1 + \tau_{1y} |g| \cos \lambda_{yx} \cos \lambda_{yz}}$$

$$f_{1y4} = f_{01y} \sqrt{1 - \tau_{1y} |g| \cos \lambda_{yx} \cos \lambda_{yz}}$$

$$f_{2y3} = f_{02y} \sqrt{1 - \tau_{2y} |g| \cos \lambda_{yx} \cos \lambda_{yz}}$$

$$f_{2y4} = f_{02y} \sqrt{1 + \tau_{2y} |g| \cos \lambda_{yx} \cos \lambda_{yz}}$$

$$f_{1z1} = f_{01z} \sqrt{1 + \tau_{1z} |g| \cos \lambda_{zx} \cos \lambda_{zy}}$$

$$f_{1z2} = f_{01z} \sqrt{1 - \tau_{1z} |g| \cos \lambda_{zx} \cos \lambda_{zy}}$$

$$f_{2z1} = f_{02z} \sqrt{1 - \tau_{2z} |g| \cos \lambda_{zx} \cos \lambda_{zy}}$$

$$f_{2z2} = f_{02z} \sqrt{1 + \tau_{2z} |g| \cos \lambda_{zx} \cos \lambda_{zy}}$$

These equations can be solved for τ 's and f_0 values as follows:

$$\tau_{1x} = \frac{1 - \left(\frac{f_{1x5}}{f_{1x6}}\right)^2}{1 + \left(\frac{f_{1x5}}{f_{1x6}}\right)^2} \cdot \frac{1}{|g| \cos \lambda_{xy} \cos \lambda_{xz}}$$

$$f_{01x} = \frac{\frac{f_{1x5}}{\sqrt{1 - \tau_{1x}|g| \cos \lambda_{xy} \cos \lambda_{xz}}} + \frac{f_{1x6}}{\sqrt{1 + \tau_{1x}|g| \cos \lambda_{xy} \cos \lambda_{xz}}}}{2}$$

$$\tau_{2x} = \frac{1 - \left(\frac{f_{2x6}}{f_{2x5}}\right)^2}{1 + \left(\frac{f_{2x6}}{f_{2x5}}\right)^2} \cdot \frac{1}{|g| \cos \lambda_{xy} \cos \lambda_{xz}}$$

$$f_{02x} = \frac{\frac{f_{2x5}}{\sqrt{1 - \tau_{2x} |g| \cos \lambda_{xy} \cos \lambda_{xz}}} + \frac{f_{2x6}}{\sqrt{1 + \tau_{2x} |g| \cos \lambda_{xy} \cos \lambda_{xz}}}}{2}$$

$$\tau_{1y} = \frac{1 - \left(\frac{f_{1y4}}{f_{1y3}}\right)^2}{1 + \left(\frac{f_{1y4}}{f_{1y3}}\right)^2} \cdot \frac{1}{|g| \cos \lambda_{yx} \cos \lambda_{yz}}$$

$$f_{01y} = \frac{\frac{f_{1y3}}{\sqrt{1 - \tau_{1y} |g| \cos \lambda_{yx} \cos \lambda_{yz}}} + \frac{f_{1y4}}{\sqrt{1 + \tau_{1y} |g| \cos \lambda_{yx} \cos \lambda_{yz}}}}{2}$$

$$\tau_{2y} = \frac{1 - \left(\frac{f_{2y5}}{f_{2y4}}\right)^2}{1 + \left(\frac{f_{2y5}}{f_{2y4}}\right)^2} \cdot \frac{1}{|g| \cos \lambda_{yx} \cos \lambda_{yz}}$$

$$f_{02y} = \frac{\frac{f_{2y4}}{\sqrt{1 - \tau_{2y} |g| \cos \lambda_{yx} \cos \lambda_{yz}}} + \frac{f_{2y5}}{\sqrt{1 + \tau_{2y} |g| \cos \lambda_{yx} \cos \lambda_{yz}}}}{2}$$

$$\tau_{1z} = \frac{1 - \left(\frac{f_{1z2}}{f_{1z1}}\right)^2}{1 + \left(\frac{f_{1z2}}{f_{1z1}}\right)^2} \cdot \frac{1}{|g| \cos \lambda_{zx} \cos \lambda_{zy}}$$

$$f_{01z} = \frac{\frac{f_{1z2}}{\sqrt{1 - \tau_{1z}} |g| \cos \lambda_{zx} \cos \lambda_{zy}} + \frac{f_{1z1}}{\sqrt{1 + \tau_{1z}} |g| \cos \lambda_{zx} \cos \lambda_{zy}}}{2}$$

$$\tau_{2z} = \frac{1 - \left(\frac{f_{2z1}}{f_{2z2}}\right)^2}{1 + \left(\frac{f_{2z1}}{f_{2z2}}\right)^2} \cdot \frac{1}{|g| \cos \lambda_{zx} \cos \lambda_{zy}}$$

$$f_{02z} = \frac{\frac{f_{2z1}}{\sqrt{1 - \tau_{2z}} |g| \cos \lambda_{zx} \cos \lambda_{zy}} + \frac{f_{2z2}}{\sqrt{1 + \tau_{2z}} |g| \cos \lambda_{zx} \cos \lambda_{zy}}}{2}$$

From these quantities we compute:

$$S\beta_x = \frac{1}{f_{01x}^2 \tau_{1x} + f_{02x}^2 \tau_{2x}} = \text{String or alternate } \beta_x \text{ value}$$

$$S\gamma_x = S\beta_x (f_{01x}^2 - f_{02x}^2)$$

$$S\beta_y = \frac{1}{f_{01y}^2 \tau_{1y} + f_{02y}^2 \tau_{2y}}$$

$$S\gamma_y = S\beta_y (f_{01y}^2 - f_{02y}^2)$$

$$S\beta_z = \frac{1}{f_{01z}^2 \tau_{1z} + f_{02z}^2 \tau_{2z}}$$

$$S\gamma_z = S\beta_z (f_{01z}^2 - f_{02z}^2)$$

We then compute:

$$K0X = f_{01x} - f_{02x}$$

$$K1X = \frac{f_{01x} \tau_{1x} + f_{02x} \tau_{2x}}{2}$$

$$K2X = \frac{f_{02x} \tau_{2x}^2 - f_{01x} \tau_{1x}^2}{8}$$

$$K3X = \frac{f_{01x} \tau_{1x}^3 + f_{02x} \tau_{2x}^3}{16}$$

$$K0Y = f_{01y} - f_{02y}$$

$$K1Y = \frac{f_{01y} \tau_{1y} + f_{02y} \tau_{2y}}{2}$$

$$K2Y = \frac{f_{02y} \tau_{2y}^2 - f_{01y} \tau_{1y}^2}{8}$$

$$K3Y = \frac{f_{01y} \tau_{1y}^3 + f_{02y} \tau_{2y}^3}{16}$$

$$K0Z = f_{01z} - f_{02z}$$

$$K1Z = \frac{f_{01z} \tau_{1z} + f_{02z} \tau_{2z}}{2}$$

$$K2Z = \frac{f_{02z} \tau_{2z}^2 - f_{01z} \tau_{1z}^2}{8}$$

$$K3Z = \frac{f_{01z} \tau_{1z}^3 + f_{02z} \tau_{2z}^3}{16}$$

In addition, for purposes of redundant checks, we compute:

$$\begin{aligned}
\Sigma f_{xs} &= f_{1xs} + f_{2xs} \\
SAf_{xs} &= f_{1xs} - f_{2xs} = \text{STRING } \Delta f_{xs} \\
\Sigma f_{xe} &= f_{1xe} + f_{2xe} \\
SAf_{xe} &= f_{1xe} - f_{2xe} \\
\Sigma f_{ys} &= f_{1ys} + f_{2ys} \\
SAf_{ys} &= f_{1ys} - f_{2ys} \\
\Sigma f_{ye} &= f_{1ye} + f_{2ye} \\
SAf_{ye} &= f_{1ye} - f_{2ye} \\
\Sigma f_{z1} &= f_{1z1} + f_{2z1} \\
SAf_{z1} &= f_{1z1} - f_{2z1} \\
\Sigma f_{z2} &= f_{1z2} + f_{2z2} \\
SAf_{z2} &= f_{1z2} - f_{2z2}
\end{aligned}$$

Alternate Scaling Program #179

Program Description for Operators

Purpose: This program computes a laboratory alignment check and scale factor determination for the Arma accelerometer using the individual string frequencies.

Usage:

Input: 4 parameter cards per run, standard 6 fields

1. Parameter Card No. 1

Field 1: Input tag No. (decimal stated point)

Fields 2 - 6: Blank

2. Parameter Card No. 2 (decimal floating point)

Field 1: λ_{xy}

Field 2: λ_{xz}

Field 3: λ_{yx}

Field 4: λ_{yz}

Field 5: λ_{zx}

Field 6: λ_{zy}

3. Parameter Card No. 3 (decimal floating point)

Field 1: f_{1xs}

Field 2: f_{2xs}

Field 3: f_{1xs}

Field 4: f_{2xs}

Field 5: f_{1ys}

Field 6: f_{2ys}

4. Parameter Card No. 4 (decimal floating point)

Field 1: f_{1y4}

Field 2: f_{2y4}

Field 3: f_{1z1}

Field 4: f_{2z1}

Field 5: f_{1z2}

Field 6: f_{2z2}

Note: As many runs as required may be submitted at the same time; the sets of cards are stacked together. It is not necessary for the sets to be separated by blank cards.

Program Stop: A zero card, placed behind the last set of cards, is required to stop the program.

1. Zero Card

Field 1: Zero (decimal stated point)

Fields 2 - 6: Blank

Output: Two high speed printer listings

1. Listing of input data and tag number. Under the headline IAMDAS is the listing of the data from parameter card 2. Under the headline F1S are the quantities f_{1xs} , f_{1ys} , f_{1z1} , f_{1z2} . Under the headline F2S are the quantities f_{2xs} , f_{2xe} , f_{2ys} , f_{2ye} , f_{2z1} , f_{2z2} .
2. Listing of answers. The 42 quantities computed are printed out with an identifying headline for each.
3. Four sets of answers per run are printed out.

Restrictions: None

Additional Programming and Operating Information:

Subroutines used: HOXS11, HOPS11, MID11, RWSGF4, RWSQF1

Space required: 1163₈ plus subroutines

Status: Machine checked

Operating Instructions: Program tape → U3, PL(3,044), floating point used

Program Print Out - Alternate Scaling

The program print out occupies two pages. The first page prints out the input parameters put into the program. The second page prints the output in the following format:

τ_{1x}	f_{01x}	τ_{2x}	f_{02x}	τ_{1y}	f_{01y}	τ_{2y}	f_{02y}
τ_{1z}	f_{01z}	τ_{2z}	f_{02z}	SB_x	SY_x	SB_y	SY_y
SB_z	SY_z	Σf_{xs}	Δf_{xs}	Σf_{ys}	Δf_{ys}	Σf_{zs}	Δf_{zs}
Σf_{ye}	Δf_{ye}	Σf_{z1}	Δf_{z1}	Σf_{z2}	Δf_{z2}	0	0

K0X	K1X	K2X	K3X	K0Y	K1Y	K2Y	K3Y
K0Z	K1Z	K2Z	K3Z	0	0	0	0

Input Data for Arma Sealing Programs

In addition to the minor errors made by the assumptions required to get the equations shown above, we must recognize measurement accuracy limitations. One of these limitations is associated with the determination of frequency. Frequency determination is accomplished by timing (with a 100 KC clock) the time interval associated with some whole number of periods of the signal of interest.

$$\text{Freq} = \frac{\# \text{ periods}}{\Delta \text{ time}} = \frac{\text{cycles}}{\text{sec}}$$

$$\text{Freq measured} = \frac{\# \text{ periods}}{\Delta t + \epsilon t}$$

$$\epsilon \text{ freq} = \frac{\# \text{ periods}}{\Delta t + \epsilon t} - \frac{\# \text{ periods}}{\Delta t}$$

$$\text{Relative } \epsilon \text{ freq} = \frac{\frac{\# \text{ periods}}{\Delta t + \epsilon t} - \frac{\# \text{ periods}}{\Delta t}}{\frac{\# \text{ periods}}{\Delta t}} = \frac{-\epsilon t}{\Delta t + \epsilon t}$$

$$|\text{Relative } \epsilon \text{ freq}| \approx \left| \frac{\epsilon t}{\Delta t} \right|$$

When the counter is operating properly, ϵt is two time counts or 20 μsec .

To keep the relative error in the frequency measurement low, Δt is taken to be at least 10 seconds. This corresponds to a 100,000 period count of the raw string frequencies, with an error of .02 cps. This is the reason for the requirement of the 100,000 period count capability on the laboratory equipment.

A 1,000 period count (approximately 17 seconds) should be used for scaling the difference frequency in the plus and minus one g field. This should introduce an error .00006 cps in the measurement. A 100 period count would have an error .0006 cps, but the extra counting length includes a comfortable margin of safety.

In the light of the above considerations, we take the measurements according to the data sheet below:

ARMA ALIGNMENT AND CALIBRATION DATA SHEET

Calibration Performed by _____ POSITION _____
 T3--West _____
 T3--North _____
 TIME START _____

Run Nr. _____
 Date _____

Data Taken by: _____

SKIN _____
 601 _____
 602 _____

X ACCELEROMETER Period Timing (Seconds)

READING	100,000	Xf_1	100,000	Xf_2	$(Xf_1 - Xf_2)$
1st	10.		10.		
2nd					
3rd					
Average					
Frequency					
Σf_x		Δf_x		Δ	

Y ACCELEROMETER Period Timing (Seconds)

Time	READING	100,000	Yf_1	100,000	Yf_2	$(Yf_1 - Yf_2)$	SKIN
	1st	10.		10.			
	2nd						601
	3rd						602
	Average						
	Frequency						
	Σf_y		Δf_y		Δ		

Z ACCELEROMETER Period Timing (Seconds)

READING	100,000	Zf_1	100,000	Zf_2	$(Zf_1 - Zf_2)$
1st	10.		10.		
2nd					
3rd					
Average					
Frequency					
Σf_z		Δf_z		Δ	

Time End _____

SKIN _____ 601 _____
 _____ 602 _____

A-12 COHERENT OSCILLATION OR SERVO ERROR, PLATFORM BALANCING

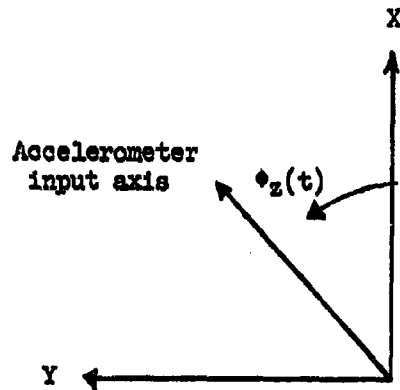
The goal in generating a reference quantity for accelerometer testing is to define what an "ideal accelerometer" undergoing the same environment as the actual accelerometer would indicate. This implies that if there are any conditions in the environment which could cause variations in the indications of "ideal instruments" we must consider them. In this discussion we limit ourselves to the dynamic environment defined by acceleration, its functions, their derivatives, and their integrals.

One of the obvious factors to consider is that an ideal instrument senses accelerations only along its input axis. In testing an accelerometer mounted on a stabilized platform, the orientation of the input axis with respect to some agreed upon coordinate system such as the tangent plane coordinates is rather accurately known. The only uncertainties associated with the orientation of such an instrument's input axis are: Initial alignment errors, unknown platform drifts, and dynamic misalignments caused by vibrations which get through the gimbal, gyro, servo system to affect the inner gimbal orientation.

By proper alignment and measurement techniques prior to first motion, the initial alignment errors may be made small enough to contribute a negligible amount to the reference quantity's error during a sled run.

If a platform is reasonably well balanced, and contains reasonably accurate gyros and correctly designed servos, the unknown gyro drifts during a sled run should not exceed a minute of arc about any axis. The downtrack accelerometers are affected only slightly by such small misalignments except in the case where the drift occurs about a pitch axis. A one minute misalignment in pitch which occurs at first motion and stays constant thereafter would give a velocity reference error of approximately $(.01 t)$ ft/sec, where t represents the time after first motion. Thus, for a 30 sec. sled run, this would mean a linear build up to approximately .3 ft/sec. velocity error at the end of the run. Such an error cannot be ignored.

The vibration induced errors are harder to estimate than the other errors because of the lack of knowledge of the environment which produces them. The physical phenomenon is simply a coherent angular oscillation coupled with a linear oscillation. Let, for example, this page represent the tangent plane with X (downtrack) pointed directly toward the top of the page. We will consider the effects of lateral vibrations coupled with angular oscillations of the platform in azimuth or about the Z axis.



The input acceleration as seen by the ideal accelerometer is given as

$$A_1(t) = \cos \phi_z(t) \cdot A_x(t) + \sin \phi_z(t) A_y(t)$$

Since the $\phi_z(t)$ value is always a small angle, we may approximate $\cos \phi_z(t)$ by 1.0 and $\sin \phi_z(t)$ by $\phi_z(t)$. Thus,

$$A_1(t) = A_x(t) + \phi_z(t) \cdot A_y(t)$$

If we take $A_1(t)$ as $A_x(t)$, we neglect the last term in the equation above. It is desirable to examine this term further. If this term is ignored, it becomes an error in the input acceleration, i.e.,

$$\phi_z(t) \cdot A_y(t) = \epsilon A_1(t)$$

The only practical method of evaluating the effect of $\epsilon \bar{A}_1$ during a sled run would appear to be on an analog computer where the product $\phi_z(t) \cdot A_y(t)$ could be formed and its integral taken to find the time history of the velocity error. For simplicity let us assume for the moment that a single sinusoidal oscillation occurs in both $\phi_z(t)$ and $A_y(t)$ (same frequency). Then the influence in ϵA_1 depends upon the phase relationship between the two oscillations

$$A_y(t) = A_y e^{j \omega t}, \quad \phi_z(t) = B_z e^{j \omega t + \theta}, \quad \epsilon \bar{A}_1 = A_y \cdot B_z \cdot \cos \theta$$

Letting: A_y be such that we have an rms g level of $1 \text{ g} \sim 32.2 \text{ ft/sec}^2$, ($A_y \approx 45 \text{ ft/sec}^2$), B_z be such that we have an rms ϕ_z level of 30 seconds

of arc or 1.5×10^{-4} radians ($B_z = 2.12 \times 10^{-4}$), and assuming complete coherence, i.e., $\cos \theta = 1.0$, we get

$$\bar{a}_1 = .95 \times 10^{-2} \text{ ft/sec}^2$$

Since this is the average error in acceleration over the interval, the built up error in velocity is equal to

$$eV = (.95) \times 10^{-2}t = (0.0095t) \text{ ft/sec.}$$

Obviously, errors of this magnitude which build up during a sled run cannot be ignored for fine grain analysis. This effect has been labelled "coherent oscillation" at HAFB. It might equally well be called "servo error," because it represents an error which can be minimized by a good tight servo design. Obviously, the most important factor contributing to this error is the degree of balancing of the inner gimbal structure of the IMU. If this balancing is not accomplished very carefully, the natural sled vibrations induce a coherent oscillation effect of excessive magnitude.

The major portion (over 90%) of the coherent oscillation effect can be removed from the data through the use of an appropriate analog computer calculation. The analog computer results are converted to digital form (see A-10) and applied to the velocity error data as a correction factor. The amount of residual error in this process depends upon the size of the coherent oscillation effect simulated. For a .1 ft/sec coherent oscillation effect (fairly significant value) the residual uncertainty in the analog computation runs about .01 ft/sec. The analog computer programming to accomplish this calculation will now be described.

The FM-FM signals to be used are the gyro roll, azimuth, and pitch angles (G_R , G_{AZ} , G_P) and the VSA accelerations downtrack, crosstrack, and vertically (A_x , A_y , and A_z). The primary phenomenon is vibrational in nature and any FM-FM subcarrier oscillator drifts will influence the overall answer if we do not filter the signals prior to calculating coherent oscillation effects. In addition, the gyro signals cannot be taken to represent the inner gimbal attitude directly since the pick-off point for these signals is not at the gyro, but in the servo loop. Let us define G_{AZ} , G_R , G_P to be the respective gyro signals after having been passed through compensational transfer functions which are the inverse of the servo transfer function characteristics. For azimuth and roll signals, this compensation is

$$\frac{(P + 587)(P + .32)}{(P + 40)(P + 4.7)}$$

For pitch this compensation is

$$\frac{(P + 423)(P + .29)}{(P + 35)(P + 3.5)}$$

These functions were obtained by independent tests at HAFB. They agree very closely with those values provided by Arma.

Let us now define G_{AZ}^* , G_R^* , G_P^* to be the compensated gyro signals (G') after having been passed through a high pass filter whose break point is 2.5 cycles/second. Similarly, let us define A_X^* , A_Y^* , and A_Z^* as the acceleration signals after having been passed through a high pass filter whose break point is 2.5 cycles/second. The required calculations are:

$$\begin{aligned} \text{X accelerometer effect} &= \int (A_Y^* \cdot G_{AZ}^*) dt + \int (A_Z^* \cdot G_P^*) dt \\ &\quad - \int (A_X^* \cdot G_P^* \cdot G_P^*) dt + \int (A_X^* \cdot G_{AZ}^* \cdot G_{AZ}^*) dt \end{aligned}$$

$$\text{Y accelerometer effect} = \int (A_X^* \cdot G_{AZ}^*) dt + \int (A_Z^* \cdot G_R^*) dt$$

$$\text{Z accelerometer effect} = \int (A_X^* \cdot G_P^*) dt + \int (A_Y^* \cdot G_R^*) dt$$

The last two terms in the X accelerometer effect account for the X thrust coupling of the Y and Z accelerometers when forced to rotate in azimuth and pitch respectively.

During phase two of the Arma sled test sequence the coherent oscillation effects were excessive in magnitude. A study of the magnitude versus the high pass filter used in the analog program showed that the effects were very strongly related to the platform shock-mount natural frequencies. This indicated that platform unbalance was the primary cause of this excessive coherent oscillation effect. The platform was subsequently balanced and the coherent oscillation effects became reasonable in magnitude.

The Simulation ProgramIntroduction

The evaluation processes to which the Vibrating String Accelerometer (VSA) data are subjected are quite complex and it is necessary to prove their validity. In particular, it is of interest to detect bias or trend errors because they may obscure the small systematic error of the accelerometer, the determination of which is one of the desired end products of guidance system sled tests. Such biases may arise from misconceptions in the design of the computer programs. An efficient way to determine any processing errors of a conceptual nature is a controlled experiment which subjects artificial data, a "test function," to the digital computer programs. The results obtained may be compared with the corresponding quantities from which the input data were derived. The difference between the original and the processed quantity is then the introduced error.

The purpose of this section is to describe the view points underlying the design of a digital program for producing artificial VSA data, and to explain their application in testing the evaluation programs. The inherent errors of the test function data, which must be made extremely small, are also presented.

Approach

Artificial data which will serve as a test function can be derived with a minimum of effort from a simplified function; i.e., a trigonometric function may be selected as an approximation of the sled acceleration profile. In this case, the theoretical value of the result of the evaluation process can be stated explicitly; however, a simplification of the actual profile may lead to wrong conclusions. It is more desirable to simulate practical data and to establish an empirical test function which closely resembles the actual profile of acceleration or velocity. This profile should faithfully represent dynamic effects such as rapidly changing acceleration and vibrations.

The problem of testing the entire evaluation process is more involved than can be seen from the above statements. In particular, the simulation of data is not restricted to the output data of the VSA themselves. The Space/Time (S/T) measuring system serves in the data reduction process as a precise position or velocity reference. Therefore, it is necessary that artificial data be prepared also to simulate the S/T data. An approach which was applied successfully in the past is chosen here again: The acceleration profile observed on the platform which carries the instruments to be tested is selected as original profile common to both the VSA and S/T data.

As outlined above, error free data processing can be proved by showing that the quantity

$$\Delta V = V_{VSA} - V_{true}$$

is sufficiently small over the entire sled run. V_{VSA} is the velocity indicated by the vibrating string accelerometer computed by the production program. For simplicity the assumed velocity is called here and hereafter V_{true} . Actually the S/T system serves as the reference. ΔV is computed as:

$$\Delta V = V_{VSA} - V_{S/T}$$

This difference is computed in a routine fashion by the production programs.

Numerical Statement of the Problem

To be simulated is the so-called difference model of the VSA, which is based on a binomial series approximation of the string frequency f :

$$f = f_0 \sqrt{1 - \tau a}$$

where a is sensed acceleration.

With the 3rd order term included, the equations of the two string frequencies become (Appendix A-7):

$$f_1 = f_{01} \left(1 + \frac{\tau_1 a}{2} - \frac{\tau_1^2 a^2}{8} + \frac{\tau_1^3 a^3}{16} \right)$$

$$f_2 = f_{02} \left(1 - \frac{\tau_2 a}{2} - \frac{\tau_2^2 a^2}{8} - \frac{\tau_2^3 a^3}{16} \right)$$

Given values for f_{01} , f_{02} , τ_1 , τ_2 , and a , we can compute f_1 and f_2 as a function of a (acceleration). The sampling rate which defined acceleration was 750 samples/second. The finally required quantities to simulate VSA performance are f_1 and f_2 . These quantities represent average frequencies over stated window times as defined in Appendix A-9. In order to determine these figures, the frequencies f_1 and f_2 must first be integrated. The physical meaning of these integrals is the total count of positive going zero crossings of the string vibration over the interval of integration. These quantities should be computed for the time sequence $t = 1t_w, 2t_w, 3t_w, 4t_w, \dots, 40.00$ seconds. (The original requirement of $t_w = 0.01$ sec for the output interval was changed later to 0.008 and 0.004 seconds. t_w is the window width.) The expressions for the average frequencies on the basis of $t_w = .01$ are:

$$\bar{f}_1 = \frac{1}{0.01} \int_t^{t+0.01} f_1 dt \quad \bar{f}_2 = \frac{1}{0.01} \int_t^{t+0.01} f_2 dt$$

The necessary precision of the computation process was defined by the requirement of using optimum scaling. If it was found that extended precision improved the result, extended precision should have been used.

Required Output Format

The quantities \bar{f}_1 , \bar{f}_2 , and the integrals of f_1 and f_2 were recorded on magnetic tape at multiples of t_w with a format equivalent to the output format of the production program, "Automatic Editing." This implies a scale-factor of 2^6 for all recorded data.

Requirement for Adjusted Rounding

The problem statement formulates this requirement as follows: Check the summation of frequency times interval length and adjust it so that it equals the original sum of zero crossings to within one round-off, i.e., at each step calculate

$$t_w \sum_{k=1}^n \bar{f}_{1k} \quad \text{and} \quad t_w \sum_{k=1}^n \bar{f}_{2k} \quad \text{and compare with}$$

$$\int_0^t f_1 dt \quad \text{and} \quad \int_0^t f_2 dt \quad \text{as previously computed.}$$

If these numbers differ by one (or more) binary bits, correct the last value of f_1 and f_2 computed so as to make these numbers coincide. This computation is really an insurance against later accumulation of round-off errors occurring in the \bar{f}_1 and \bar{f}_2 computation.

It is important to note that simulating the average frequencies as stated above does not mean that the output of VSA is simulated in its original form. The required format corresponds to the output of the second program in the sequence of the data evaluation process, the "Automatic Editing" program. This approach is chosen because the "String Reader" program and the "Automatic Editing" program are not expected to introduce any significant trend error. Simulating data in the format of the "String Reader" input would require a much higher sampling rate and consequently an essentially greater computational effort.

Computational Procedure

Acceleration Profile

The acceleration profile from run 3-5C was selected as typical from among the early phase II runs. While in the test functions developed for the Minuteman and Titan evaluation, the acceleration was measured by a commercial vibration accelerometer, in the present case the output of the precision string accelerometer itself is used for this purpose. To obtain the acceleration signal in analog form, the output of the string accelerometer has to be frequency-demodulated by an additional discrimination process. Figure A-4 is a strip chart of the telemetered tape recorded acceleration plotted with two time scales. The graph at the top shows well the dynamic effects during the boost phase in an expanded scale, with limitations set by the inertia of the recorder pen. Platform oscillations with the dominating natural frequency of about 12 cps can be seen. The curve below represents velocity as computed on an analog computer. This velocity function derived by analog computation serves only as qualitative information. The next two records below show the two profiles in a compressed time scale over the entire run.

Block Diagram

The above acceleration profile served as input (on FM-FM tape) to the processes and computations indicated by the blocks in Figure A-5. Two discriminators are necessary to produce the analog acceleration signal. The second discriminator is adjustable and had to be tuned quite carefully to avoid a bias of the center frequency which is equivalent to a bias of acceleration. The simulated velocity (V_{true}) differed from the actual sled velocity (from which the measurement was taken) by about 60 ft/sec at burnout, due to misadjustment and to non-linearities of the 2nd discriminator. This deviation is immaterial with regard to the objective of the simulation. Low pass filtering and digitizing are indicated by the next two blocks. During the sampling process a small error is made due to foldback. However, new frequency components caused by foldback and even DC drift have no bearing on the result of the analysis, because the digital data are declared as "true" data of acceleration. These data are then fed into the two branches of the actual simulation process. The branch for simulating VSA data shows two blocks; one for computing the string frequencies and one for integrating these frequencies. Provisions are made to change the parameters, f_{01} , f_{02} , T_1 , and T_2 and to set the nonlinear contributions $\int a^2 dt$ and $\int a^3 dt$ equal to zero.

Two integrations are performed in the branch for simulating S/T data. They yield sled-velocity and distance versus time and are referred to as "true" velocity and position. Since the S/T data represent

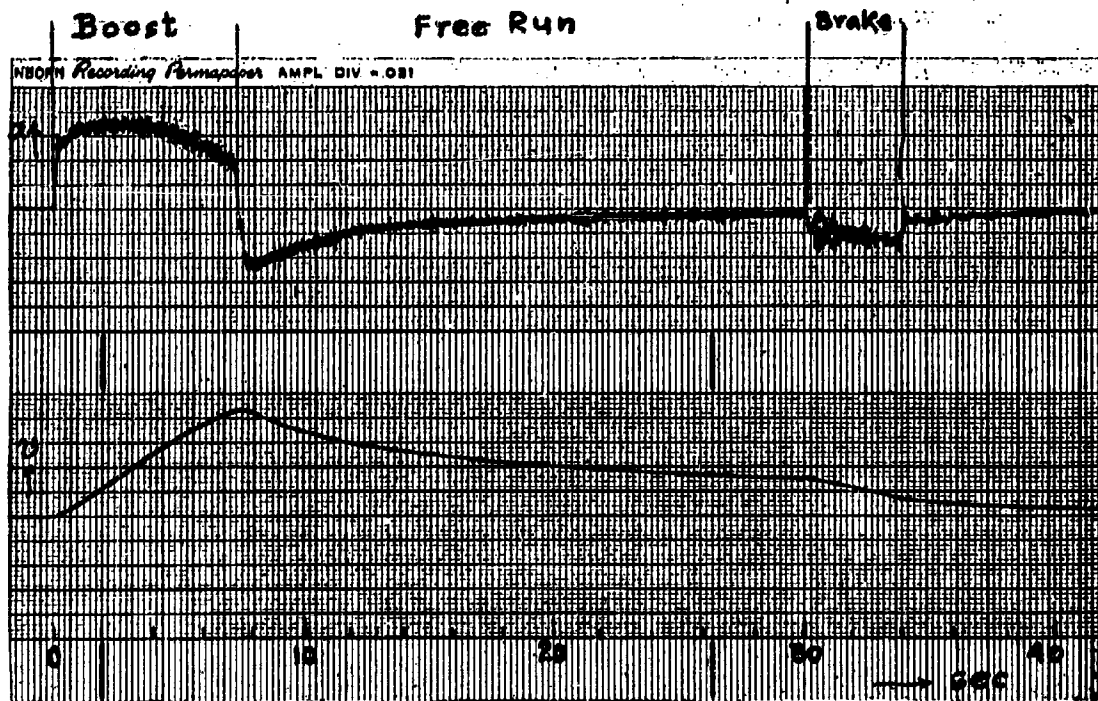
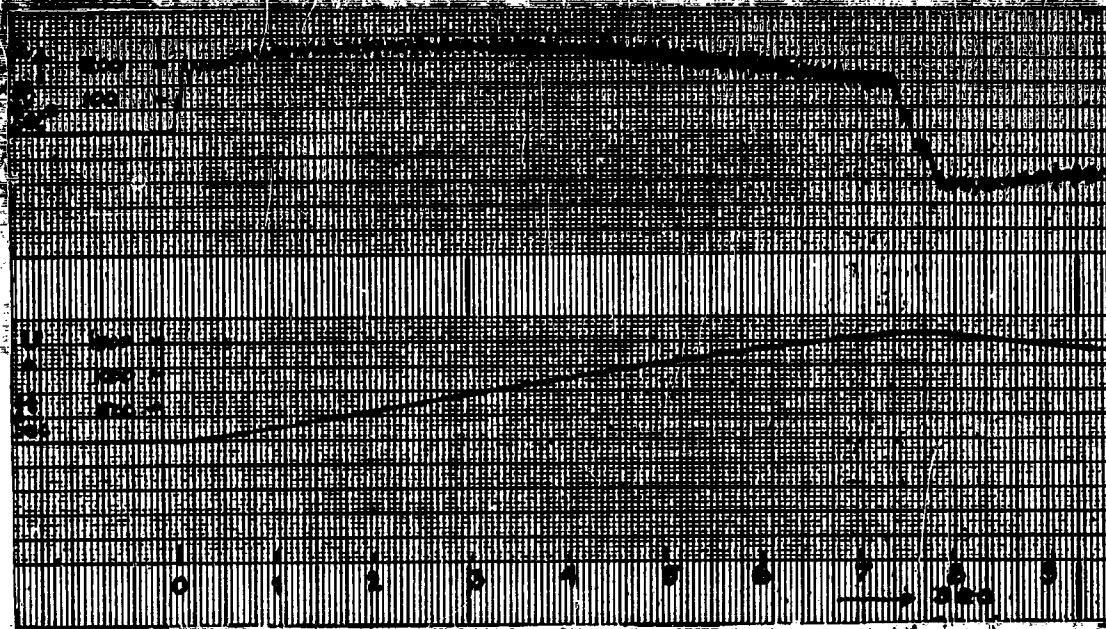


FIGURE A-4
ACCELERATION AND VELOCITY PROFILE
SLID RUN 3-5C

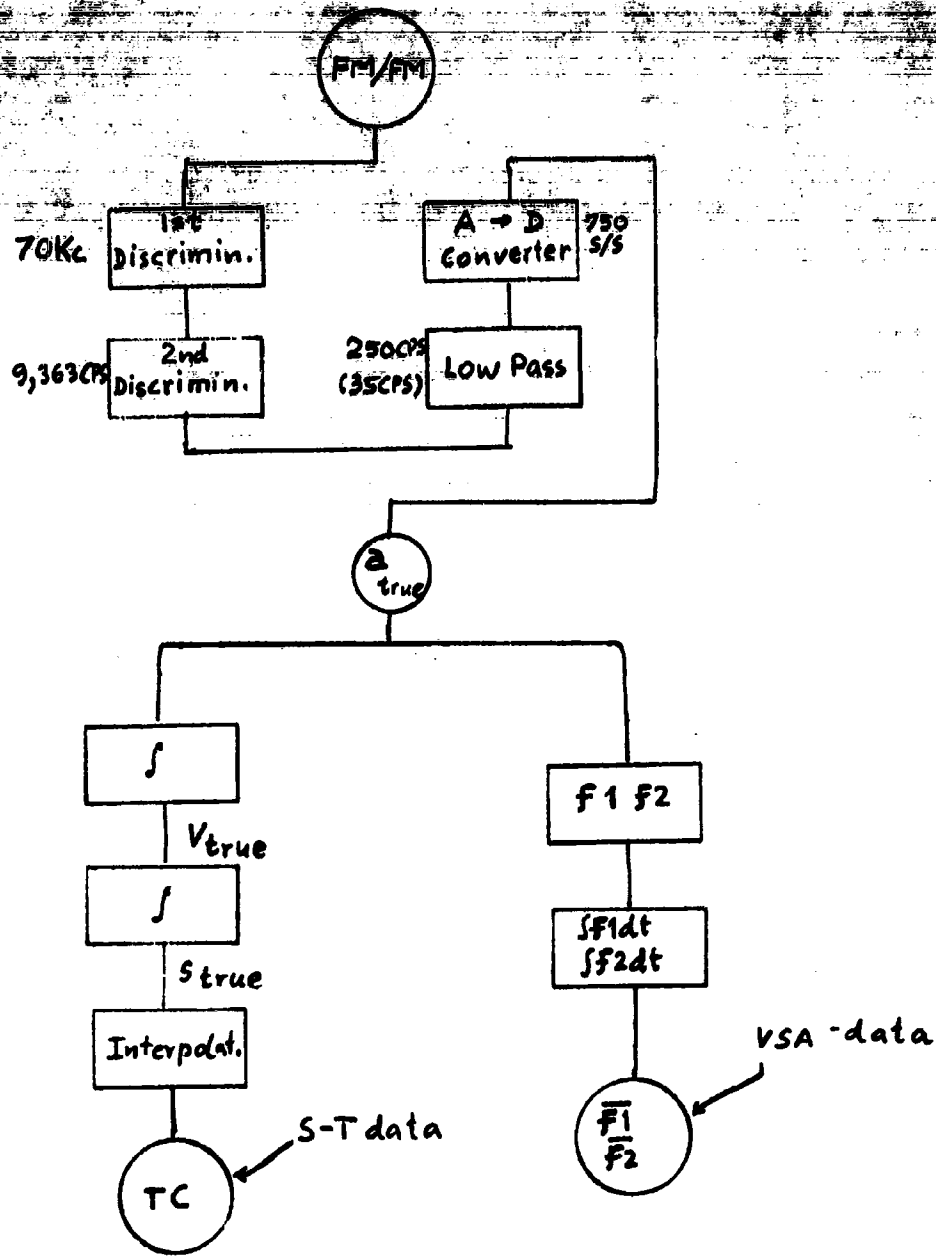


FIGURE A-5
 BLOCK DIAGRAM
 OF
 SIMULATED DATA FLOW

times as function of position, an inverse (parabolic) interpolation is then performed to produce the time values at given marker stations. They are recorded on tape and can now be processed by the routine digital programs.

Integration Procedure

The results reported in a later paragraph indicate that Simpson's Rule yields valid results when applied properly to integrate the fluctuating acceleration data. An interesting problem arose from the specific output requirements. The question was: How can Simpson's weights be modified to provide results for each data point? In other words, can Simpson's Rule be combined with a parabolic interpolation? Since a parabola is used in the integration procedure, it appears straightforward to use the same parabolic segment for this purpose. If that can be done, results become available, readily and accurately, at multiples of the original sampling step. For instance, they would be available every 4 msec, the "window width" required for the last program version of Phase III.

A set of weights for the desired intermediate results was derived from the general expression for the integral of a parabolic segment through 3 points y_1 , y_2 , and y_3 , which is:

$$I(t) = \int_0^t \left\{ y_1 + (2y_2 - 1.5y_1 - 0.5y_3) \frac{t}{h} + (0.5y_1 - y_2 - 0.5y_3) \frac{t^2}{h^2} \right\} dt$$

Setting the upper limit to $2h$ one obtains Simpson's coefficients

$$\frac{h}{3}, \frac{4h}{3}, \text{ and } \frac{h}{3}.$$

With the limits set from 0 to h and from h to $2h$ the expressions for single step integration are found as

$$I_{0-h} = (5y_1 + 8y_2 - y_3) \frac{h}{12}$$

$$\text{and } I_{h-2h} = (-y_1 + 8y_2 + 5y_3) \frac{h}{12}$$

The latest version of the integration program used the weights as shown below:

$$\frac{5h}{12}, \frac{8h}{12}, -\frac{h}{12}$$

$$-\frac{h}{12}, \frac{8h}{12}, \frac{5h}{12}$$

in an alternating fashion. It is noted that the sum of these weights yields Simpson's coefficients.

Another interpolation scheme was tried out first which led to erroneous results. Two overlapping integration chains were used in this procedure with a shift of the initial starting points of one sampling interval. The error caused by this shift was surprisingly high and seems to be of interest in this context. Figure A-6a shows the velocity error function using the original interpolation scheme which is supposed to be zero or, at least, should show no trend. This error function resulted from the "Vector Comparison" program and from subsequent filtering with an averaging process. The averaging period was about 0.3 second.

In order to prove the assumed origin of the unexpected low frequency trend error which reaches about 0.5 ft/sec, an auxiliary computation was performed. During a period from 4.650 to 4.786 seconds, where the error grows quite rapidly by about 0.18 ft/sec, acceleration data were integrated. The integration was performed twice, with one time increment of 4/3 msec shift between the starting points. The initial and the end conditions of the integrals were properly set up with the above-mentioned single step weights. The computed total difference in velocity was

Integration 1	$V_1 =$	30.998 ft/sec
Integration 2	$V_2 =$	30.808 ft/sec
$V_1 - V_2 =$.190 ft/sec

The difference $V_1 - V_2$ agrees well with the observed trend error in velocity. The very reason for this effect is the high frequency content of the acceleration data. This was proved by an experiment with acceleration bandwidth limited to 35 cps. The error was reduced significantly (Figure A-6b). In comparing Figures A-6b and A-6a, the difference of the scale-factors of the ordinates should be noted.

After the time shift was eliminated by changing programs, a significant improvement was achieved as can be seen from Figure A-7. However, the function plotted in this graph contains errors which were found to be related to round-off errors as explained in the next section.

Precision Problems

One purpose of the simulated test function was to detect very small errors in the design of production type programs. This imposed a stringent accuracy requirement on the test function itself. The error in the simulated data had to be at least one order of magnitude smaller than the errors to be detected. In particular, it was required that round-off errors should not be allowed to accumulate. A trivial consequence was to carry as many significant places as possible. For this reason "optimum scaling" with fixed binary point was applied in the first version of the program; i.e., the numbers were scaled so that their maximum values reached a value between 2^{34} and 2^{35} . Later the fixed point system was changed to a simplified floating point system which utilized the full register length of 36 bits. To keep the programming effort as small as possible and in



Fig. A-6a $\Delta V = V_{RA} - V_B/T$ ($f_c = 250$ cps, $t_d = .008$ sec)
Effect of Time Shift between Integrations

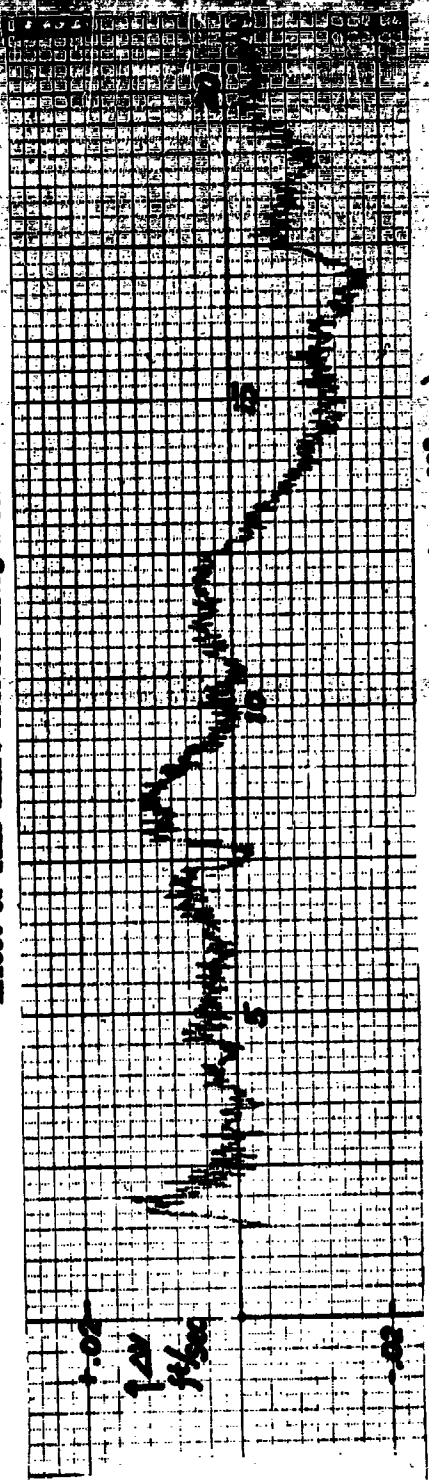


Fig. A-6b $\Delta V = V_{RA} - V_B/T$ ($f_c = 35$ cps, $t_d = .008$ sec)
Effect of Time Shift between Integrations

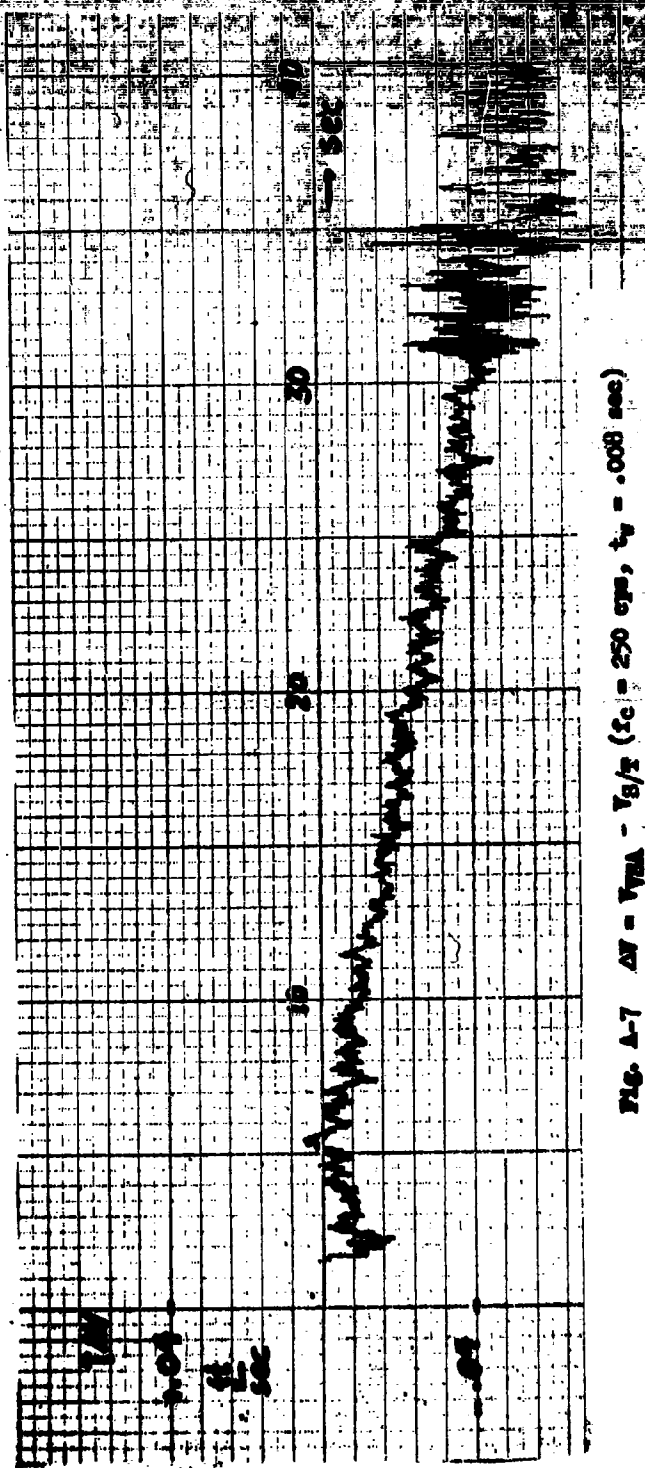


Fig. A-7 $\Delta V = V_{PA} - V_{B/Z}$ ($f_c = 250$ cps, $t_d = .008$ sec)
 Effect of Head-off Errors

order to save computer time, the floating point computation was applied only to those operations for which the full length of the register was essential. In both versions rounding-off was used at the least significant bit.

A problem occurred in connection with the accuracy of the average frequencies \bar{f}_1 and \bar{f}_2 . The precision of these quantities was restricted considerably by the format scaling requirement (2^6) and a careful adjustment of round-off errors was necessary. For practical reasons the computation which derives these quantities from the integrals of the frequencies was performed in fixed point format. The following expressions were used in an early version of the program:

$$\bar{f}_1 \cdot 2^6 = \left(\frac{1}{t_w}\right) \left(\int_0^{nt_w} f_1 dt \cdot 2^{16} - t_w \sum_0^{(n-1)t_w} (\bar{f}_1 \cdot 2^6) 2^{10} \right) 2^{-10}$$

$$\bar{f}_2 \cdot 2^6 = \left(\frac{1}{t_w}\right) \left(\int_0^{nt_w} f_2 dt \cdot 2^{16} - t_w \sum_0^{(n-1)t_w} (\bar{f}_2 \cdot 2^6) 2^{10} \right) 2^{-10}$$

By computing the values of \bar{f}_1 and \bar{f}_2 as the difference between the total integral and the sum of the previously computed values the total round-off error of $\Sigma \bar{f}_1$ and $\Sigma \bar{f}_2$ was compelled not to exceed the desired one bit maximum. The proper dimensions were observed by multiplying with t_w or its reciprocal. Figure A-7 is a plot of the velocity error function derived from data computed by the above equations. As shown, this process gave rise to a negative drift error of 0.05 ft/sec maximum magnitude at about 40 seconds. This unexpected error was carefully investigated and it was proved that it originates from round-off errors in \bar{f}_1 and \bar{f}_2 . Although the total sum of the error in $\Sigma \bar{f}_1$ and $\Sigma \bar{f}_2$ were kept under control as outlined, the individual errors caused the small drift in the final result. It is noted for the purpose of clarification that no drift error occurs if velocity is derived from Σf_1 and Σf_2 , the quantities with adjusted total round-off error. The round-off errors in f_1 and f_2 accumulate when the expressions $\Sigma(\bar{f}_1 \cdot t_w)$ and $\Sigma(\bar{f}_2 \cdot t_w)$ are computed in the "Integration" program. To keep the sum of these errors small enough, it is necessary that the individual round-off errors in f_1 and f_2 be kept small when these quantities are computed. A relatively small change in the numerical procedure helped to reduce the observed drift significantly. An inspection of the new expressions shown below shows that the difference was now taken from numbers increased in size by the value of $\frac{1}{t_w}$. It is noted that in the particular case which was studied, $\frac{1}{t_w}$ had the value of 125.

$$\bar{f}_1 \cdot 2^6 = \left(\frac{1}{t_w}\right) \left(\int_0^{nt_w} f_1 dt \cdot 2^{16} - \sum_0^{(n-1)t_w} (\bar{f}_1 \cdot 2^6) 2^{10} \right) 2^{-10}$$

$$\bar{f}_2 \cdot 2^8 = \left(\frac{1}{t_w} \int_0^{nt_w} f_2 dt \cdot 2^{10} - \sum_0^{(n-1)t_w} (\bar{f}_2 \cdot 2^8) 2^{10} \right) 2^{-10}$$

Using the above expressions for computing the average frequencies, the drift error was significantly reduced.

Pre-Run Computation

One further requirement for the simulation to match the actual data processing was to include a pre-run period (from computational zero to first motion) of approximately 7.5 seconds. During this time, the input acceleration should theoretically be zero. At first, the additional effort as required to include this period with zero acceleration appears small. However, experience has shown that based on this requirement double precision commands had to be worked into the program.

Precision Problems - Pre-Run

The latest program (single precision) of the VSA test function was tried out to find the effect of the acceleration data being zero before first motion. The table which follows is a small section of a high speed printer listing which shows the noise effects in the simulated data of average string frequencies f_1 and f_2 :

DOUBLE PRECISION EFFECT ON FREQUENCY COMPUTATION NOISE DURING PRE-RUN

<u>Time Seconds</u>	<u>Single Precision</u>		<u>Double Precision</u>	
	<u>f₁ cps</u>	<u>f₂ cps</u>	<u>f₁ cps</u>	<u>f₂ cps</u>
7.380	9,339.999 8	9,342.391 8	9,340.000 0	9,342.400 0
7.384	9,340.000 0	9,342.400 8	9,340.000 0	9,342.400 0
7.388	9,340.000 1	9,342.394 2	9,340.000 0	9,342.400 0
7.392	9,340.000 2	9,342.403 1	"	"
7.396	9,340.000 4	9,342.396 4	"	"
7.400	9,340.000 6	9,342.405 5	"	"
7.404	9,340.000 7	9,342.402 6	"	"
7.408	9,340.000 9	9,342.396 0	"	"
7.412	9,340.001 0	9,342.404 9	"	"
7.416	9,340.001 2	9,342.398 3	"	"
7.420	9,340.001 3	9,342.407 3	"	"
7.424	9,340.001 5	9,342.400 6	"	"
7.428	9,340.001 6	9,342.394 0	"	"
7.432	9,339.998 0	9,342.402 9	"	"
7.436	9,340.002 0	9,342.396 3	"	"

The small scatter in the frequency values around their nominal values 9,340.0000 cps and 9,342.4000 cps (see columns 2 and 3) caused the initial velocity at first motion time recovered from the simulated data to be different from zero. In order to reduce this error and to reduce the noise in the frequency values, double precision arithmetic was chosen for the next versions of the program. The errors to be eliminated were small. Yet the idea was to avoid errors whenever it was possible, in order not to obscure other errors which the simulation should detect. In columns 4 and 5 it can be seen that the noise disappears at the 4th decimal place behind the point. Only those numerical operations which required it were performed with double precision, namely the integration of f_1 and f_2 and the summation of f_1 and f_2 . To simplify computations, fixed octal point was used. The same scale-factors selected as an optimum for acceleration and that selected for the string frequencies f_1 and f_2 were then used also as scale-factors for the integrals or sums of these quantities. The resulting accumulated numbers exceed one register length and two registers have to be provided. Rounding is applied to the time increment which occupies (in most cases) one full register length. The same principle of round-off error control is applied as described previously. With the new scale-factors, the expression for average string frequencies becomes:

$$\bar{f}(t_1) \cdot 2^6 = \left\{ \frac{1}{t_w} \int_0^{t_1} f \, dt \cdot 2^{21} - \left(\sum_0^{t_1-1} \bar{f} \cdot 2^6 \right) 2^{15} \right\} 2^{-15}$$

Some practical difficulties were observed using this expression which will be discussed later.

Reference Velocity for VSA

In order to better predict (and trouble shoot) the values of velocity computed from the hot-run production programs using VSA data, a VSA reference velocity was included in the simulation and computed as follows:

$$V_{refVSA} = \frac{(\sum \bar{f}_1 - \sum \bar{f}_2) t_w - K_0 t}{K_1} - \frac{K_2}{K_1} \int a^2 dt - \frac{K_3}{K_1} \int a^3 dt$$

The flow chart (Figure A-8) shows the final version of the simulation program.

In the previous simulation setup the VSA indicated distance function was derived from acceleration by double integration. The advantage of the new setup can be explained as follows: Velocity as indicated by the VSA is computed by first changing the physical units of acceleration to physical units of frequency. This conversion implies a numerical process which produces some numerical error. This error accumulates to about 0.00065 ft/sec at the end of the sled run. This error may essentially be eliminated by the computation scheme indicated by Figure A-8.

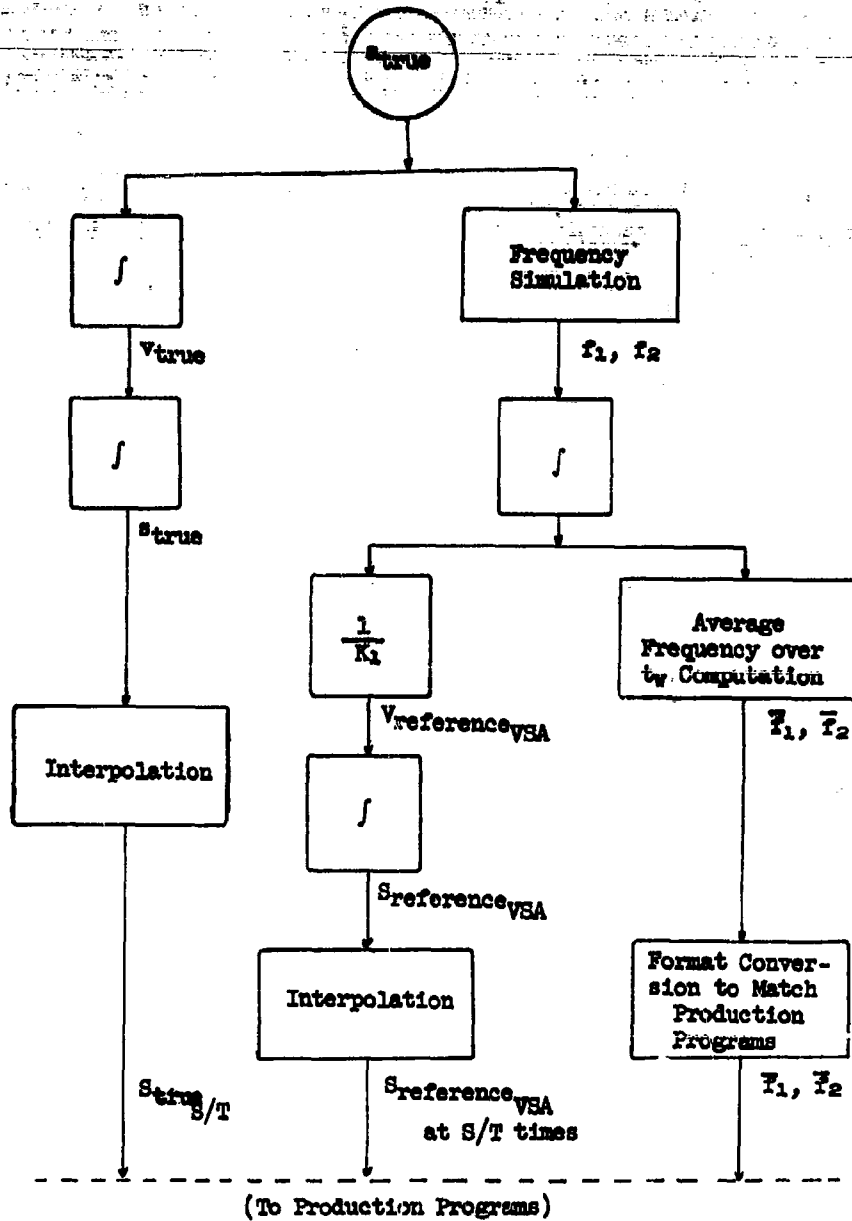


Fig. A-8 Flow Diagram of VSA Simulation

The quantities $\int f_1 dt$ and $\int f_2 dt$ are related to velocity by a scale-factor $1/K_1$. It is appropriate to declare the velocity found from $\int f_1 dt$ and $\int f_2 dt$ as reference velocity rather than the velocity "V_{true}" which is found by integrating the acceleration data. By doing this, an error is eliminated which would show up in the results obtained from the production programs.

Partial Error Analysis

Reference Velocity

As mentioned, the quantity V_{refVBA} is the actual underlying velocity which serves for the simulation of \bar{f}_1 and \bar{f}_2 , the average string frequencies. The quantity $\Delta V_1 = V_{ref} - V_{true}$ as in Figure A-9 shows a negative drift with nearly constant slope. It reaches -0.00065 ft/sec at 45 seconds. This error function can be approximated by a straight line through the origin with a slope of about -0.000013 ft/sec². Therefore, it is preferable to use S_{refVBA} for the simulation of interrupter times which serve as a reference. Of course, if the least square fitting procedure which is used to find error coefficients includes the K_0 term for fitting the bias error component, the error equivalent to using S_{true}/T instead of using S_{refVBA} is extracted at least approximately and does not spoil the least square solutions essentially.

The observed error (Figure A-9) is probably caused by the different scale-factors of "f" and "a" which are 2^{16} and 2^{24} respectively and which may lead to different round-off errors.

Velocity Computed by the "Arma Integration" Program

A more serious error is discovered if we process the simulated data f_1 and f_2 through the production program which computes acceleration ("Sum and Difference" program) and then integrate these acceleration data to find the indicated velocity V_{ind} ("Arma Integration" program). The error $\Delta V = V_{ind} - V_{ref}$ shows a systematic character with a peak of about 0.0035 ft/sec in the neighborhood of burnout (16 sec.) (see Figure A-10). We find that over the greater part of the simulated sled run, the sum model and the difference model yield an error ΔV_2 of similar magnitude.

The greater part of this error originates as we can show from the deficiency of the chosen procedure in handling vibrational components of acceleration. Inspecting the tables which follow we find that the recovered integrals $\int a^2 dt$ and $\int a^3 dt$ computed by the "Coordinate

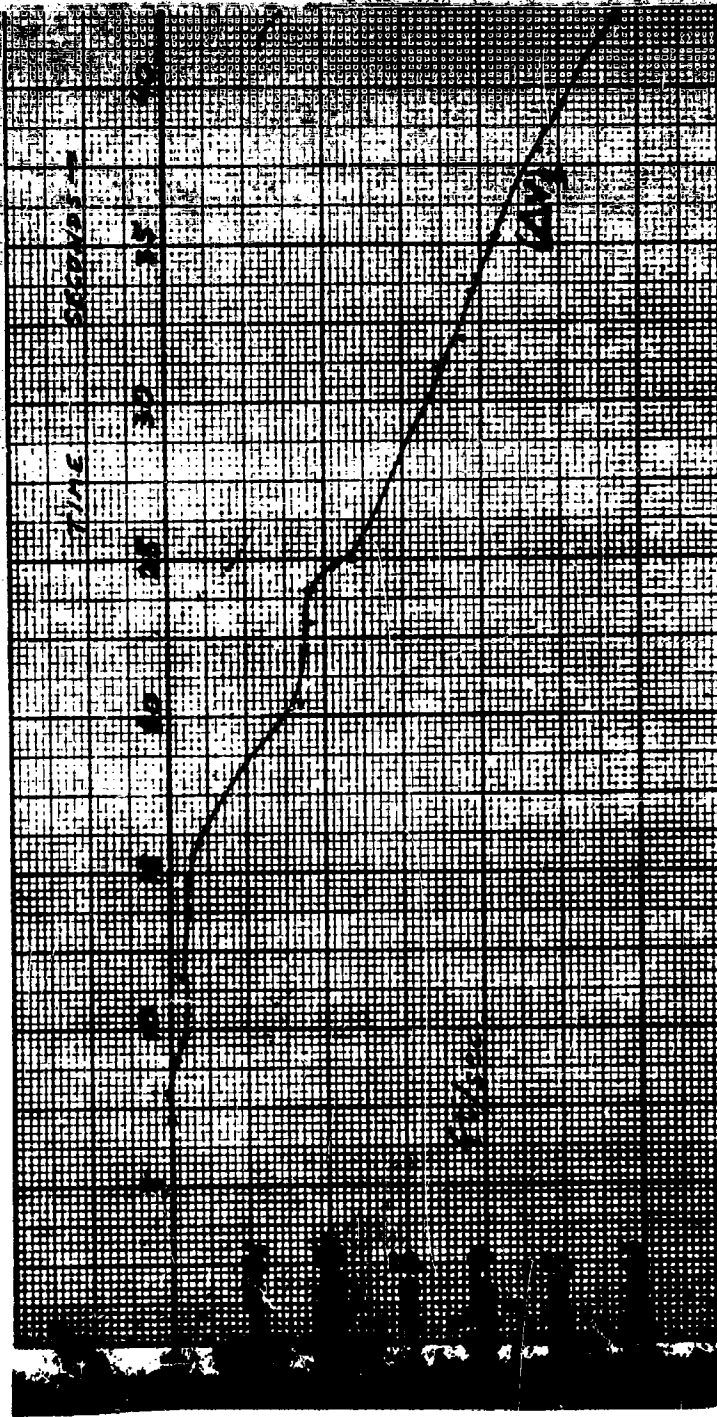


Fig. A-9 $\Delta V = \text{Final} - \text{Version}$
 FINAL VERSION
 SIMULATION ΔV ERROR

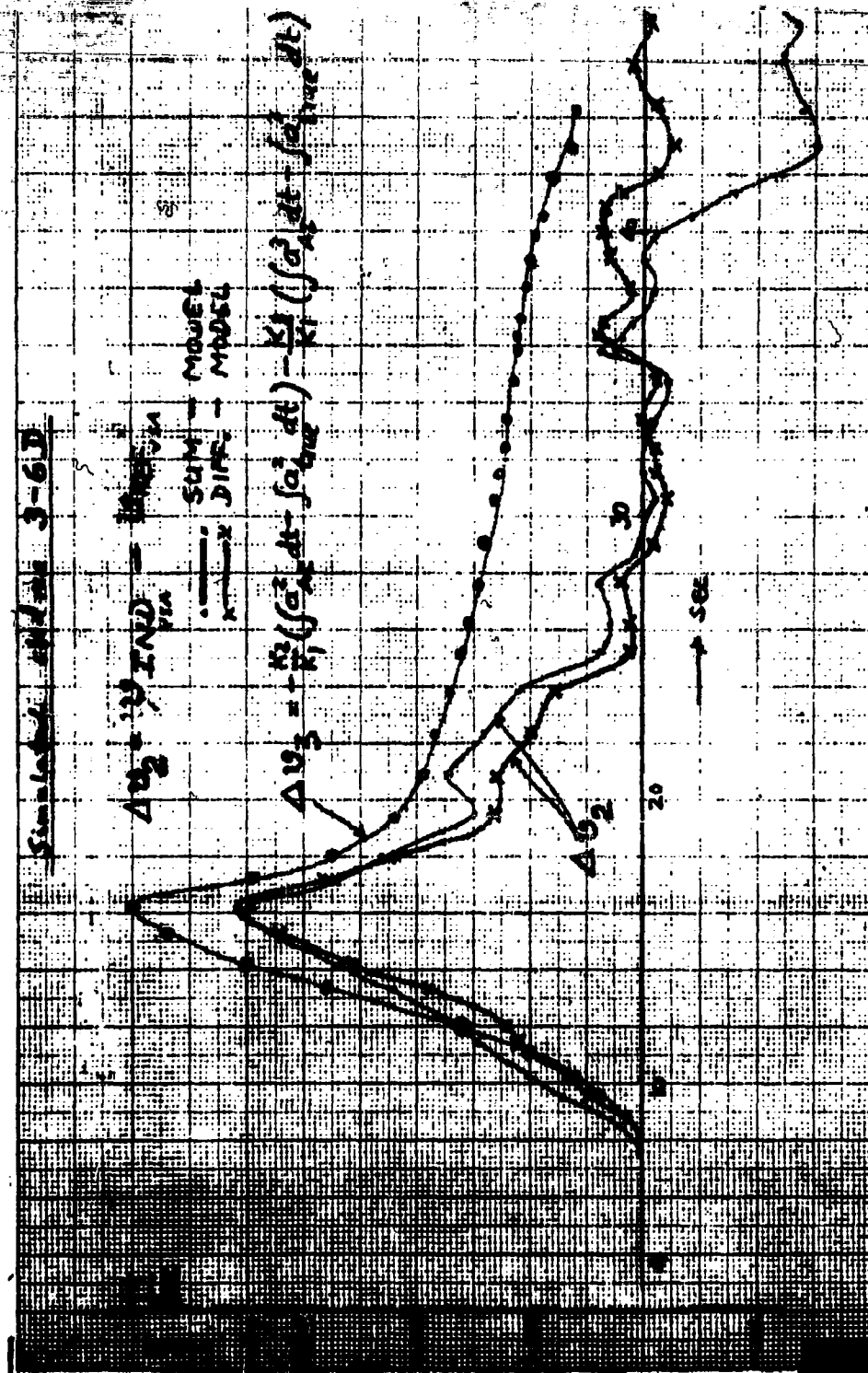


Fig. A-10 Errors in Velocity
 Observed Quadratic
 and Cubic Effects

TABLE OF $\int a^2 dt - (t_w = .004 \text{ sec})$

<u>Time Seconds</u>	<u>$\int a_{\text{true}}^2 dt$</u>	<u>$\int a_{\text{AI}}^2 dt$</u>	<u>$\int a_{\text{AI}}^2 dt - \int a_{\text{true}}^2 dt$</u>	<u>$\int a_{\text{AI}}^2 dt - \int a_{\text{true}}^2 dt$ (%)</u>
8.7	39,340	39,307	- 33	-0.084
9.5	80,090	79,994	- 96	- .12
10.2	123,706	123,565	- 141	- .11
11.0	168,865	168,638	- 227	- .13
12.0	216,374	216,029	- 345	- .16
13.2	258,982	258,312	- 670	- .26
14.2	280,904	279,987	- 917	- .33
15.1	297,667	296,507	-1160	- .39
16.1	307,087	305,618	-1469	- .48
17.1	330,403	328,637	-1766	- .54
18.0	346,343	344,351	-1992	- .58
19.4	361,875	359,644	-2231	- .62
20.9	368,795	366,415	-2380	- .64
22.3	372,405	369,935	-2470	- .66
23.8	374,979	372,388	-2591	- .69
25.2	376,887	374,176	-2711	- .72
26.2	377,879	375,081	-2798	- .74
27.6	379,123	376,202	-2921	- .77
29.0	380,109	377,085	-3024	- .79
30.5	381,019	377,866	-3153	- .83
31.4	381,504	378,275	-3229	- .85
32.4	381,986	378,687	-3299	- .86
33.4	382,411	379,044	-3367	- .88
34.8	382,990	379,532	-3458	- .90
35.8	383,424	379,902	-3522	- .92
36.3	383,594	380,045	-3549	- .92
36.7	383,788	380,209	-3579	- .93
37.9	384,111	380,463	-3648	- .95
38.9	384,907	381,198	-3709	- .96
39.8	386,888	383,123	-3765	- .97
40.6	389,707	385,896	-3811	- .98
41.3	394,935	391,091	-3844	- .97
42.0	401,844	397,952	-3892	- .97
42.9	408,860	404,930	-3930	- .96
44.2	410,715	406,741	-3974	- .97
45.7	411,356	407,345	-4011	- .98
47.3	411,603	407,559	-4044	- .98

TABLE OF $\int a^3 dt$ - ($t_w = .004$ sec)

Time Seconds	$\int a_{true}^3 dt$	$\int a_{AI}^3 dt$	$\int a_{AI}^3 dt - \int a_{true}^3 dt$	$\int a_{AI}^3 dt - \int a_{true}^3 dt$ (%)
8.7	7,602,159	7,583,986	- 18,173	-0.24
9.5	16,980,321	16,921,759	- 58,562	- .34
10.2	27,464,883	27,369,420	- 95,463	- .35
11.0	38,212,213	38,057,580	-154,633	- .40
12.0	48,849,222	48,616,747	-232,475	- .48
13.2	57,036,237	56,621,116	-415,121	- .73
14.2	60,422,571	59,897,363	-525,208	- .87
15.1	62,732,225	62,110,437	-621,788	- .99
16.1	63,331,068	62,662,376	-668,692	-1.06
17.1	59,600,956	59,070,175	-530,781	-0.89
18.0	57,412,856	56,974,526	-438,330	- .76
19.4	55,753,891	55,388,466	-365,425	- .66
20.9	55,239,706	54,905,358	-334,348	- .61
22.3	55,046,373	54,725,384	-320,989	- .58
23.8	54,922,774	54,616,314	-306,460	- .56
25.2	54,840,767	54,547,159	-293,608	- .54
26.2	54,802,119	54,516,072	-286,047	- .52
27.6	54,755,821	54,479,806	-276,015	- .50
29.0	54,722,337	54,453,758	-268,579	- .49
30.5	54,690,713	54,430,229	-260,484	- .48
31.4	54,675,306	54,419,321	-225,985	- .47
32.4	54,659,820	54,407,674	-252,146	- .46
33.4	54,646,926	54,398,144	-248,782	- .46
34.8	54,630,846	54,386,111	-244,735	- .45
35.8	54,618,153	54,376,140	-242,013	- .44
36.3	54,613,562	54,372,614	-240,948	- .44
36.7	54,607,953	54,368,307	-239,646	- .44
37.9	54,599,967	54,363,064	-236,903	- .43
38.9	54,560,482	54,327,753	-232,729	- .43
39.8	54,438,672	54,212,599	-226,073	- .42
40.6	54,219,976	54,001,594	-218,382	- .40
41.3	53,715,173	53,506,462	-208,711	- .39
42.0	53,000,706	52,805,238	-195,468	- .37
42.9	52,298,674	52,113,257	-185,417	- .35
44.2	52,217,385	52,036,823	-180,562	- .35
45.7	52,201,304	52,022,821	-178,483	- .34
47.3	52,197,129	52,019,785	-177,344	- .34

TABLE OF $\Delta V_s(t)$ - ($t_w = .004$ sec)

<u>Time Seconds</u>	<u>$-\frac{K_2}{K_1} / a^2 dt \times 10^6$</u>	<u>$-\frac{K_3}{K_1} / a^3 dt \times 10^6$</u>	<u>$\Delta V_s(\text{ft/sec})$</u>
8.7	- 5	128	0.000 12
9.5	- 16	413	0.000 40
10.2	- 23	673	0.000 65
11.0	- 37	1091	0.001 05
12.0	- 57	1641	0.001 58
13.2	-112	2930	0.002 82
14.2	-153	3703	0.003 55
15.1	-194	4389	0.004 20
16.1	-245	4720	0.004 47
17.1	-295	3747	0.003 45
18.0	-333	3094	0.002 76
19.4	-373	2579	0.002 21
20.9	-398	2360	0.001 96
22.3	-413	2266	0.001 85
23.8	-433	2163	0.001 73
25.2	-453	2072	0.001 62
26.2	-468	2019	0.001 55
27.6	-488	1948	0.001 46
29.0	-506	1896	0.001 39
30.5	-527	1838	0.001 31
31.4	-540	1807	0.001 27
32.4	-552	1780	0.001 23
33.4	-563	1756	0.001 93
34.8	-578	1727	0.001 49
35.8	-589	1708	0.001 12
36.3	-593	1701	0.001 11
36.7	-599	1691	0.001 09
37.9	-610	1672	0.001 06
38.9	-620	1643	0.001 02
39.2	-630	1596	0.000 97
40.6	-637	1541	0.000 90
41.3	-643	1473	0.000 83
42.0	-651	1379	0.000 73
42.9	-657	1308	0.000 65
44.2	-665	1274	0.000 61
45.7	-671	1260	0.000 59
47.3	-676	1252	0.000 58

Function" program are too small in comparison to the integrals which were computed from a_{true} . This error, which amounts to -1.06% maximum for $\int a^2 dt$ and -0.97% maximum for $\int a^3 dt$, is a "rectification" error caused by the sampling rate of 250 samples/sec, which is too low, and possibly by shortcomings of the integration process.

If we multiply the difference of the integrals by K_2/K_1 or K_3/K_1 and add the two products, we obtain a function ΔV_3 (see Table of $\Delta V_3(t)$ and Figure A-10) very similar to the function ΔV_2 in Figure A-10.

$$\Delta V_3 = - \frac{K_2}{K_1} \left(\int a^2_{A_1} dt - \int a^2_{true} dt \right) - \frac{K_3}{K_1} \left(\int a^3_{A_1} dt - \int a^3_{true} dt \right)$$

where $K_2/K_1 = 0.167\ 367 \times 10^{-8}$

$K_3/K_1 = 0.705\ 973 \times 10^{-8}$ for the given model of the VSA instrument.

Comparing the nonlinear terms $\int a^2 dt$ and $\int a^3 dt$ with those obtained with $t_w = 8$ msec corresponding to only 125 samples/sec, a small advantage of .11% in the recovered value of $\int a^3 dt$ is found for $t_w = 4$ msec. However, $\int a^2 dt$ is found to be slightly better with $t_w = 8$ msec.

The question arises: What causes the difference between ΔV_2 and ΔV_3 in Figure A-10? There is still a small systematic error ($\Delta V_2 - \Delta V_3$) which reaches about 0.0015 ft/sec at 31 seconds. A possible explanation is this: In the process of computing a in the "Sum and Difference" program, the nonlinear terms

$$- \frac{K_2}{K_1} \left(\frac{f_1 - f_2 + K_0}{K_1} \right)^2 \quad \text{and} \quad - \frac{K_3}{K_1} \left(\frac{f_1 - f_2 + K_0}{K_1} \right)^3$$

are computed as contributions to the total \tilde{a} . These terms are then integrated in the "Arma Integration" program approximately and implicitly as part of the summation process $\sum \tilde{a} t_w$ to form the correction terms

$$- \frac{K_2}{K_1} \int a^2 dt \quad \text{and} \quad - \frac{K_3}{K_1} \int a^3 dt.$$

The numerical process of finding the terms $-\frac{K_2}{K_1} \int a^2 dt$ and $-\frac{K_3}{K_1} \int a^3 dt$ in this fashion is not the same as the process of computing the integrals $\int a^2 dt$ and $\int a^3 dt$ as independent coordinate functions in the "Coordinate Functions" program. These integrals were used and interpolated to find ΔV_3 . Further analysis is needed to prove the validity of this hypothesis.

We note at this point that the above investigations thoroughly validate the hot-run production program techniques up to a residual velocity error with a maximum value on the order of .0035 ft/sec. Further reduction of this error (although possible) was not seriously attempted in the production programming. We are now ready to examine the results of error coefficient recovery by the production programming when artificial error coefficients were inserted into the simulation of VSA information.

The Simulation Results

After having shown that the hot-run data processing introduced negligible error (max \approx .003 ft/sec as previously noted), it was then necessary to insert artificial error coefficients into the test program and attempt to recover them using the hot-run average velocity comparison and least squares regression analysis. The following table illustrates the recovery accuracy achieved for $\tau = .3$ seconds.

ERROR COEFFICIENT RECOVERY ($\tau = .3$)

Coefficient	Inserted Value	Recovered Value	Recovered -Inserted	Max Velocity Error during Sled Run (ft/sec)	Relative Velocity Error - 1 Part in xxx of V_{max}
δK_0	0	-.19473-5	-.19473-5	-.0001	15,000,000
δK_1	+.28785-4	+.32679-4	+.03894-4	+.0058	257,000
δK_2	+.36077-7	+.34574-7	-.01503-7	-.0006	2,500,000
δK_3	-.70912-9	-.69672-9	+.01240-9	+.0009	1,650,000
δK_A	0	-.1475 -5	-.1475 -5	-.0004	3,750,000
Const	0	-.217 -2	-.217 -2	-.0022	690,000

A study was undertaken to determine the effects of variations in τ . The results of this study are shown in Figures A-11 through A-16. The deviations of the recovered coefficients from the reference coefficients are plotted vertically. The independent (abscissa) variable is τ , the averaging time. As may be seen from these figures, all solutions are very nearly equivalent in the range $.1 \leq \tau \leq .5$. Outside of this range the individual coefficients behave differently, and in general the least squares solution begins to break down. Each figure contains a set of reference levels expressed as 1 part in xxx

"Function" program are too small in comparison to the integrals which were computed from a_{true} . This error, which amounts to -1.06% maximum for $\int a^3 dt$ and -0.97% maximum for $\int a^2 dt$, is a "rectification" error caused by the sampling rate of 250 samples/sec, which is too low, and possibly by shortcomings of the integration process.

If we multiply the difference of the integrals by K_2/K_1 or K_3/K_1 and add the two products, we obtain a function ΔV_3 (see Table of $\Delta V_3(t)$ and Figure A-10) very similar to the function ΔV_2 in Figure A-10.

$$\Delta V_3 = -\frac{K_2}{K_1} \left(\int a^2_{AI} dt - \int a^2_{true} dt \right) - \frac{K_3}{K_1} \left(\int a^3_{AI} dt - \int a^3_{true} dt \right)$$

where $K_2/K_1 = 0.167367 \times 10^{-6}$

$K_3/K_1 = 0.705973 \times 10^{-8}$ for the given model of the VSA instrument.

Comparing the nonlinear terms $\int a^2 dt$ and $\int a^3 dt$ with those obtained with $t_w = 8$ msec corresponding to only 125 samples/sec, a small advantage of .11% in the recovered value of $\int a^2 dt$ is found for $t_w = 4$ msec. However, $\int a^2 dt$ is found to be slightly better with $t_w = 8$ msec.

The question arises: What causes the difference between ΔV_2 and ΔV_3 in Figure A-10? There is still a small systematic error ($\Delta V_2 - \Delta V_3$) which reaches about 0.0015 ft/sec at 31 seconds. A possible explanation is this: In the process of computing a in the "Sum and Difference" program, the nonlinear terms

$$-\frac{K_2}{K_1} \left(\frac{f_1 - f_2 + K_0}{K_1} \right)^2 \quad \text{and} \quad -\frac{K_3}{K_1} \left(\frac{f_1 - f_2 + K_0}{K_1} \right)^3$$

are computed as contributions to the total \bar{a} . These terms are then integrated in the "Arma Integration" program approximately and implicitly as part of the summation process $\sum \bar{a} t_w$ to form the correction terms

$$-\frac{K_2}{K_1} \int a^2 dt \quad \text{and} \quad -\frac{K_3}{K_1} \int a^3 dt.$$

The numerical process of finding the terms $-\frac{K_2}{K_1} \int a^2 dt$ and $-\frac{K_3}{K_1} \int a^3 dt$ in this fashion is not the same as the process of computing the integrals $\int a^2 dt$ and $\int a^3 dt$ as independent coordinate functions in the "Coordinate Functions" program. These integrals were used and interpolated to find ΔV_3 . Further analysis is needed to prove the validity of this hypothesis.

We note at this point that the above investigations thoroughly validate the hot-run production program techniques up to a residual velocity error with a maximum value on the order of .0035 ft/sec. Further reduction of this error (although possible) was not seriously attempted in the production programming. We are now ready to examine the results of error coefficient recovery by the production programming when artificial error coefficients were inserted into the simulation of VSA information.

The Simulation Results

After having shown that the hot-run data processing introduced negligible error (max \approx .003 ft/sec as previously noted), it was then necessary to insert artificial error coefficients into the test program and attempt to recover them using the hot-run average velocity comparison and least squares regression analysis. The following table illustrates the recovery accuracy achieved for $\tau = .3$ seconds.

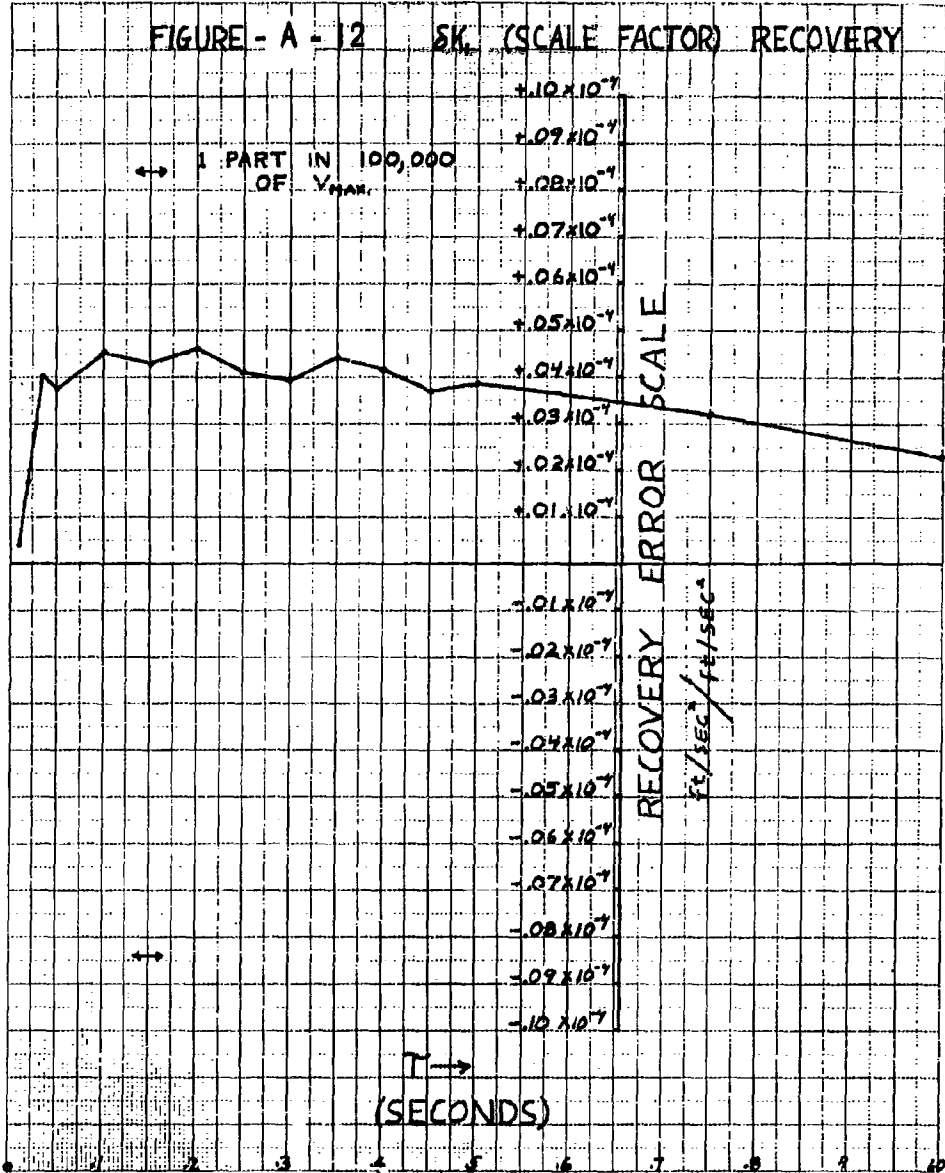
ERROR COEFFICIENT RECOVERY ($\tau = .3$)

Coefficient	Inserted Value	Recovered Value	Recovered - Inserted	Max Velocity Error during Sled Run (ft/sec)	Relative Velocity Error - 1 Part in xxx of V_{max}
δK_0	0	-.19473-5	-.19473-5	-.0001	15,000,000
δK_1	+.28785-4	+.32679-4	+.03894-4	+.0058	257,000
δK_2	+.36077-7	+.34574-7	-.01503-7	-.0006	2,500,000
δK_3	-.70912-9	-.69672-9	+.01240-9	+.0009	1,650,000
δK_A	0	-.1475 -5	-.1475 -5	-.0004	3,750,000
Const	0	-.217 -2	-.217 -2	-.0022	690,000

A study was undertaken to determine the effects of variations in τ . The results of this study are shown in Figures A-11 through A-16. The deviations of the recovered coefficients from the reference coefficients are plotted vertically. The independent (abscissa) variable is τ , the averaging time. As may be seen from these figures, all solutions are very nearly equivalent in the range $.1 \leq \tau \leq .5$. Outside of this range the individual coefficients behave differently, and in general the least squares solution begins to break down. Each figure contains a set of reference levels expressed as 1 part in xxx

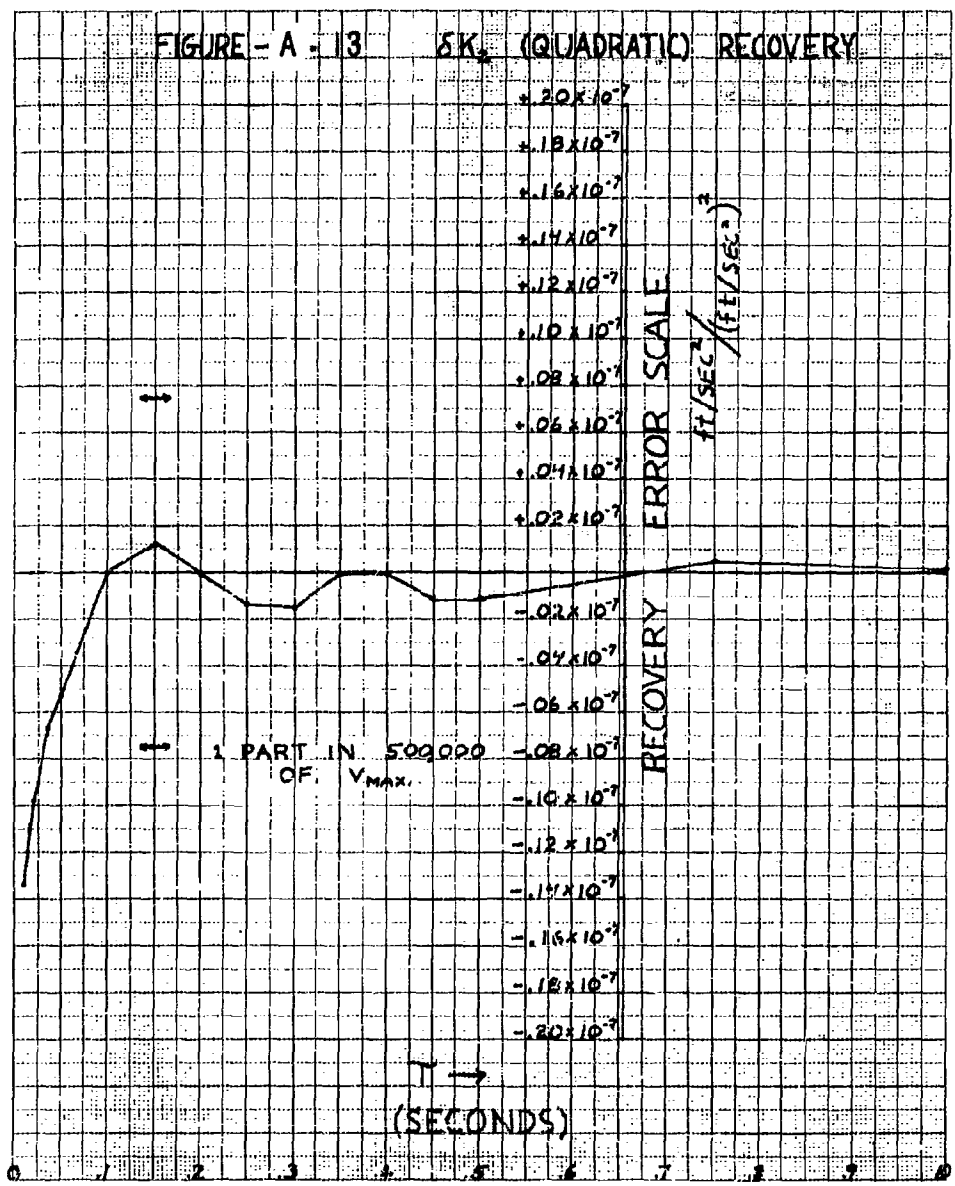
OPERATIONAL UNIT NO. 40 CIVIL ENGINEERING 1 B-17 CIVIL ENGINEERING

NO. OF RESEARCH PROJECTS INVESTIGATED 15 100% OF DESIGN



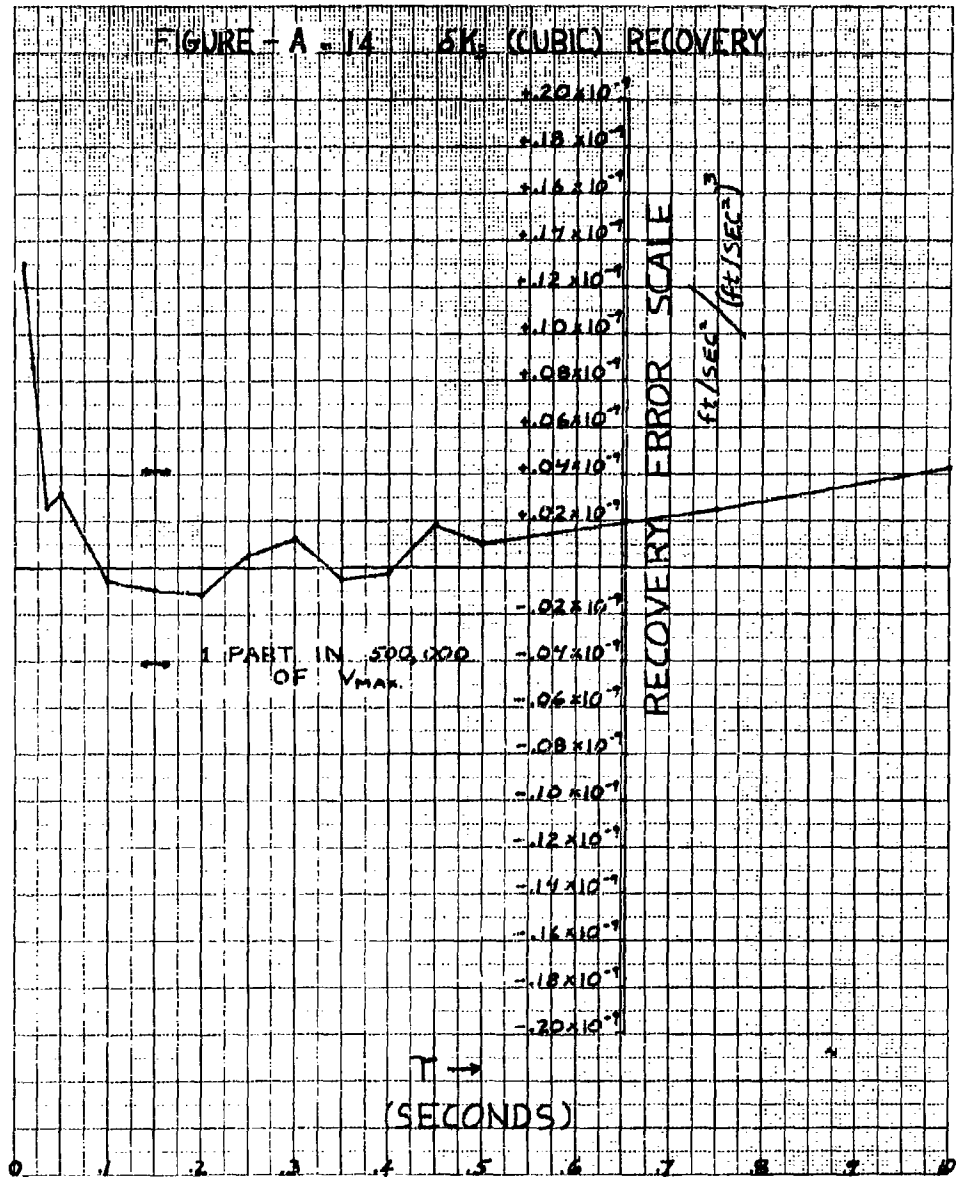
CERNATIONAL INSTRUMENTS CO. INC. 300 BAY ST. NEW YORK 7, N.Y.

MODEL 1000



CITIZENSHIP WORK CO. NO. 5284 AIR-TEL-521 200 SA 500 P/121018

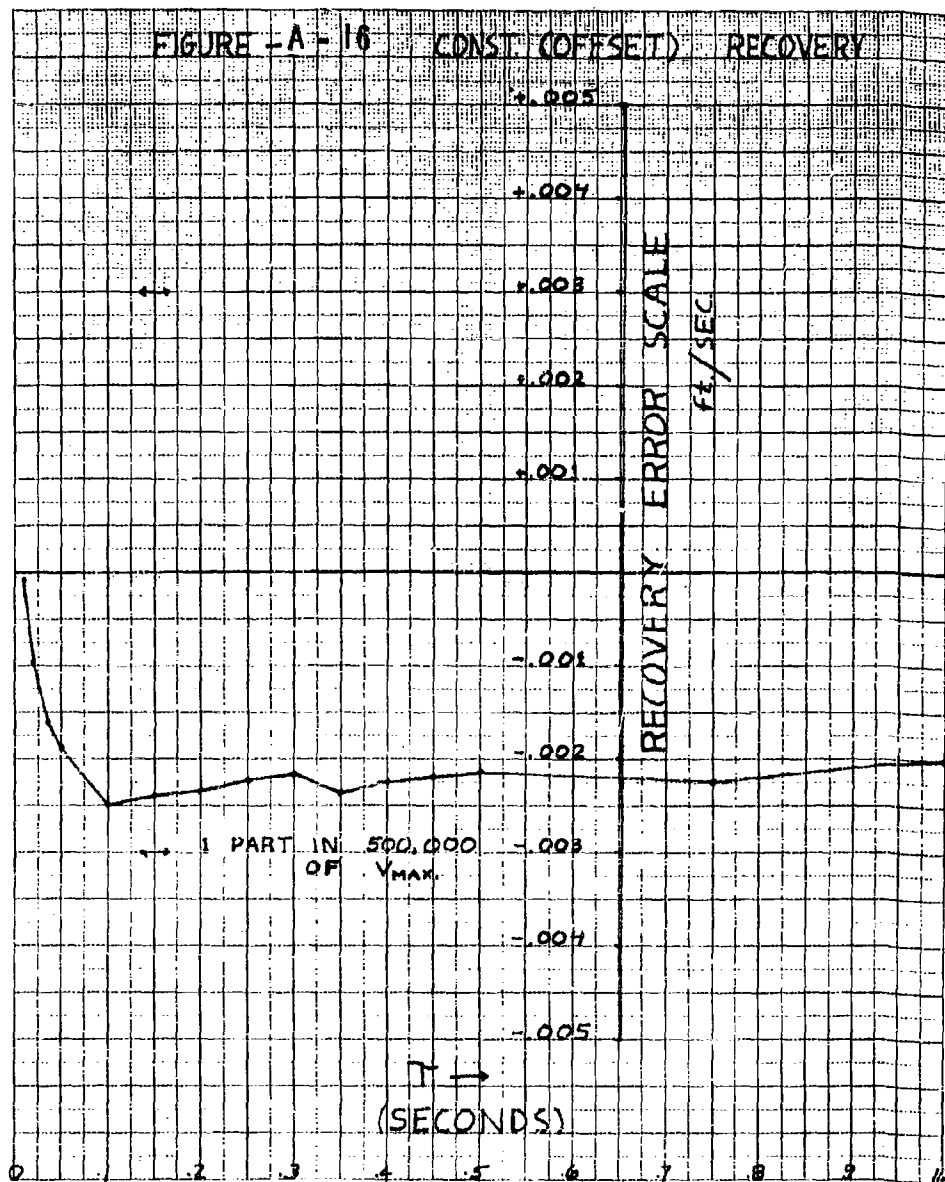
REPRODUCED BY THE NATIONAL ARCHIVES FROM RG 226



CITIZENS AND SONS CO. NO. 308 WASHINGTON ST. ST. LOUIS, MO. 63102

RECOVERY

RECOVERY ERROR SCALE
FT./SEC.



of V_{max} . These levels allow a quick evaluation of how drastic the effects of the noted errors in coefficient recovery would be for a typical sled run. As may be noted, no error on any figure exceeds 1 part in 173,000 of V_{max} . This shows that over the entire investigation range .01 τ 1.0, the accuracy of the error coefficient recovery was equivalent to a relative error of less than 1 part in 173,000 of V_{max} .

If the averaging time (τ) is allowed to get longer and longer the accuracy of the comparison becomes similar to that of a pure distance comparison. The following table shows the results of an error coefficient evaluation on the distance level using the dynamic simulation. The error coefficient recovery is actually quite good, but it does not match the accuracy obtainable from the average velocity comparison method. Thus, the regression analysis does not break down on the distance level, it is simply not as good as it is on the average velocity level. It might be that an iterative regression technique could be employed to obtain the error coefficients from a combination of the two comparisons. For example: One might evaluate the scale factor (δK_1) and offset (Const.) from a least squares on the distance level, extract these error sources from the accelerometer output indication and then solve for the remaining error coefficients by a regression on the residual error using an average velocity comparison. Many possible variations of such an approach could be employed to optimize the recovery of some specified set of error coefficients. As shown in these last two tables, the ability to use track test data to calibrate an inertial accelerometer is essentially proved.

DISTANCE COMPARISON

Coefficient	Inserted Value	Recovered Value	Recovered - Inserted	Max Velocity Error during Sled Run (ft/sec)	Relative Velocity Error - 1 Part in xxx of V_{max}
δK_0	0	-.15607-3	-.15607-3	-.0078	192,000
δK_1	+.28785-4	+.26025-4	-.02760-4	-.0041	352,000
δK_2	+.36077-7	+.20082-7	-.15995-7	-.0064	234,000
δK_3	-.70912-9	-.48838-9	+.22074-9	+.0155	97,000
δK_A	0	-.9668 -5	-.9668 -5	-.0026	572,000
Const	0	+.10249-2	+.10249-2	+.0010	1,500,000